

FACILITY FORM 602	N71-12664	(ACCESSION NUMBER)	(THRU)
	89	(PAGES)	63
	CR-108750	(NASA CR OR TMX OR AD NUMBER)	11
			(CATEGORY)

DEVELOPMENT OF METEOROID SIMULATORS

FOR HYPERVELOCITY IMPACT STUDIES

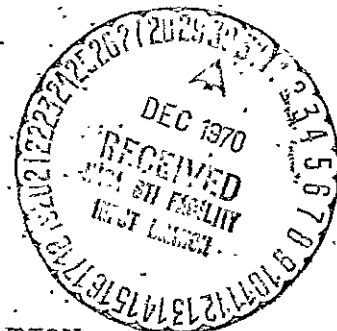
by: R. L. Woodall and E. R. Berus

Distribution of this report is provided in the interest of information exchange. Responsibility for the contents resides in the author or organization that prepared it.

October 1970

Prepared under Contract No. NAS 9-9343 by
THE FIRESTONE TIRE & RUBBER COMPANY
Defense Research Division
Akron, Ohio

for



NATIONAL AERONAUTICS AND SPACE ADMINISTRATION

Reproduced by
NATIONAL TECHNICAL
INFORMATION SERVICE
Springfield, Va. 22151

CR-108750

DEVELOPMENT OF METEOROID SIMULATORS

FOR HYPERVELOCITY IMPACT STUDIES

by: R. L. Woodall and E. R. Berus

October 1970

Prepared under Contract No. NAS 9-9343 by
THE FIRESTONE TIRE & RUBBER COMPANY
Defense Research Division
Akron, Ohio

for

NATIONAL AERONAUTICS AND SPACE ADMINISTRATION
MANNED SPACECRAFT CENTER
Houston, Texas 77058

ABSTRACT

The results of a contract to develop one gram aluminum meteoritic simulators using shaped charge techniques are reported. The results of the project were very encouraging. It was established that using specially designed shaped charges, jet-pellets with velocities of 8, 11 and 15 km/sec can be produced. Furthermore, the ability to control the jet-pellet length and to isolate the jet-pellet from the following debris was demonstrated. Further development work is required on the shaped charge systems to obtain refined final designs.

TABLE OF CONTENTS

	Page Numbers
SUMMARY	1
INTRODUCTION	4
TEST FACILITY	7
TEST RESULTS AND DISCUSSION	7
Slug and Debris Trap Development	7
One inch diameter aperture slug and debris trap	8
One-half inch diameter aperture slug and debris trap	10
Inhibitor Development	10
Composite liner inhibiting	10
Skirted liner inhibiting	11
Combined composite-skirted liner inhibiting	11
8 km/sec Jet-Pellet Development	12
Standard C/M Testing (Charge-to-Mass Ratio)	12
Reduced C/M Testing	12
11 km/sec Jet-Pellet Development	13
Liner Wall Thickness Effect	13
Liner Angle Effect	14
14 km/sec Jet-Pellet Development	14
Preliminary Bi-Explosive Tests	15
New Bi-Explosive Design Tests	15
Comp. B - Octol Charges	15
Pentolite - Comp. B Charge	16
Aluminum Material Study	16
1100 Aluminum	16
6061 Aluminum	16
CONCLUSIONS	17
Slug and Debris Trap Development	17
Inhibitor Development	18
8 km/sec Jet-Pellet Development	18
11 km/sec Jet-Pellet Development	18
14 km/sec Jet-Pellet Development	18
Aluminum Material Study	18
RECOMMENDATIONS	19
Slug and Debris Trap Development	19
Inhibitor Development	19
8 km/sec Jet-Pellet Development	19
11 km/sec Jet-Pellet Development	20
14 km/sec Jet-Pellet Development	20
APPENDIX A - Development of Design Criterion for Constant Cross-	21
Sectional Area Liner and Constant Cross-Sectional	
Area Explosive Charge	
B - Analysis of Shaped Charge Jetting Process Using	25
the Steady-State Theory	
C - Basic Design Equations for Bi-Explosive Shaped	30
Charges	
REFERENCES	33
TABLES	34
FIGURES	40

TABLES

Table	I	Slug and Debris Trap Tests
	II	Inhibitor Tests
	III	8 km/sec Jet-Pellet Test Results
	IV	11 km/sec Jet-Pellet Tests
	V	Preliminary Tests of 1100-O Aluminum Hyperbolic Liners in Bi-Explosive Charge
	VI	14 km/sec Jet-Pellet Tests

FIGURES

- Fig. 1. Side view sketch of the Open Test Site facility.
- Fig. 2. Side view block diagram of the electrical equipment for the Open Test Site facility.
- Fig. 3. 40° hyperbolic test assembly with 1-in. diameter aperture slug and debris trap.
- Fig. 4. 40°, 0.030-in. wall thickness, hyperbolic liner.
- Fig. 5. Explosive loading procedure for hyperbolic charges.
- Fig. 6. Loading fixture for 40° hyperbolic charge.
- Fig. 7. Explosive loading procedure for 1-in. diameter aperture slug and debris trap charges.
- Fig. 8. One inch diameter aperture slug and debris trap liner.
- Fig. 9. Radiographs of 1-in. diameter aperture slug and debris trap functioning.
- Fig. 10. One-half inch diameter aperture slug and debris trap liner.
- Fig. 11. Explosive loading procedure for 1/2-in. diameter aperture slug and debris trap charges.
- Fig. 12. Photographs of crater formed by 11 km/sec jet-pellet.

- Fig. 13. Radiographs of composite inhibited jet-pellets.
- Fig. 14. 30°, 0.030-in. wall thickness hyperbolic liner.
- Fig. 15. Inside skirted inhibited 30°, 0.030-in. wall thickness, hyperbolic liner.
- Fig. 16. Outside skirted inhibited 30°, 0.030-in. wall thickness, hyperbolic liner.
- Fig. 17. Inside & outside skirted inhibited 30°, 0.030-in. wall thickness, hyperbolic liner.
- Fig. 18. Radiographs of skirted inhibited jet-pellets.
- Fig. 19. Skirted - composite inhibited 35°, 0.030-in. wall thickness, hyperbolic liner.
- Fig. 20. Radiographs of skirted - composite inhibited jet-pellet.
- Fig. 21. Flanged 60°, 0.030-in. wall thickness, hyperbolic liner.
- Fig. 22. Radiographs of standard C/M 8 km/sec jet-pellet.
- Fig. 23. Radiographs of reduced C/M 8 km/sec jet-pellets.
- Fig. 24a. Graphic representation of jet-pellet velocity differential vs. reduced C/M loading fixture angle.
- Fig. 24b. Graphic representation of jet-pellet velocity vs. reduced C/M loading fixture angle.
- Fig. 25. 30°, 0.020-in. wall thickness, hyperbolic liner.
- Fig. 26. Adapter plate for hyperbolic liners.
- Fig. 27. 30°, 0.030-in. wall thickness, hyperbolic liner.
- Fig. 28. 30°, 0.040-in. wall thickness, hyperbolic liner.
- Fig. 29. Loading fixture for 30° hyperbolic liners.
- Fig. 30. Radiographs of jet-pellets from 30° hyperbolic liners of various wall thicknesses.
- Fig. 31. 35°, 0.030-in. wall thickness, hyperbolic liner.
- Fig. 32. Loading fixture for 35° hyperbolic liners.
- Fig. 33. 40°, 0.010-in. wall thickness, hyperbolic liner.

- Fig. 34. Radiographs of jet-pellets from hyperbolic liners with various apex angles and wall thicknesses.
- Fig. 35. Bi-Explosive test assembly developed under NASA contract NAS1-6886.
- Fig. 36. 50°, 0.020-in. wall thickness (non-linear wall area variation) hyperbolic liner.
- Fig. 37. 5-inch bi-explosive charge test assembly.
- Fig. 38. Explosive loading procedure for 5-inch bi-explosive charge.
- Fig. 39. Flanged 90°, 0.030-in wall thickness, hyperbolic liner.
- Fig. 40. Radiographs of jet-pellets from 5-inch bi-explosive charges.
- Fig. 41. Radiographs of jet-pellets from annealed (1100-O) and unannealed (1100-F) aluminum hyperbolic liners.
- Fig. 42. Radiographs of jet-pellets from annealed (6061-O) and unannealed (6061-T6) aluminum hyperbolic liners.

FINAL REPORT

DEVELOPMENT OF METEOROID SIMULATORS FOR HYPERVELOCITY IMPACT STUDIES

SUMMARY

The main objective of this contract was to develop a series of shaped charge designs which would produce one gram aluminum jet-pellets with velocities ranging from 8 to 14 km/sec.

The tasks to be accomplished in achieving the above objective were listed in the contract as:

1. Inhibitor - Develop an inhibiting technique for controlling the length of the shaped charge jet to a length-to-diameter ratio (L/D) less than three. This task will be accomplished by modifying the base of the shaped charge liner or by applying other appropriate techniques.

2. Diverter - Develop a diverter charge which will divert the low velocity slug and other low velocity jet material from the path of the high velocity shaped charge jet-pellet.

3. Shaped Charge - Develop shaped charges that will produce jet-pellets with the following properties:

PROPERTIES	CHARGE TYPE		
	a	b	c
Material	aluminum	aluminum	aluminum
Approximate mass (gm)	1	1	1
Velocity (km/sec)	8 ± 1	11 ± 1	14 ± 1
L/D	$\frac{3}{3}$	$\frac{3}{3}$	$\frac{3}{3}$
Type jet	integral	integral	integral"

Under the task of Shaped Charge Development, it was planned to develop shaped charges based on two new shaped charge designs that had been developed by Firestone during meteoroid simulator development work conducted under NASA contracts NAS1-5212 and NAS1-6886. They are referred to as the "hyperbolic charge" and the "bi-explosive charge." The hyperbolic charge is designed such that both the shaped charge liner wall and the explosive charge cross-sectional area are controlled so as to produce a short integral jet-pellet. (Most shaped charge designs incorporate a conical liner that produces a long segmenting jet). The bi-explosive charge, which utilizes two explosives with different detonation rates, is designed to produce integral jets at

velocities in excess of 11 km/sec. It was explained in NASA Report CR-66615 that the convergent conical detonation waves produced by the bi-explosive charge are needed for the generation of high jet velocities from large angle liners and that the large angle liners are needed to circumvent a limitation on cohesive jet formation which occurs when high velocity jets are formed. This limitation is related to the sound velocity of the liner material, and it was shown that the velocity barrier could be circumvented by employing large angle liners.

For the program being reported it was planned to form one gram aluminum jet-pellets at velocities of 8 and 11 km/sec using the hyperbolic charge. Both experience and theory indicate that at jet velocities in the neighborhood of 12 km/sec, the aluminum jets will become radially unstable when generated by a conventional conically lined charge or by a hyperbolic charge. Therefore, the 14 km/sec jet-pellet was to be formed using a bi-explosive charge that would incorporate large angle liners.

Development work conducted on the 8 km/sec jet-pellet shaped charge design showed that the objective can be accomplished with a 60 degree hyperbolic liner. The last design tested produced a jet-pellet with a small velocity gradient (0.17 km/sec from tip to tail) and it was expected that a steady-state jet would be achieved by a slight modification in the charge configuration. However, work was terminated on the 8 km/sec design at this point in response to a request from NASA. It was desired to use the remaining funds on the 11 km/sec and 14 km/sec designs.

A shaped charge incorporating a 35° hyperbolic liner was developed which produced an integral jet-pellet at 11 km/sec. Development work was conducted on an inhibiting mechanism for this design which effected a reduction of the jet-pellet length such that the required maximum length-to-diameter ratio of 3 was obtained. Further development work will be necessary to increase the separation between the jet-pellet and the trailing low velocity debris.

A five-inch diameter bi-explosive shaped charge was designed, aimed at producing a 14 km/sec jet-pellet. The design incorporated a 90 degree hyperbolic liner. Jet-pellet velocities of 15.1 and 15.3 km/sec, which were greater than anticipated, were produced by this charge. These results demonstrated the effectiveness of the bi-explosive approach in obtaining high jet velocities from large angle liners (a jet tip velocity of about 7 km/sec would normally be obtained from a 90° aluminum liner in a conventional mono-explosive shaped charge). The jet-pellets exhibited some degree of radial instability, presumably due to the jets being formed under supercritical conditions (the liner wall flow velocity, V_2 exceeded the sonic velocity of aluminum). It is recommended that in any further development effort a 100° liner be

tested in the present bi-explosive charge. This will lower the jet velocity slightly, but should increase the jet stability. Another approach suggested is the use of a beryllium-aluminum alloy which has a high sonic velocity (10.4 km/sec compared to 2.79 km/sec for aluminum). This should permit the formation of radially stable jet-pellets by the 90° liner at velocities above 15 km/sec.

Under the task of Inhibitor, concurrent to the development of the 11 km/sec jet-pellet, a mechanism for controlling the length of the jet-pellet was developed.

It was found that by introducing a discontinuity into the shaped charge liner, a discontinuity in the subsequent jet results. Basically, the bar of material, from which the liner was to be machined, was separated into two pieces, then cemented together. The liner was machined from the bar of material so that the cemented joint was located at the desired position in the finished liner. This two piece liner assembly was referred to as a composite inhibited liner. This technique of inhibiting produces a clean separation in the jet-pellet and the length of the main jet can be adjusted by changing the position of the cemented joint.

Increasing the thickness of the liner wall near the base of the liner, referred to as skirting, was found to produce an inhibiting effect. It was found that when the extra liner material was added to the outside surface of the uninhibited liner design, the tail of the jet-pellet was less disturbed than when material was added to the inside surface of the liner.

Both of the mechanisms described were shown to be effective, however, more development is needed to obtain a greater degree of separation between the jet and the trailing material.

Under the task of Diverter, a new device was developed to destroy, instead of divert, the low velocity slug and other undesirable low velocity jet material. This device was referred to as the slug and debris trap. An auxiliary shaped charge liner was made to collapse around the slug and debris material, thus stopping it and in some cases propelling it in a direction opposite to that of the jet-pellet. The design was found to be very effective. The closing of the trap at the proper time and position behind the jet-pellet is controlled primarily by geometry. In one case simply putting two units in tandem resulted in improved effectiveness. The final design of a slug and debris trap unit must depend on the particular shaped charged design to which it will be assembled, since the jet-pellet velocity is different for each design.

The results of the project are very encouraging. It has been established that jet-pellets with velocities of 8, 11 and 15 km/sec can be produced. Furthermore, the ability to control the jet-pellet length and to isolate the jet-pellet from the following debris has been demonstrated. Further development work is required on the shaped charge systems to obtain refined final designs.

INTRODUCTION

The main objective of this contract was to develop a series of shaped charge designs which would produce one gram aluminum jet-pellets with velocities ranging from 8 to 14 km/sec. This would allow hypervelocity impact investigators to correlate shaped charge jet-pellet impact results with those from light gas guns at the lower velocity of 8 km/sec. Beyond this point it would provide the capability of obtaining data at the more significant higher velocities. The relationship between hypervelocity pellet energy and crater volume is, at this time, uncertain in the region above 10 km/sec due to lack of experimental data. The ability to generate these data should result in both a better theoretical model of the cratering process and a greater certainty in predicting damage to a given structure.

Firestone in collaboration with Ballistic Research Laboratories, Aberdeen Proving Ground, had conducted meteoritic simulator development work on three previous NASA contracts. These contracts were directed at developing a shaped charge meteoritic simulator which would accelerate a minimum of 2 grams of the materials nickel and iron to velocities in excess of 12 km/sec. The meteoritic simulators of known mass, density, velocity, and material composition were to be carried above the earth via rocket and then projected downward through the atmosphere. The light intensity from the reentering meteoritic simulator was to be recorded by photographic means and used to determine the luminous efficiency for each velocity level and material.

On contract NAS1-4187 (Ref. 1) an attempt was made to develop a 15 km/sec jet-pellet using a bi-metallic cylindrical liner. The bi-metal cylinder was composed of an inner cylinder of the material to be jetted and an outer cylinder of beryllium which was intended to effect a cohesive jet by modifying the jet formation process. Small quantities of jet material with velocities near 15 km/sec were produced; however, the jet material was not cohesive.

A second attempt was made to produce 15 km/sec nickel and iron jet-pellets on contract NAS1-5212 (Ref. 2). In this case the approach was to begin the development with small angle shaped

charge liners ($20^\circ - 30^\circ$) which would produce jet velocities of 10 to 11 km/sec. These designs would then be modified to increase the jet velocity. Using this approach, it was not possible to form cohesive jet material beyond 11 km/sec for nickel and 8.5 km/sec for 1020 steel. During the course of the work on contract NAS1-5212 a new shaped charge (called the hyperbolic design) was developed. Also, both the hyperbolic charge and a slightly modified version of a BRL shaped charge design were calibrated for mass and velocity of the jet-pellets (Ref. 3). Three of the hyperbolic designs, assembled with nickel liners, and three of the BRL designs, assembled with iron liners, were delivered to NASA for rocket reentry tests.

Work done on Contract NAS1-5212 had shown that an integral jet could be produced from a conical liner by keeping C/M nearly constant along the charge-liner axis. (The C/M is defined as the ratio of the explosive charge mass to the metal mass propelled by the explosive. In this application the ratio of the charge to liner cross-sectional areas, measured in a plane perpendicular to the charge-liner axis, is multiplied by the ratio of the explosive to liner material densities to obtain the C/M ratio.) Both the explosive charge area and the liner area were controlled for the design developed on contract NAS1-5212. It was required that C/M remain constant. This meant that both the charge and liner wall cross-sectional areas were required to remain constant at all points along the liner axis (so that their ratio would be constant).

It was found that when a liner with a conical exterior is required to have a constant cross-sectional area, the inside surface of the liner has to be hyperboloid (see Appendix A for the mathematical development). That is, it is generated by revolving a hyperbola about its axis of symmetry. Liners designed on this principle were referred to as hyperbolic liners. Similarly, when an explosive charge loaded around a shaped charge liner with conical exterior surface is required to have a constant cross-sectional area, the outside surface of the charge has to be hyperboloid (again, see Appendix A for the mathematical development). In this case, the surface is generated by revolving a segment of a hyperbola about a line perpendicular to its axis of symmetry.

In practice, the hyperbolic surface for the explosive was approximated by a conic surface which caused a relatively small variation in C/M. The resultant shaped charge design produced an integral jet. Thus, it was shown that an integral jet could be produced by controlling C/M. The entire jet (neglecting some non-steady state material) produced by this design was utilized for the meteoritic simulator; whereas, for a conventional conical design, only the jet tip, which is a small fraction of the total jet, could be utilized.

During work on contract NAS1-5212 and a subsequent contract NAS1-6886 (Ref. 4), it was found that the radial instability of the jet was related to the shaped charge liner cone angle. Furthermore, investigation of the shaped charge theory revealed that this angle effect was predictable if it was assumed that the liner material sound velocity was an important parameter in the jet formation process (see Appendix B). Specifically, based on the latter assumption, when the liner material flows into the stagnation point of the jet at supersonic velocity, a shock wave is formed and jet instability problems begin.

Under contract NAS1-6886, based on this observation, a series of shaped charge tests were conducted where large angle liners were evaluated in specially designed shaped charges. It was found that the concept of employing large angle liners for the production of cohesive jets was a valid one. For the first time cohesive nickel and iron jet material was observed at velocities in the neighborhood of 12 km/sec.

In order to produce high velocity jet material from large angle liners another problem had to be overcome. That is, in general as the liner cone angle is increased the jet velocity decreases. Therefore, a way had to be found for delivering more energy to the shaped charge jet. This problem was solved by developing a bi-explosive charge which produced a convergent conical detonation wave. The bi-explosive charge, which utilizes two explosives with different detonation rates, delivers more energy to the shaped charge jet because of a higher effective detonation rate (u_d) and because of a smaller angle (θ) between detonation front and the liner wall (Appendix C).

The tasks to be accomplished in achieving the objectives of the program being reported were as follows:

- a. Develop an inhibiting technique for controlling the shaped charge jet length by modifying the base of the shaped charge liner.
- b. Develop a diverter charge which will isolate the shaped charge jet-pellet from the slug and other low velocity jet material.
- c. Develop a series of shaped charge designs which will produce aluminum jet-pellets with masses of one gram and velocities of 8, 11, and 14 km/sec.

Under the task of Shaped Charge Development, it was planned to form one gram aluminum jet-pellets at velocities of 8 and 11 km/sec using hyperbolic designs. Both experience and theory indicated that at jet velocities in the neighborhood of

12 km/sec, the aluminum jets would become radially unstable when generated by a conventional conically lined charge or by a hyperbolic charge. Therefore, the 14 km/sec jet-pellet was to be formed using a bi-explosive charge that would incorporate large angle liners.

In order to minimize uncontrolled parameters, all of the hardware made for this program were 100% inspected to assure quality.

TEST FACILITY

All design testing was done at the Defense Research Division test facility at Ravenna Army Ammunition Plant. The test site used to study the experimental shaped charge designs is referred to as the Open Test Site. The Open Test Site, shown schematically in Fig. 1, was used to examine jet formation and jet integrity at distances up to 30-inches from the base of the test charge. All testing was done in air (i.e., atmospheric pressure).

At the Open Test Site the charges were placed 8 to 12-inches in front of blast-resistant cassettes (protective film holders used to cushion film from the shock of the explosive detonation). The upper cassette was used to radiograph the collapse process of the liner and the resultant jet formation. It was also used to radiograph the jet-pellet at distances of about 2 to 4-inches from the base of the test charge. A second "window" in the upper cassette permitted a radiograph of the jet-pellet at approximately 10-inches of travel. The second cassette (below the first one) was used to radiograph the jet-pellet at 25 to 30-inches of travel. Figure 2 presents a block diagram of the electronic equipment used. Field E mission Corp Model 233 X-ray pulsers (maximum voltage 300 KV) were used for the radiography. Times used to determine the velocity were recorded using Beckman Model 7270 digital read out counters (triggered to start during the initiation of the tetryl booster and to stop by current viewing resistors mounted on the face of the X-ray pulsers).

TEST RESULTS AND DISCUSSION

Slug And Debris Trap Development

At the start of the contract this development was referred to as the Diverter Charge Development. The purpose of this program was to develop a mechanism which would isolate the jet-pellet from the slug and other low velocity jet material which normally follows the jet-pellet. This can be accomplished by pro-

PELLING the unwanted material off the jet-pellet trajectory using an asymmetric auxiliary charge, as has been done by the Ballistic Research Laboratories, Aberdeen Proving Ground. Another possible technique would be to collapse an auxiliary shaped charge liner around the slug and debris material, thus stopping it and possibly propelling it in a direction opposite to that of the jet-pellet. A test assembly with a slug and debris trap is shown in Fig. 3.

It was decided to evaluate the latter approach first because if it proved successful it would destroy the slug and debris rather than change its trajectory a few degrees. Tests were conducted to evaluate the effectiveness of the slug and debris trap concept. For most of these tests, 40° hyperbolic charges were used. Figure 3 shows the 40° hyperbolic liner. Figure 4 shows the basic explosive loading sequence for a hyperbolic charge. The twelve holes through the flange portion of the hyperbolic liner, (Fig. 4), were cast with 65/35 octol explosive during the casting of the hyperbolic shaped charge, (Figs. 5 and 6). These twelve holes provided initiation sources for the slug and debris trap.

One inch diameter aperture slug and debris trap. - The basic explosive loading sequence for the 1.0-inch diameter aperture slug and debris trap charge is shown in Fig. 7. The test assembly used 42°, 0.100-inch wall thickness, aluminum trap liners with a 1.0-inch aperture diameter, see Fig. 8. The complete test assembly is shown in Fig. 3. and in Fig. 3.

A radiographic study of the functioning of the basic slug and debris trap was conducted. Since uninhibited 40° hyperbolic liners were used, a heavy burden was placed on the slug and debris trap because in addition to the slug, there was a large amount of trailing jet material to impact the trap liner. A composite view of the functioning of the basic slug and debris trap is shown in Fig. 9. Table I presents the test data for the test shots shown in Fig. 9 (FTR DRD Rnd. Nos.: 1028-2, 1028-4, 1028-6) as well as a summary of all of the slug and debris trap tests. The following comments refer to Fig. 9:

(1.) At $t=31$ microseconds (after initiation of the hyperbolic shaped charge), the trap liner can be seen as a football shape in the upper portion of the radiograph. (Because of poor contrast in the original radiograph, white dots have been used to indicate the observed contour of the trap liner.) The bottom of the trap had just closed and entrapped the trailing jet and slug.

(2.) At $t=41$ microseconds, the trailing jet was impacting the bottom part of the trap liner. The resulting impact was of the hypervelocity type which reduced the trailing jet and a portion of the trap liner to a cloud of very fine particles that were dispersing radially.

(3.) At $t=83$ microseconds, the slug had entered the trap liner and was being impacted at its lower end. This impact would also reduce the undesired trailing debris, in this case the slug, to a dust like form.

Apparently the trap liner did not completely consume the slug because a piece of slug (approximately 3/8-inch long) was recovered from one of the test shots. After every test shot, the trap liner residue was recovered in one piece. In all but one case, the trap liner residue displayed no impact damage, indicating that it had a resultant velocity near zero. In one case, the residue trap liner had impacted the target at low velocity.

Following this basic function study other radiographic tests were fired to evaluate variations of the slug and debris trap liner design. Both thicker and thinner wall aluminum liners were tested (FTR DRD Rnd. Nos. 1028-3, and 1028-8 and 1037-8, respectively). Variation of the wall thickness was found to permit fine adjustment of the time of closure of the aperture.

From these tests, it was determined that the closure time of even the 0.050-inch wall aluminum, 1.0-inch diameter aperture trap would be too late for an 11 km/sec jet-pellet with L/D less than 3. Therefore, one more design was tested with the 1.0-inch diameter aperture trap charge. In this test the trap liner was removed after the explosive cast had been made. This design would use the high density gasses from the detonating high explosive charge to impact the slug and debris. The unlined trap, FTR DRD Rnd. No. 1028-7, closed slightly earlier than the 0.050-inch wall aluminum trap liner but not early enough for an 11 km/sec jet-pellet with L/D less than 3.

In addition to the tests of closure time, just discussed, two other variations were tested. In one test a trap liner was removed from a cast trap charge and sectioned into two pieces. Then one half of the trap liner was inserted in the trap charge. Upon firing this test, FTR DRD Rnd. No. 1028-5, it was evident that this design was not as effective as the full trap liner designs.

It had been observed in the unlined trap tests that the high density gasses of the unlined trap design were effective against the trailing jet, but not very effective against the slug. Therefore, two trap liners were removed from trap charges and cut into two pieces. The upper half of each liner was inserted in each trap charge. This lined portion was to act on the slug while the high density gasses would act on the trailing jet material. Upon firing these tests, FTR DRD Rnd. Nos. 1037-6 and 9, it was found that the design did function well.

The evaluation of the 1.0-inch aperture trap liner designs showed the 0.100-inch wall thickness aluminum trap liner to be most effective in destroying the trailing jet material. None of the liner designs tested were successful in completely destroying the slug. Although the closure time for the 1-inch dia-

meter aperture was not early enough for an 11 km/sec jet-pellet with L/D less than 3, it should be very close to the time required for an 8 km/sec jet-pellet with L/D less than 3.

One-half inch diameter aperture slug and debris trap. - The second design of the slug and debris trap (Fig. 10) had a 1/2-inch aperture diameter. This smaller aperture permitted earlier closure of the trap. The basic explosive loading sequence for the 1/2-inch slug and debris trap is shown in Fig. 11. Full trap liners of 0.100-inch wall aluminum and 0.030-inch wall copper were tested (FTR DRD Rnd. Nos. 1028-10, 1028-9 and 1057-2 Table I). It was found that the closure time was approximately the time required for an 11 km/sec jet-pellet with L/D less than 3. The aluminum liner was found to be slightly more effective than the copper liner in destroying the trailing jet.

One other variation in trap design was tested. Two trap charges were assembled, one above the other, to provide double trapping. The trap charges used were the only ones remaining and were not chosen for optimum effect. The results of the test shot, FTR DRD Rnd. No. 1057-3, can be seen in Fig. 12 and Table I. The double trap assembly stopped all of the trailing jet as was evidenced by the lack of secondary impacts in the aluminum target crater. Unfortunately the inhibiting system used on the hyperbolic liner did not effectively separate the jet-pellet from the trailing jet and the trap liner shocked the jet-pellet. But, even with these non-ideal conditions, the typical crater formed by hypervelocity impact demonstrated the feasibility of the slug and debris trap concept.

Inhibitor Development

The function of an inhibitor is to control the L/D (length-to-diameter) ratio of the jet-pellet and to stop the jetting process at a predetermined stage of liner collapse.

Composite liner inhibiting. - A mechanism was devised for controlling the length of a steady-state shaped charge jet. It consists of introducing a discontinuity into the shaped charge liner which results in a discontinuity in the subsequent jet which is formed. The discontinuity was introduced into the bar of material from which the liner was machined. Basically, the bar of material was separated into two pieces and then cemented together with Loctite 307 adhesive and baked at 200° F for 30 minutes. Then the liner was machined from the bar of material so that the cemented joint was located at the desired position in the finished liner.

This two piece liner assembly was referred to as a composite inhibited liner. The basic testing of this form of

inhibiting was done with 40° hyperbolic liners, Fig. 4. Four variations in liner separation were tested in a radiographic study. The results can be seen in Fig. 13 and Table II, FTR DRD Rnd. Nos. 1034-1 through 5 inclusive. The angle used for Design 2 was chosen by using the steady-state collapse theory to predict the direction of motion of the liner inner surface. The angle for Design 3 was chosen as a mirror of the angle for Design 2. The most interesting result of the tests was the lack of difference in the shape of the zone of separation in the jet-pellets from the four different designs. Although some sort of difference was expected, no appreciable difference was observed. Therefore, the design chosen for further testing was Design 4, since it afforded manufacturing advantages over the other designs.

Although the separation in the liner resulted in a reasonably clean separation in the jet-pellet, the rate of separation was too slow to provide adequate separation to permit a slug and debris trap to function and destroy the rear segment and trailing jet without affecting the main pellet. Therefore, the liner needed some device such as a skirt to further reduce the velocity of the rear segment of jet-pellet or prevent its formation.

Skirted liner inhibiting. - Three basic skirted liner designs were tested using 30° hyperbolic liners. The basic uninhibited 30° hyperbolic liner is shown in Fig. 14. The three forms of skirting were: internal, Fig. 15; external, Fig. 16; internal and external, Fig. 17. The radiographs shown in Fig. 18 present the effect of each of the three inhibitor designs tested. Although the two designs using internal skirting reduced the trailing jet more than the externally skirted design, they also damaged the rear of the jet-pellet more severely. Table II presents the basic data for these skirted inhibitor tests (FTR DRD Rnd. Nos.: 1036-1, 1037-3, 1037-4 (1029-1 is listed in Table IV)).

In addition to the above tests of these three skirted liners, two liners of each type were assembled from two pieces of metal (Design 1 composite inhibiting) to test the interaction of the skirting and the liner separation. The cemented joint was located 1.4-inches from the bottom of the flanged liner surface, 0.5-inch above the skirting. The test results appear in Table II (FTR DRD Rnd. Nos.: 1036-2, 1037-5 through 8, inclusive). The internally skirted designs did not exhibit any effect on the separation. The externally skirted design produced a two piece jet-pellet, but the trailing portion was not traveling at a greatly reduced velocity as was required.

Combined composite - skirted liner inhibiting. - From the above inhibitor tests, it appeared that an externally skirted

liner assembled from two pieces of metal with the cemented joint located at the top edge of the skirting might provide the inhibiting desired. Figure 19 shows the inhibited liner design tested next. The radiographs shown in Fig. 20 present the results and the basic test data is shown in Table II (FTR DRD Rnd. Nos.: 1057-1 through 3 inclusive). The jet-pellet formed in round 1057-1 had been shortened to the desired L/D ratio, but there was no improvement in the separation rate of the trailing jet. The other two test shots with this type of liner used slug and debris trap assemblies. They indicated that the trap closure time was slightly early for this test assembly since both jet-pellets were shocked by the slug and debris trap liners.

No further inhibiting tests were conducted under this contract. Suggestions for new designs to be tested are discussed later in this report.

8 km/sec Jet-Pellet Development

The 60°, 0.030-inch wall thickness, hyperbolic liner used in the 8 km/sec testing is shown in Fig. 21. Two loading fixtures were designed to determine the magnitude of C/M needed to produce an 8 km/sec jet-pellet. One loading fixture was referred to as an 18° standard C/M and the other was referred to as a 19° reduced C/M loading fixture.

Standard C/M testing. - The jet-pellet produced by the 18° standard C/M loading fixture, using comp. B explosive, is shown in Fig. 22 and the basic test data are presented in Table III (FTR DRD Rnd. Nos.: 1040-1 and 1040-3). The jet-pellets were cohesive and stable, but had velocities of 8.66 and 8.48 km/sec. Except that the velocity exceeded the desired 8 km/sec, the jet-pellet was a good candidate for inhibiting tests.

Reduced C/M testing. - The jet-pellet produced by the 19° reduced C/M loading fixture, using comp. B explosive, is shown in Fig. 23 and the basic test data are presented in Table III (FTR DRD Rnd. No. 1040-2). The jet-pellet was cohesive, but exhibited a tip-to-tail velocity differential of 0.37 km/sec and segmented into four pieces. The jet-pellet overall velocity was 8.26 km/sec, closer to the 8 km/sec objective. Two new reduced C/M loading fixtures were designed in an attempt to reduce the velocity gradient in the reduced C/M jet-pellet. The new loading fixtures had loading fixture angle (ϕ) values of 20° and 21°. The resulting jet-pellets are included in Fig. 24 and the basic test data is presented in Table III (FTR DRD Rnd. Nos.: 1040-4 and 1040-5). As the loading fixture angle (ϕ) was increased from 19° to 21°, the jet-pellet tip-to-tail velocity differential decreased from 0.37 km/sec to 0.17 km/sec. The 0.17 km/sec

velocity difference broke the jet-pellet into two pieces. By graphically presenting the test data (Fig. 24) it appears that a stable jet-pellet would be produced by a reduced C/M loading fixture with loading fixture angle (ϕ) of 22.7°. The jet-pellet velocity would be approximately 7.7 km/sec. No further 8 km/sec jet-pellet tests were conducted under this contract in response to a request from NASA. The contract funds were to be conserved and directed toward the other development efforts.

11 km/sec Jet-Pellet Development

In previous meteoritic simulator development contracts the liner material was either nickel or iron and the hyperbolic liners were assembled with an aluminum adapter plate (flange). Since the liner material used in this contract was aluminum, it was decided to make the liner and flange in one piece, thereby simplifying the manufacture of the liner. One test shot (FTR DRD Rnd. No. 1028-1) was fired to verify that no change in jet-pellet character would be effected by the change in liner design. The basic test data are shown in Table IV. The jet-pellet was normal and of excellent integrity. Therefore, it was determined that either type of flange, cemented or integral, was satisfactory.

Liner wall thickness effect. - A radiographic study of the effect of liner wall thickness on the jet-pellet from the 30° hyperbolic liner was made. The liner wall thickness was tested in the following three values:

(1) 0.020-in. - Fig. 25, which used an aluminum adapter plate, Fig. 26 (FTR DRD Rnd. Nos. 1029-2 and 4 in Table IV)

(2) 0.030-in. - Fig. 27, which used an aluminum adapter plate, Fig. 26 (FTR DRD Rnd. Nos. 1029-1 and 3 in Table IV) note - this liner assembly is equivalent to flanged liner DRB-23-2404, Fig. 14

(3) 0.040-in. - Fig. 28, which had an integral flange (FTR DRD Rnd. Nos. 1048-1 and 2 in Table IV)

The loading fixture used is shown in Fig. 29. Typical radiographs are shown in Fig. 30. The 0.020-in. wall thickness hyperbolic liner produced a jet-pellet with a velocity of 11.32 km/sec but with marginal stability evident at 24 inches of travel. The 0.030-in. wall thickness hyperbolic liner produced a jet-pellet with a velocity of 11.07 km/sec which still exhibited some characteristics of marginal radial stability. At 95-inches travel the pellet was almost completely destroyed. The 0.040-in. wall thickness hyperbolic liner produced a jet-pellet with a velocity of 10.77 km/sec which was radially stable.

Liner angle effect. - It was decided that additional possible designs for an 11 km/sec jet-pellet should be studied. Up to this point, the liners tested had 30° apex angles. The following two angle and wall thickness variations in hyperbolic liners were tested:

(1) 0.030-in. wall, 35°, Fig. 31 (FTR DRD Rnd. Nos. 1046-1 and 2) The loading fixture used is shown in Fig. 32

(2) 0.010-in. wall, 40°, Fig. 33, which used an aluminum adapter plate, Fig. 26 (FTR DRD Rnd. Nos. 1043-1 and 2)

The 0.010-in. wall, 40° hyperbolic liner definitely violated the wall thickness lower limit established above, but was necessary to keep the jet-pellet velocity at about 11 km/sec. The results of the radiographic study can be seen in Fig. 34 and Table IV (FTR DRD Rnd. Nos. 1046-1 and 2, and 1043-1 and 2). The jet-pellet velocity for the 35°, 0.030-in. wall thickness design was 10.70 km/sec and the jet-pellet integrity was excellent. The 40°, 0.010-in. wall thickness design produced jet-pellets with velocities of 11.13 and 11.28 km/sec which were slightly radially unstable. The larger angle of the 40° liner tended to make the jet-pellet cohesive, but the wall thickness effect was strong enough to make the overall resultant jet-pellet integrity unsatisfactory.

14 km/sec Jet-Pellet Development

In order to accelerate a shaped charge jet-pellet to a velocity of 14 km/sec with the available explosives, it appears that either a cylindrical liner (tubular liner) or a waveshaped charge must be employed. Cylindrical liners produce very little jet and in general the jet formed is not cohesive. Under NASA contract NAS1-6886 (Ref. 1) Firestone developed a charge referred to as a bi-explosive charge, which is a waveshaped charge.

The functioning of these charges depended upon the use of two explosives with different detonation rates and an inert waveshaper (detonation barrier). These charges produced a converging conical detonation wave, causing the effective detonation rate to be constant as the detonation wave swept the liner. A conical detonation wave was required because the general approach to obtaining a cohesive 14 km/sec jet-pellet included the use of large angle liners (80° to 100°) and the principal way known to obtain high jet-pellet velocities from the large angle liners was to increase the effective detonation rate of the explosive charge.

The angle between the conical detonation wave and the liner is referred to as the theta (θ) angle. For a given explosive

in contact with the liner, the greatest jet-pellet velocity should occur for the condition where the theta angle is zero. A brief discussion of basic design equations is presented in Appendix C. A detailed discussion of the design of the bi-explosive charge was published in the Final Report for NASA Contract NAS1-6886 (Ref. 1).

Preliminary bi-explosive tests. - Four preliminary test shots using aluminum liners in bi-explosive charges were fired. The bi-explosive design used was one of the designs developed under Contract NAS1-6886. The basic test assembly is shown in Fig. 35. The test charges were loaded with 60/40 comp. B and 65/35 octol explosives and used the 43° polyurethane waveshaper (DRB-23-2542) developed for this charge. One 60° (similar to DRC-23-2418-1, Fig. 21) and three 50°, DRB-23-2544, (Fig. 36) aluminum hyperbolic liners were tested. The test results are shown in Table V. The jet-pellets were not expected to be stable. The item of main interest was the velocity obtained. In every test the velocity was greater than expected. This indicated that the velocity of the jet-pellets obtained from a newly designed bi-explosive charge could easily be in the range of 13 to 14 km/sec.

New bi-explosive design tests. - A new bi-explosive charge was designed and necessary loading hardware was manufactured. The new bi-explosive design employed many design improvements over the design shown in Fig. 35. The liner register surface was modified to better locate and secure the liner. A new, filled, aluminum waveshaper was designed to improve the explosive casts produced. The method of manufacturing the new loading fixtures provided a better match of the innerface of the inner and outer explosive charges. The basic test assembly is shown in Fig. 37. The loading sequence is shown in Fig. 38. Three 90°, 0.030-in. wall thickness hyperbolic liners were tested in this new charge. The 90° hyperbolic liner is shown in Fig. 39. With a 90° liner and 60/40 comp. B - 65/35 octol explosives, it was estimated that the new bi-explosive design would produce a conical detonation front with a theta angle of 5°.

Comp. B - octol charges: Two of the 90° hyperbolic liners were loaded with 60/40 comp. B and 65/35 octol explosives. One used a steel end plate (FTR DRD Rnd. No. 1056-1) and the other used an aluminum end plate (FTR DRD Rnd. No. 1056-3). The test results are presented in Fig. 40 and Table VI. The jet-pellet from the charge using an aluminum end plate had a velocity of 15.3 km/sec, but was stretching lengthwise very rapidly. The jet-pellet from the charge using a steel end plate had a velocity of 15.1 km/sec, but was shocked and expanding radially. In both cases, the jet-pellet velocity was well above the design velocity of 13 - 14 km/sec for the 90° hyperbolic liner. Since the velocity was greater than expected, the jet-pellet integrity

suffered due to the concomitant increase in flow rate of the liner wall into the jet formation point. Although the jet-pellets were not stable, the velocity obtained shows the potential of the bi-explosive charge for producing high velocity jet-pellets.

It should be noted that the appearance of the jet-pellets in Fig. 40 has been affected by poor contrast in the radiographic negatives which resulted from problems in film development.

Pentolite - comp. B charge: One of the 90° hyperbolic liners was loaded with 50/50 pentolite and 60/40 comp. B explosives in an attempt to obtain a slower jet-pellet than was obtained with the comp. B-octol explosive charge. An aluminum end plate was used (FTR DRD Rnd. No. 1056-2). The test results are presented in Fig. 40 and Table VI. The jet-pellet had a velocity of 11.6 km/sec. Although the jet-pellet velocity was below the design velocity, which should have improved the jet-pellet integrity, the jet-pellet was radially unstable. The poor stability of the jet-pellet was attributed to the quality of the charge. The 50/50 pentolite had a much higher casting shrinkage factor than the 60/40 comp. B. This high shrinkage factor produced a poor fit between the inner and outer charges and also introduced considerable porosity in the pentolite charge that was not present in the comp. B charge.

Aluminum Material Study

Two types of aluminum were considered for use in making liners of this contract. The two types of aluminum were, 1100, and 6061. The basic testing was done with 30° and 40°, 0.030-in. wall thickness hyperbolic liners.

1100 aluminum. - Commercially pure aluminum, 1100-F was used for the basic bar stock for making liners for this contract. The 1100-F, as received aluminum was compared with 1100-O, annealed, aluminum. The test results are presented in Fig. 41 and Table IV (FTR DRD Rnd. Nos. 1037-2 and 1029-1). As can be seen in Fig. 41 the unannealed aluminum had a tendency to produce a very poor jet-pellet. This tendency was not always evident as was demonstrated in two other test shots: FTR DRD Rnd. No. 1037-1, see Table II; FTR DRD Rnd. No. 1040-3, see Table III. In comparison, the 1100-O, annealed, aluminum consistently performed well. A typical example is shown in Fig. 41 (FTR DRD Rnd. No. 1029-1).

6061 aluminum. - One aluminum alloy was chosen to be evaluated as a potential liner material. The 6061 alloy of aluminum was chosen for its good machining characteristics and its constituent metals. The 6061-T6 aluminum was compared with 6061-O,

annealed, aluminum. The test results are presented in Fig. 42 and Table IV (FTR DRD Rnd. Nos. 1041-1 and 2). As can be seen in Fig. 42, the unannealed aluminum alloy, i.e., the T6 tempered aluminum, produced a jet-pellet of very poor integrity. Although the annealed 6061 aluminum produced a slightly better jet-pellet than the 6061-T6 aluminum, neither produced a jet-pellet of satisfactory integrity. The 1100-0 aluminum was therefore found to be the most suitable for manufacturing hyperbolic liners for this contract.

CONCLUSIONS

Significant advancements were made in the field of meteoroid simulation by shaped charges during the course of this project. Mechanisms were developed for both controlling the length of the jet-pellets and for isolating them from trailing low velocity debris. Shaped charges were designed which produced jet velocities in the range desired. The most important result was the formation of a relatively massive jet (about one gram) at a velocity in excess of 15 km/sec.

Further development is needed on each of the three designs which were the goals of this project. The amount of additional effort to complete the 11 km/sec design appears to be minimal.

The following is a summary of the results achieved during the course of this project.

Slug and Debris Trap Development

1. The feasibility of the slug and debris trap liner has been demonstrated.
2. The 0.100-inch wall thickness aluminum trap liner was found to be more effective than a .050-inch thickness or no trap liner in destroying the slug and debris.
3. Fine adjustment of closure time can be made by varying the slug and debris trap liner wall thickness.
4. The one inch aperture slug and debris trap, see Figs. 7 and 8, was found to have approximately the required closure time for use with an 8 km/sec jet-pellet.
5. The one-half inch aperture slug and debris trap (Fig. 11) was found to have approximately the required closure time for use with an 11 km/sec jet-pellet.
6. Double trap assemblies (one trap assembly immediately followed by another trap assembly) were found to be most effective in destroying the slug and debris.

Inhibitor Development

1. Composite liner inhibiting has been shown to be an effective method of controlling jet-pellet length.

2. The design 4 composite liner assembly was found to be the most satisfactory of the four composite designs tested.

3. External skirting was found to be preferable to internal skirting for inhibiting purposes.

8 km/sec Jet-Pellet Development

1. A reduced C/M 60/40 comp. B hyperbolic charge design, with a phi angle of approximately 22.7° , should produce a stable jet-pellet with a velocity of approximately 7.7 km/sec from a 60° , 0.030-in. wall thickness hyperbolic liner.

2. A standard C/M 60/40 comp. B hyperbolic charge design, with a phi angle of 18° , produces a stable jet-pellet with a velocity of approximately 8.5 km/sec from a 60° , 0.030-in. wall thickness hyperbolic liner.

11 km/sec Jet-Pellet Development

1. A 35° , 0.030-in. wall hyperbolic liner (Fig. 31) in a 65/35 octol hyperbolic charge produces a stable jet-pellet with a velocity of 10.7 km/sec.

14 km/sec Jet-Pellet Development

1. The new bi-explosive design, (Fig. 37) produces a jet-pellet with a velocity of approximately 15 km/sec using a 90° , 0.030-in. wall thickness hyperbolic liner.

2. The end plate material used on the test assembly affects the longitudinal stability of the jet-pellet produced.

Aluminum Material Study

1. The most suitable form of aluminum of the four forms tested for manufacture of hyperbolic liners is 1100-O. This was found to be better than 1100-F, 6061-O, or 6061-T6 aluminum.

RECOMMENDATIONS

The results of this project indicate that it is possible to form integral, one gram aluminum jet-pellets with velocities of 8 and 11 km/sec and that it may be possible to form integral, one gram aluminum jet-pellets with a velocity in the neighborhood of 14 km/sec. It is recommended that to achieve these goals in further development, the following approaches be taken.

Slug And Debris Trap Development

Double slug and debris traps should be incorporated into future designs. If it is not possible to obtain enough separation between the jet-pellet and the trailing jet material to permit the slug and debris trap to destroy all the trailing jet material, a slower closing slug and debris trap could be employed and an additional trap charge located about 24-in. from the hyperbolic liner could be added. The additional trap charge would be detonated after a predetermined delay allowed the jet-pellet to pass through. This arrangement would permit more time for the jet-pellet to separate from the trailing jet material.

Inhibitor Development

The skirted portion of the liner shown in Fig. 19 could be made of a different metal, such as Meehanite, Grade GE. This change in metal should produce a greater separation between the jet-pellet and the trailing jet material.

Another possible approach would involve a two angle liner. The liner would be similar to that shown in Fig. 19 but while the outside contour would be retained, the inside contour would change from the cemented joint toward the flange end. The skirted portion would be hollowed out so that the wall thickness, measured normal to the outside liner surface, would be constant at about 0.050-in. This design would force the lower liner portion to travel farther before reaching the central axis to produce jet. The delay in the jet formation for the lower portion should produce a greater separation between the jet-pellet and the trailing jet material.

8 km/sec Jet-Pellet Development

A reduced C/M loading fixture with a phi angle of approximately 22.7° should be made. Using this loading fixture with a 60° , 0.030-in. wall thickness, 1100-0 aluminum hyperbolic liner and 60/40 comp. B explosive charge, a stable jet-pellet should be obtained. This design would then require refinement of the inhibiting and slug and debris trap designs.

11 km/sec Jet-Pellet Development

A suitable inhibitor mechanism should be applied to the basic 35°, 0.030-in. wall thickness, 1100-O aluminum hyperbolic liner. Combining this inhibited liner with a suitable slug and debris trap assembly should produce the one gram, 10.7 km/sec jet-pellet required.

14 km/sec Jet-Pellet Development

A 100°, 0.030-in. wall thickness, 1100-O aluminum hyperbolic liner should be tested in the newly developed bi-explosive charge. This should reduce the jet-pellet velocity enough to produce a more cohesive jet-pellet.

Another bi-explosive charge could be designed which would exhibit a lower effective detonation rate thus producing a slower jet-pellet from the 90°, 0.030-in. wall thickness hyperbolic liner. By reducing the jet-pellet velocity, a more cohesive jet-pellet should be obtained.

A 90°, 0.030-in. wall thickness, beryllium-aluminum alloy hyperbolic liner should be tested in the existing bi-explosive charge. The beryllium-aluminum alloy has a very high sound velocity which should result in a cohesive jet-pellet with a velocity in excess of 15 km/sec.

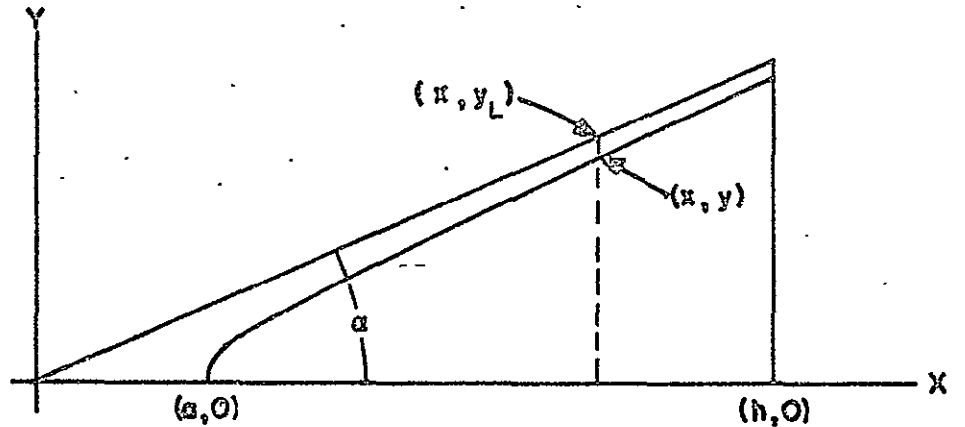
The thickness and material of the end plate should be evaluated as a means to control longitudinal stability of jet-pellets from these bi-explosive charges.

APPENDIX A

DEVELOPMENT OF DESIGN CRITERION FOR CONSTANT CROSS-SECTIONAL AREA LINER AND CONSTANT CROSS-SECTIONAL AREA EXPLOSIVE CHARGE

Determination of the curve which will generate a surface inside a conical liner such that the cross-sectional area will remain constant along the liner axis:

The lines which will generate the conical surface and the interior surface in the x, y plane can be shown as:



Let it be required that the cross-sectional area between the surfaces be a constant, A_L , from $x = a$ to $x = h$

$$\pi (y_L^2 - y^2) = A_L \quad (1)$$

but

$$y_L = mx \quad \text{where } m = \tan \alpha \quad (2)$$

thus

$$\pi [(mx)^2 - y^2] = A_L \quad (3)$$

or

$$\frac{x^2}{A_L/\pi m^2} - \frac{y^2}{A_L/\pi} = 1 \quad (4)$$

since m is a constant and we require that A_L be a constant, we can let

$$a^2 = A_L / \pi m^2 \quad (5)$$

$$b^2 = A_L / \pi \quad (6)$$

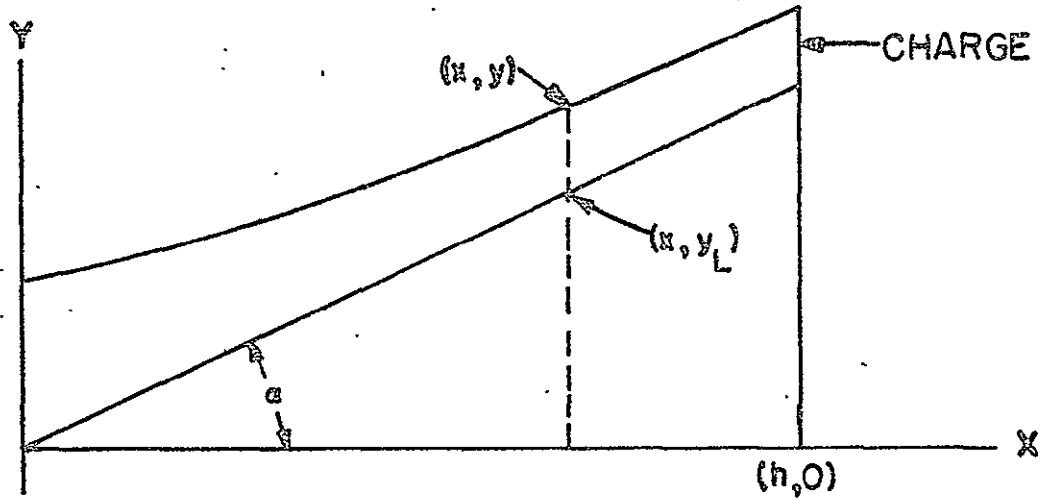
thus

$$\frac{x^2}{a^2} - \frac{y^2}{b^2} = 1 \quad (7)$$

which is a hyperbola, symmetric about the x axis and open in the positive x direction.

Determination of the curve which will generate a surface outside a conical liner such that the cross-sectional area will remain constant along the liner axis:

The lines which will generate the conical surface and the exterior surface in the x, y plane can be shown as:



Let it be required that the cross-sectional between the two surfaces be a constant, A_c , from $x = 0$ to $x = h$

$$\pi(y^2 - y_L^2) = A_c \quad (8)$$

but $y_L = mx$ where $m = \tan \alpha$ (9)

thus $\pi [y^2 - (mx)^2] = A_c$ (10)

or $\frac{y^2}{A_c/\pi} - \frac{x^2}{A_c/\pi m^2} = 1$ (11)

since m is constant and we require that A_c be a constant we can let

$$a^2 = A_c / \pi m^2 \quad (12)$$

$$b^2 = A_c / \pi \quad (13)$$

thus
$$\frac{y^2}{b^2} - \frac{x^2}{a^2} = 1 \quad (14)$$

which is a hyperbola, symmetric about the y axis and open in the positive y direction.

APPENDIX B

ANALYSIS OF SHAPED CHARGE JETTING PROCESS USING THE STEADY-STATE THEORY

Results of tests conducted with various shaped charge designs have indicated that for a given shaped charge liner cone angle and liner material there is an upper limit to the jet velocity beyond which the jet material becomes progressively less cohesive as the jet velocity is increased (by using more energetic explosive, thinning the liner wall, etc.). This phenomenon can be explained by the existing steady-state shaped charge theory if it is accepted that the sound velocity of the liner material is an important limiting parameter.

Consider the steady-state shaped charge process as shown in Fig. B-1. The figure, based on the shaped charge theory developed by Birkhoff et. al. (Ref. 5), shows the relationships between the shaped charge variables from the point of view of a laboratory coordinate system (Fig. B-1a) and from the point of view of a coordinate system moving with velocity V_1 (Fig. B-1b). The velocity of the liner wall, V_2 , flowing into the stagnation point, relative to the moving coordinate system, is the object of this analysis. This velocity has been considered by shaped charge investigators such as Eichelburger (Ref. 6) and Walsh et. al., (Ref. 7) to be critical in the sense that when it exceeds the sound velocity in the liner material, shock waves appear in the region of the stagnation point. Furthermore, if V_2 is sufficiently high the shock waves occur right at the stagnation point and prevent a jet from being formed.

In order to find how V_2 varies as a function of other shaped charge parameters, consider the following set of relationships provided by the steady-state charge theory

$$V_J = V_o \frac{\cos(\alpha/2)}{\sin(\beta/2)} \quad (15)$$

where. V_J = Jet velocity
 V_o = Collapse velocity of liner material
 α = Half angle of conical liner
 β = Collapse angle of liner material

$$\beta = 2 \sin^{-1} \frac{V_o \cos \alpha}{2 U_d} + \alpha \quad (16)$$

where U_d = Detonation rate of explosive

$$V_1 = V_o \frac{\cos 1/2 (\beta - \alpha)}{\sin \beta} \quad (17)$$

where V_1 = Stagnation point velocity

$$V_2 = V_J - V_1 \quad (18)$$

where V_2 = Liner wall flow velocity relative to moving coordinate system

It can be shown that the above equations can be solved to give the following relationship

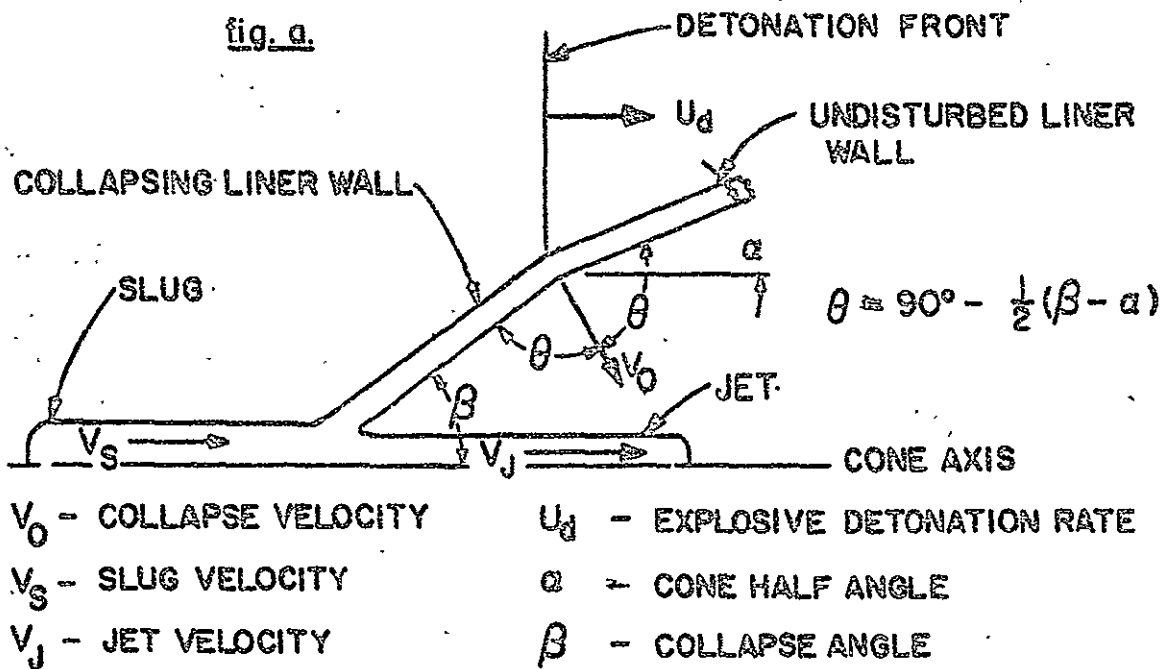
$$V_2 = \frac{V_J}{2} \left[1 - \frac{\tan \alpha/2}{\cot(\alpha/2) - \frac{V_J}{U_d} \cot \alpha} \right] \quad (19)$$

where V_2 is the velocity under discussion and V_J , α and U_d are the jet² velocity, cone half angle and explosive detonation rate, respectively. It is seen that in this form the jet velocity is treated as an independent variable. A plot of V_2 as a function of three parameters is shown in Fig. B-2. In studying this figure it must be kept in mind that some of the points on the curves shown may not be physically possible. All that is implied here is that if it is possible to obtain a given jet velocity (V_J) with a given cone angle (2α) and a given detonation rate (U_d), then the indicated liner wall flow velocity (V_2) must have existed.

The sound velocity of aluminum is shown as a horizontal line in Fig. 3-2. It is seen that the constant jet velocity curves intersect the sound velocity line. The important point to be seen is that the coordinate points $(V_2, 2\alpha)$ on the constant jet velocity curves, which lie above the sound velocity line, have a V_2 greater than the sound velocity in the liner material and those that lie below have a value of V_2 less than the sound velocity in the aluminum liner material. Furthermore, the value of V_2 decreases as the cone angle (2α) increases.

Thus, if it is assumed that jet instability is related to the value of V_2 and that it is desirable to keep the value of V_2 less than the velocity of sound in the liner material, then it is expedient to form the jet with a liner that has as large a cone angle as possible.

LABORATORY COORDINATE SYSTEM



MOVING COORDINATE SYSTEM

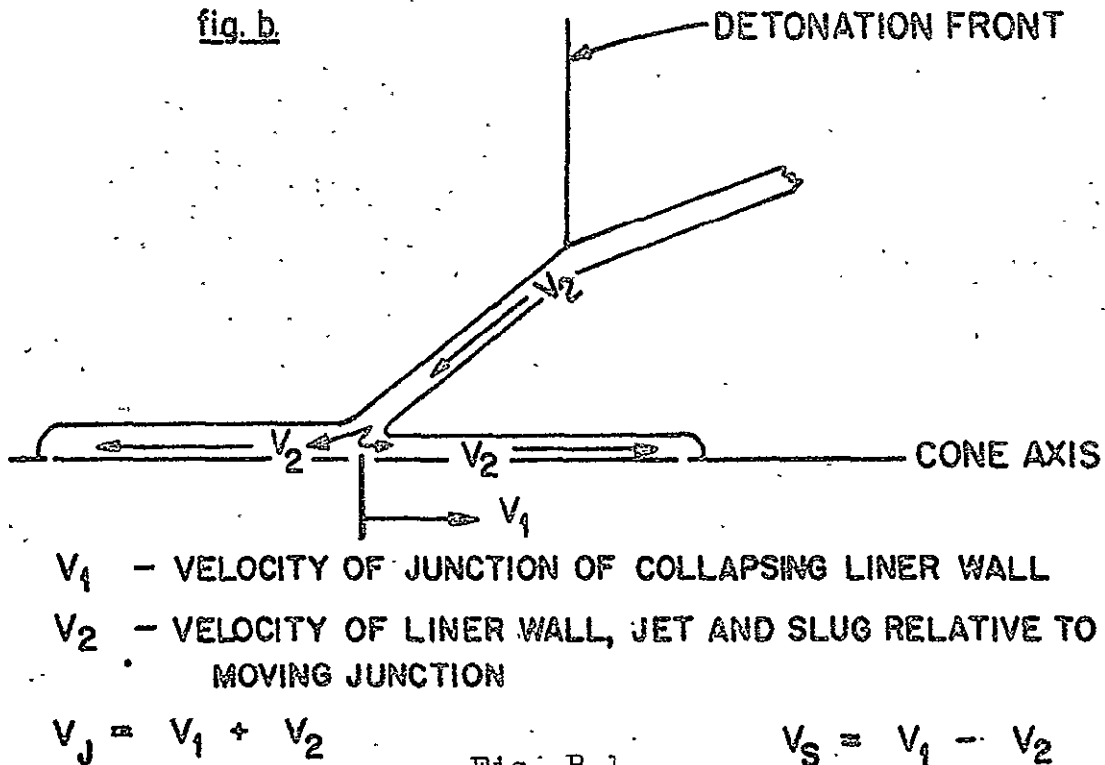


Fig. B-1.

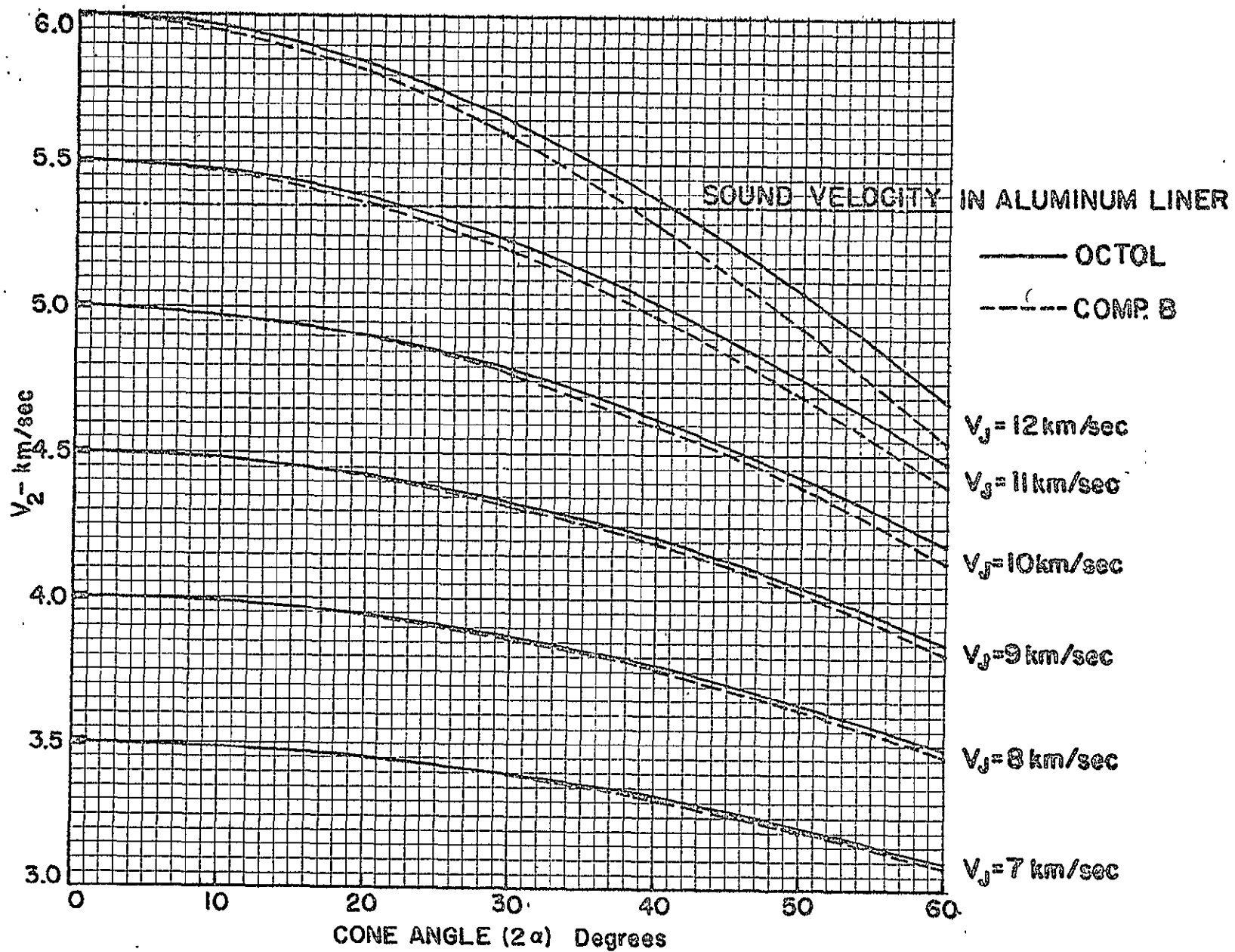


Fig. B-2.

APPENDIX C
 BASIC DESIGN EQUATIONS FOR
 BI-EXPLOSIVE SHAPED CHARGES

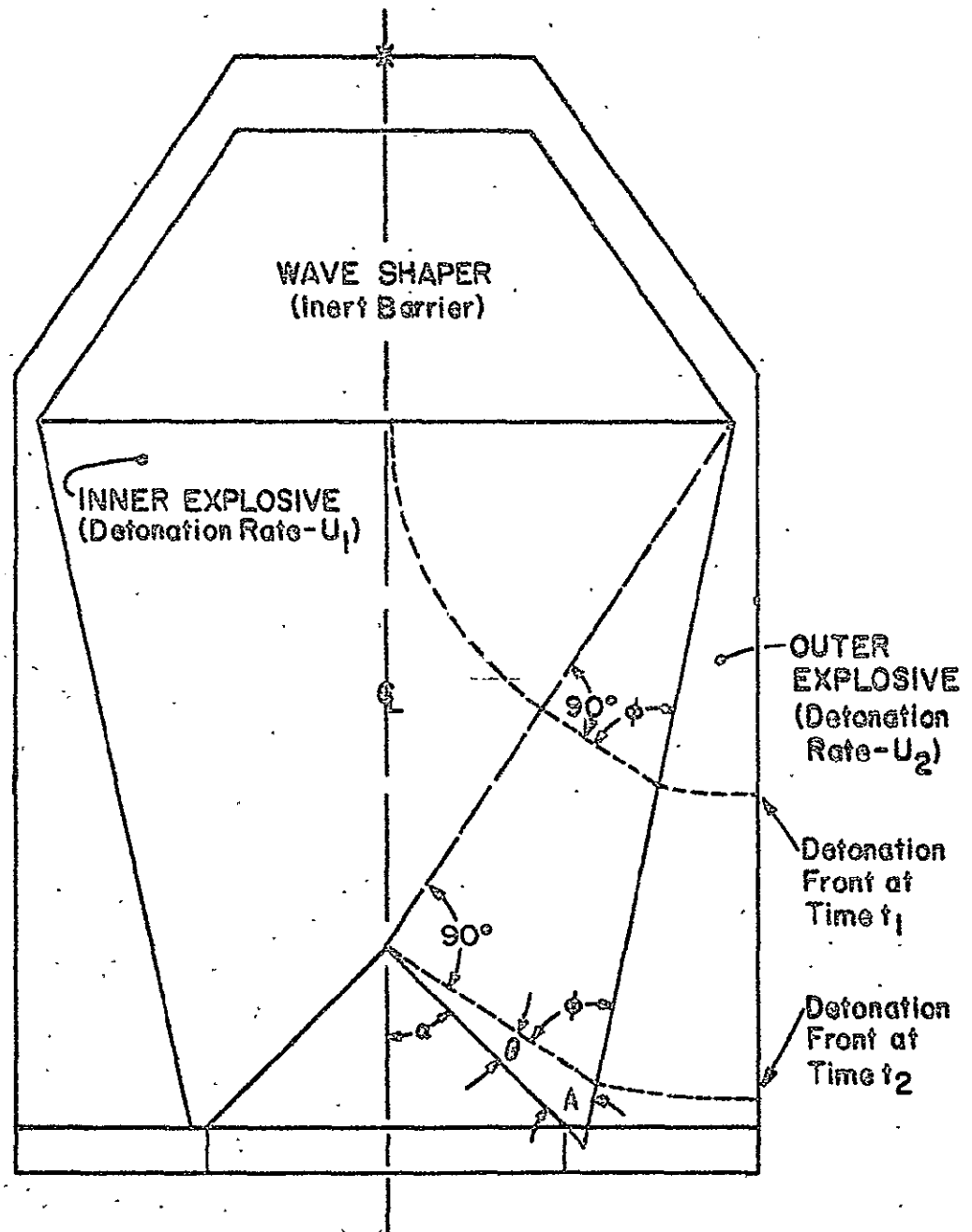


Fig. C-1.

In Fig. C-1, the following two angle parameters determine the angle between the conic detonation front and the liner surface, the angle theta (θ): angle phi (ϕ), and angle A.

The angle A is determined by choice of charge dimensions. The angle ϕ (ϕ) is determined by the detonation rates of the inner and outer explosives as follows:

$$\sin \phi = u_1/u_2 \quad , \text{ where } u_1 \text{ is the detonation rate of the new inner explosive and } u_2 \text{ is the detonation rate of the new outer explosive.} \quad (20)$$

The angle θ (θ) can be calculated with the following equation.

$$\theta = \phi - A \quad (21)$$

Having determined θ (θ) for a given bi-explosive system it would be of interest to develop an effective detonation rate. Conventional shaped charge designs assume the detonation front travels as a plane wave, which is normal to the liner central axis, moving down the liner central axis. Therefore, if the conic detonation wave front of the bi-explosive design sweeps the liner surface in a time interval Δt , the effective detonation rate could be defined as the rate at which a conventional plane detonation front would sweep the liner surface in the same time interval Δt . The following development arrives at an equation for the effective detonation rate (u_E).

, where u_1 is the detonation rate of the inner explosive, u_a is the rate at which the conic detonation front sweeps the liner surface, u_E is the effective detonation rate.

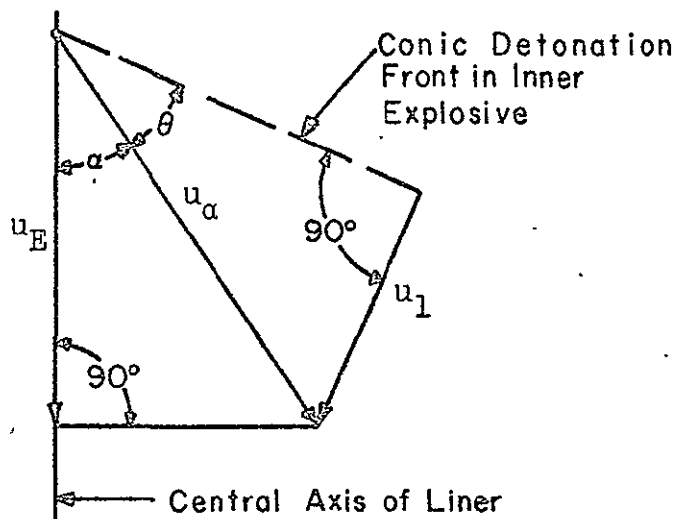


Fig. C-2. Sketch for bi-explosive charge configuration effective detonation rate development.

In Fig. C-2:

$$\sin \theta = u_1 / u_\alpha \quad (22)$$

or,
$$u_\alpha = u_1 / \sin \theta \quad (23)$$

and,
$$\cos \alpha = u_E / u_\alpha \quad (24)$$

or,
$$u_E = u_\alpha \cos \alpha \quad (25)$$

Substituting u_α from Eqn. 23 into Eqn. 25:

$$u_E = (u_1 \cos \alpha) / \sin \theta$$

REFERENCES

1. Berus, E. R.; and Clark, E. L.: Development and Testing of Shaped Charge Meteoritic Simulators. Defense Research Division, The Firestone Tire and Rubber Company (Contract NAS1-4187) for National Aeronautics and Space Administration Oct. 1965.
2. Berus, E. R.; and Clark, E. L.: Development and Testing of Advanced Shaped Charge Meteoritic Simulators. Part I - Shaped Charge Design and Development. NASA CR-66215, Nov. 1966.
3. Woodall, R. L.; and Clark E. L.: Development and Testing of Advanced Shaped Charge Meteoritic Simulators. Part II - Calibration of Flight Guns. NASA CR-66216. Nov. 1966.
4. Design and Testing of Bi-Explosive Shaped Charge Meteoritic Simulators. NASA CR-66615. April 1968.
5. Birkhoff, G.; MacDougall, D. P.; Pugh, E.M.; Taylor, G.: Explosives with Lined Cavities, J. of Appl. Phy. 19,563 (1948).
6. Eichelberger, R. J.: Shaped Charge Warheads: Potential Improvements and Problems. Proceedings, of Non-Nuclear Warhead Symposium. Picatinny Arsenal 29th, 30th Sept. and 1 Oct. 1964, Vol. I.
7. Walsh, J. M.; Schreffler, R. G.; Willig, F. S.: Limiting Conditions for Jet Formation in High Velocity Collisions, J. of Appl. Phy. 24,349 (1953).

Table I

SLUG AND DEBRIS TRAP TESTS
(Using 65/35 octol explosive loaded aluminum hyperbolic
liners and Slug and Debris Trap Charges)

FTR DRD Round Number	Trap						Hyperbolic Liner				Comments
	Aperture Diameter (inches)	Liner Mat.	Liner Wall Thck. (in.)	Liner Dwg. No.	Additional Description	1st Flash Radio- graph (μ sec)	Apex Angle (deg.)	Dwg. No.	Inhibitor Type	Jet- Pellet Velocity (km/sec)	
1028-3	1.00	Al	0.150	DRB-23-2681-1 Item 1	Full Trap Liner	30.1	40	DRC-23-2391	None	10.2	Trap liner has almost closed - Jet-Pellet undamaged
1028-2	1.00	Al	0.100	DRB-23-2681-1 Item 1	Full Trap Liner	30.6	40	DRC-23-2391	None	10.6	Trap liner has just closed - Jet-Pellet undamaged
1028-4	1.00	Al	0.100	DRB-23-2681-1 Item 1	Full Trap Liner	40.6	40	DRC-23-2391	None	10.2	Trap liner impacting trailing jet material- Jet-Pellet undamaged
1028-6	1.00	Al	0.100	DRB-23-2681-1 Item 2	Full Trap Liner	80.4	40	DRC-23-2391	None	--	Trap liner impacting slug material-Jet- Pellet undamaged
1028-8	1.00	Al	0.050	DRB-23-2681-1 Item 3	Full Trap Liner	29.9	40	DRC-23-2391	None	--	Trap liner has impacted rear of jet-pellet - Rear of jet-pellet slightly damaged
1037-8	1.00	Al	0.050	DRB-23-2681-1 Item 3	Full Trap Liner	28.9	30	DRC-23-2405 M.P.	Int. & Ext. Skt. - *	11.36	Trap liner has not closed - Inhibitor has flared the rear of the pellet
1028-7	1.00	None	None	--	Unlined Trap Charge	79.1	40	DRC-23-2391	None	--	Trap gasses impacting slug material - rear of jet-pellet damaged
1028-5	1.00	Al	0.150	DRB-23-2681-1 Item 1 M.P.	Sectioned Half Trap Liner	40.1	40	DRC-23-2391	None	--	Trap liner and gasses impacting trailing jet material - Rear of jet-pellet asym- metrically hit
1037-6	1.00	Al	0.100	DRB-23-2681-1 Item 1 M.P.	Upper Half Trap Liner	79.6	30	DRC-23-2407 M.P.	Ext. Skt. *	--	Trap liner impacting slug material - Pellet separated into 2 pieces
1037-9	1.00	Al	0.100	DRB-23-2681-1 Item 1 M.P.	Upper Half Trap Liner	28.7	30	DRC-23-2405 M.P.	Int. Skt. *	11.25	Trap gasses impacting trailing jet material- Inhibitor has flared the rear of the pellet
1028-10	0.50	Al	0.100	DRB-23-2718 Item 1	Full Trap Liner	42.9	40	DRC-23-2391 M.P.	**	10.27	Trap liner impacting trailing jet material- Jet-Pellet shocked from rear
1028-9	0.50	Cu	0.030	DRB-23-2718 Item 2	Full Trap Liner	42.7	40	DRC-23-2391 M.P.	***	10.54	Trap liner impacting trailing jet material- Jet-Pellet shocked from rear
1057-2	0.50	Al	0.100	DRB-23-2718 Item 1	Full Trap Liner	23.2 45.9	35	DRC-23-2460	Dbl. Angle Ext. Skt.	10.94	Trap liner has not closed/Jet-pellet shocked from rear (in 2nd radiograph)
1057-3	0.50 0.50	Cu None	0.030 None	DRB-23-2718 Item 1 None	Dbl. Trap Assy.-full Trap Liner Over Unlined Trap	36.0	35	DRC-23-2460	Dbl. Angle Ext. Skt.	10.96	Trap gasses impacting trailing jet material- Jet-Pellet shocked from rear

*Composite inhibited - Design 1 assembly with cemented joint located 1.405 inch from flanged base.
 **Composite inhibited - Design 3 assembly with cemented joint located 0.875 inch from flanged base.
 ***Composite inhibited - Design 2 assembly with cemented joint located 0.875 inch from flanged base.

Table II

INHIBITOR TESTS
(Using 65/35 octol explosive loaded aluminum hyperbolic liners - Note 1)

FTR DRD Round Number	Hyperbolic Liner				Jet- Pellet Velocity (km/sec)	Flash Radiograph Times (μ sec)	Comments
	Apex Angle (deg.)	Wall Thickness (in.)	Inhibitor Type	Dwg. No.			
1034-1	40	0.030	Composite - Design 1 (2)	DRC-23-2391	10.20	29.5/49.4/91.3	Jet-Pellet slowly separated into 2 pieces - Jet-Pellet integrity excellent
1034-2	40	0.030	Composite - Design 1 (2)	DRC-23-2391	10.29	29.5/49.3/91.3	Jet-Pellet slowly separated into 2 pieces - Jet-Pellet integrity excellent
1034-3	40	0.030	Composite - Design 3 (2)	DRC-23-2391	--	25/45/82.6 (7)	Jet-Pellet slowly separated into 2 pieces - Jet-Pellet integrity excellent
1034-4	40	0.030	Composite - Design 2 (2)	DRC-23-2391	--	25/45/84.6 (7)	Jet-Pellet slowly separated into 2 pieces - Jet-Pellet integrity excellent
1034-5	40	0.030	Composite - Design 4 (3)	DRC-23-2391	10.20	20.2/46.0/83.6	Jet-Pellet slowly separated into 2 pieces - Jet-Pellet integrity excellent
1037-1	30	0.030	Composite - Design 1 (4) (6)	DRC-23-2404	11.17	29.4/90.2/82.5	Jet-Pellet slowly separated into 2 pieces - Jet-Pellet slightly splitting lengthwise from rear
1036-1	30	0.030	External Skirted	DRC-23-2407	11.14	28.8/45.4/75.1	Jet-Pellet shortened but splitting lengthwise from rear
1036-2	30	0.030	Ext. Skt. - Comp. Des. 1 (4)	DRC-23-2407	11.20	29.7/50.6/82.4	Jet-Pellet shortened and slowly separating into 2 pieces but splitting lengthwise from rear
1037-6	30	0.030	Ext. Skt. - Comp. Des. 1 (4)	DRC-23-2407	--	79.6/79.6/80.2	Trapped assy. - Jet-Pellet same as 1036-2
1037-4	30	0.030	Internal Skirted	DRC-23-2406	11.30	29.5/49.6/82.7	Jet-Pellet shortened but splitting lengthwise from rear and damaged at rear
1037-7	30	0.030	Int. Skt. - Comp. Des. 1 (4)	DRC-23-2406	--	29.1/43.9/78.0	Jet-Pellet shortened but splitting lengthwise from rear and damaged at rear
1037-9	30	0.030	Int. Skt. - Comp. Des. 1 (4)	DRC-23-2406	11.25	28.7/48.5/81.2	Trapped Assy. - Jet-Pellet same as 1037-7 (Jet-Pellet not separating into 2 pieces)
1037-3	30	0.030	Int. & Ext. Skt.	DRC-23-2405	11.35	29.7/49.6/82.5	Jet-Pellet shortened but splitting lengthwise from rear and damaged at rear
1037-5	30	0.030	Int. & Ext. Skt. - Comp. Des. 1 (4)	DRC-23-2405	11.14	29.1/49.2/82.5	Jet-Pellet shortened but splitting lengthwise from rear and damaged at rear
1037-8	30	0.030	Int. & Ext. Skt. - Comp. Des. 1 (4)	DRC-23-2405	11.36	28.9/48.8/81.2	Trapped Assy. - Jet-Pellet same as 1037-5 (Jet-Pellet not separating into 2 pieces)
1057-1	35	0.030	Dbl. Ext. Skt. - Comp. Des. 4 (5)	DRC-23-2460	10.67	25.7/44.9/85.6	Jet-Pellet shortened but has trailing jet following
1057-2	35	0.030	Dbl. Ext. Skt. - Comp. Des. 4 (5)	DRC-23-2460	10.94	24.5/45.9/86.4	Trapped assy. - Jet-Pellet shocked by trap assy.
1057-3	35	0.030	Dbl. Ext. Skt. - Comp. Des. 4 (5)	DRC-23-2460	10.96	36.0/52.2/90.1	Dbl. Trapped Assy. - Jet-Pellet shocked by trap assy.

Notes: (1) The following loading fixtures were used for the indicated liner angles: 40°-DRC-11-2239
35°-DRC-11-2427
30°-DRC-11-2052

- (2) Cemented joint located 0.875 inch from flanged base.
(3) Cemented joint located 0.985 inch from flanged base.
(4) Cemented joint located 1.405 inch from base.
(5) Cemented joint located 1.367 inch from base.
(6) "F temper"
(7) Instrumentation difficulties.

Table III

JET-PELLET TEST RESULTS (8 KM/SEC)
 (60°, 0.030-in. wall thickness 1100-0 aluminum hyperbolic
 liners (DRC-23-2418) using 60/40 comp. B explosive charge)

FTR DRD Round Number	LOADING FIXTURE			JET-PELLET				Comments
	Dwg. No.	C/M	ϕ Angle (deg.)	Tip Velocity (km/sec)	Tail Velocity (km/sec)	Tip-to-Tail Velocity (km/sec)	$\frac{(\text{Tip}+\text{Tail Vel.})}{2}$ (km/sec)	
1040-1	DRC-11-2417	Std. (10.74)	18.0	8.66	8.66	0	8.66	Longitudinally and Radially Stable
1040-3*	DRC-11-2417	Std. (10.74)	18.0	8.48	8.48	0	8.48	Longitudinally and Radially Stable
1040-2	DRC-11-2419	Red. (8.12)	19.0	8.44	8.07	0.37	8.26	Radially Stable but Elongating
1040-4	DRC-11-2429	Red. (8.12)	20.0	8.19	7.92	0.27	8.06	Radially Stable but Elongating
1040-5	DRC-11-2428	Red. (8.12)	21.0	7.99	7.82	0.17	7.91	Radially Stable but Elongating

*"F" temper, i.e., work hardened (as received).

Table IV

JET-PELLET TEST RESULTS (11 KM/SEC)
(65/35 octol explosive charges - Note 1)

FTR DRD Round Number	Liner				Jet-Pellet	
	Apex Angle (deg.)	Wall Thickness (in.)	Aluminum Type (Note 2)	Dwg. No.	Velocity (km/sec)	Comments
1028-1	40	0.030	1100-0	DRC-23-2391	10.33	Test of flanged liner - Jet-pellet integrity excellent
1041-1	40	0.030	6061-T6	DRC-23-2391	10.48	Test of Aluminum Alloy - Jet-pellet radially delaminating
1041-2	40	0.030	6061-0	DRC-23-2391	10.53	Test of Annealed Aluminum Alloy - Jet-pellet longitudinally segmenting
1029-1	30	0.030	1100-0	DRB-23-2143	11.07	Test of 30° Hyp. Liner - Jet-pellet slightly splitting from rear
1029-3	30	0.030	1100-0	DRB-23-2143	--	Long Flight View (95 inches from liner) - Jet-pellet almost destroyed by air drag
1037-2	30	0.030	1100-F	DRB-23-2404	11.35	Test of unannealed 30° Hyp. Liner - Jet-pellet violently splitting lengthwise - pellet destroyed
1037-1	30	0.030	1100-F	DRB-23-2404 M.P. ^{Note 3}	11.17	Test of unannealed, inhibited 30° Hyp. Liner - Jet-pellet segmented longitudinally into 2 pieces
1029-2	30	0.020	1100-0	DRB-23-2173-1	11.30	Test of 30° Hyp. Liner - Jet-pellet splitting from rear
1029-4	30	0.020	1100-0	DRB-23-2173-1	--	Long Flight View (95 inches from liner) - Jet-pellet destroyed by air drag
1048-1	30	0.040	1100-0	DRC-23-2423	10.80	Test of 30° Hyp. Liner - Jet-pellet radially and longitudinally stable
1048-2	30	0.040	1100-0	DRC-23-2423	10.77	Test of 30° Hyp. Liner - Jet-pellet radially and longitudinally stable
1046-1	35	0.030	1100-0	DRC-23-2422	10.70	Test of 35° Hyp. Liner - Jet-pellet radially and longitudinally stable
1046-2	35	0.030	1100-0	DRC-23-2422	10.70	Test of 35° Hyp. Liner - Jet-pellet radially and longitudinally stable
1043-1	40	0.010	1100-0	DRB-23-2172-2	11.13	Test of 40° Hyp. Liner - Jet-pellet radially slightly unstable and longitudinally segmenting
1043-2	40	0.010	1100-0	DRB-23-2172-2	11.28	Test of 40° Hyp. Liner - Jet-pellet radially slightly unstable and longitudinally segmenting

Notes: 1.) The following loading fixtures were used for the indicated liner angles: 40° - DRC-11-2239

35° - DRC-11-2427

30° - DRC-11-2052

2.) The "F temper" and "T6 temper" were as received bar stock. The "O temper" was annealed after rough machining.

3.) Composite inhibited - Design 1 assembly with cemented joint located 1.405 inches from flanged base.

Table V

PRELIMINARY TESTS OF 1100-O ALUMINUM HYPERBOLIC
 LINERS IN BI-EXPLOSIVE CHARGE PER DRC-23-2172 (FIG. 35)
 (65/35 octol outer and 60/40 comp. B inner explosive charge, polyurethane wave shaper)

FTR DRD Round Number	Liner			End Plate Material	Detonation Front		Jet Pellet	
	Apex Angle (deg.)	Wall Thickness (inches)	Dwg. No.		Angle θ (deg.)	Eff. Det. Rate (km/sec)*	Velocity (km/sec)	Comments
1047-1	60	0.030	DRB-23-2445	Steel	37.7	11.2	11.4	Radially stable but elongating
1047-2	50	0.020	DRB-23-2544	Steel	42.7	10.6	11.9	Destroyed
1047-3	50	0.020	DRB-23-2544	Steel	42.7	10.6	11.6	Radially stable but shocked from rear
1047-4	50	0.020	DRB-23-2544	Aluminum	42.7	10.6	12.1	Radially unstable but not elongating

*The following detonation rates were used for calculations: 65/35 Octol, 8.3 km/sec; 60/40 Comp. B, 7.9 km/sec.

Table VI

JET-PELLET TEST RESULTS (14 KM/SEC)
 (90°, 0.030-in. wall thickness, 1100-O aluminum hyperbolic
 liners DRB-23-2725, bi-explosive charge per DRC-23-2438 Fig. 37)

FTR DRD Round Number	Explosive Charge		End Plate Material	Detonation Front		Jet-Pellet	
	Inner	Outer		Angle θ (deg.)	Eff. Det. Rate (km/sec)*	Velocity (km/sec)	Comments
1056-1	60/40 Comp. B	65/35 Octol	Steel	5.00	64.1	15.1	Radially unstable with slight positive velocity gradient
1056-3	60/40 Comp. B	65/35 Octol	Aluminum	5.00	64.1	15.3	Radially unstable with large positive velocity gradient
1056-2	50/50 Pentolite	60/40 Comp. B	Aluminum	2.34	128.2	11.6	Radially unstable with large positive velocity gradient

*The following detonation rates were used for calculations: 65/35 Octol, 8.3 km/sec; 60/40 Comp. B, 7.9 km/sec;
 50/50 Pentolite, 7.4 km/sec.

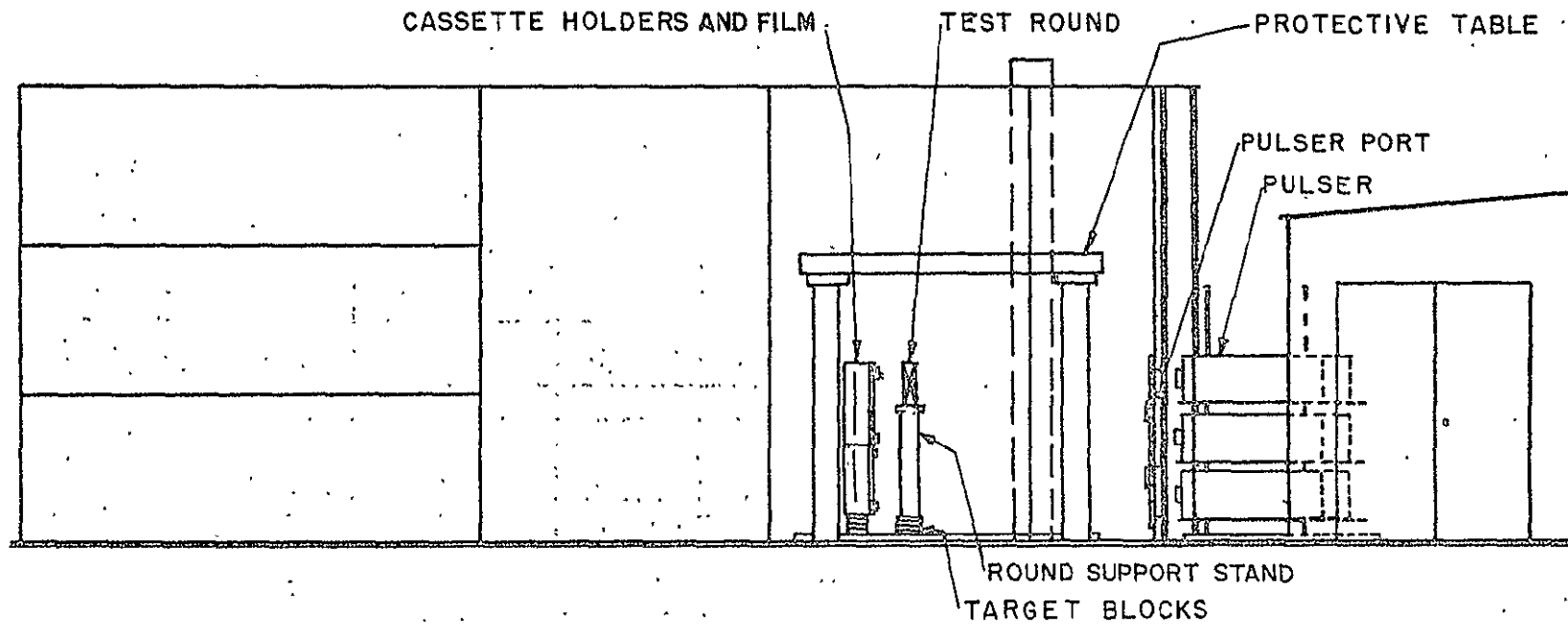


Fig. 1. Side view sketch of the Open Test Site facility.

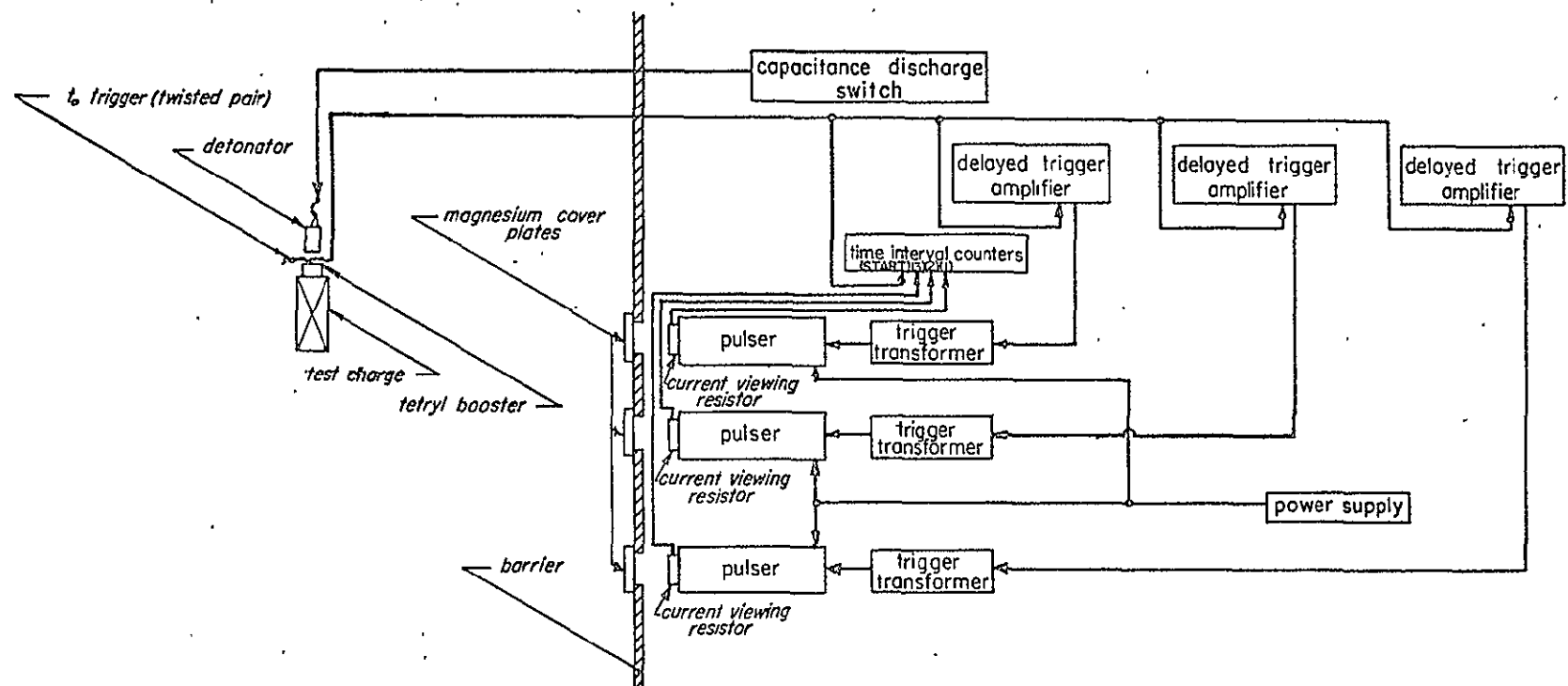


Fig. 2. Block diagram of the electrical equipment - Open Test Site.

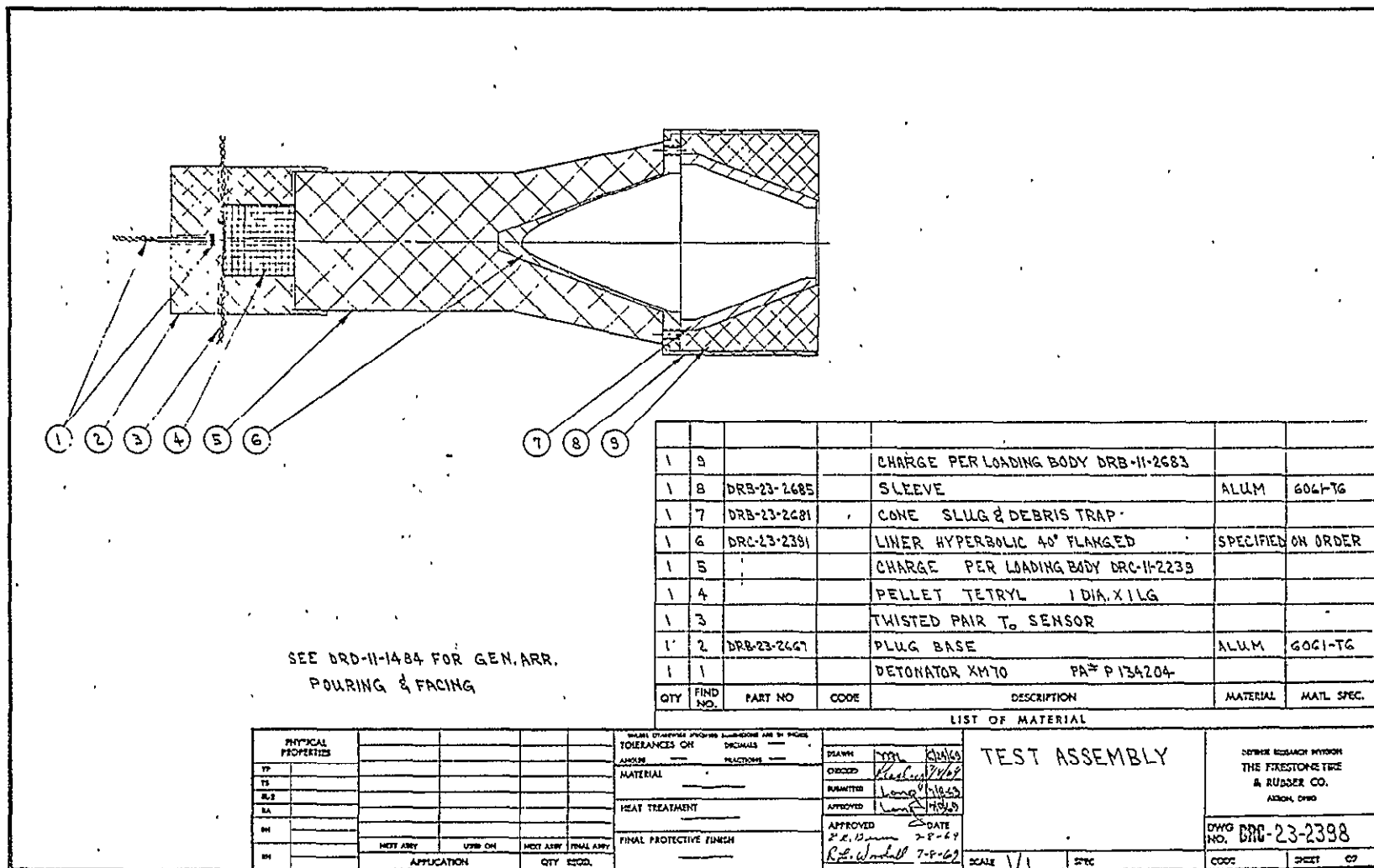


Fig. 3. 40° hyperbolic test assembly w/1-in. aperture slug and debris trap.

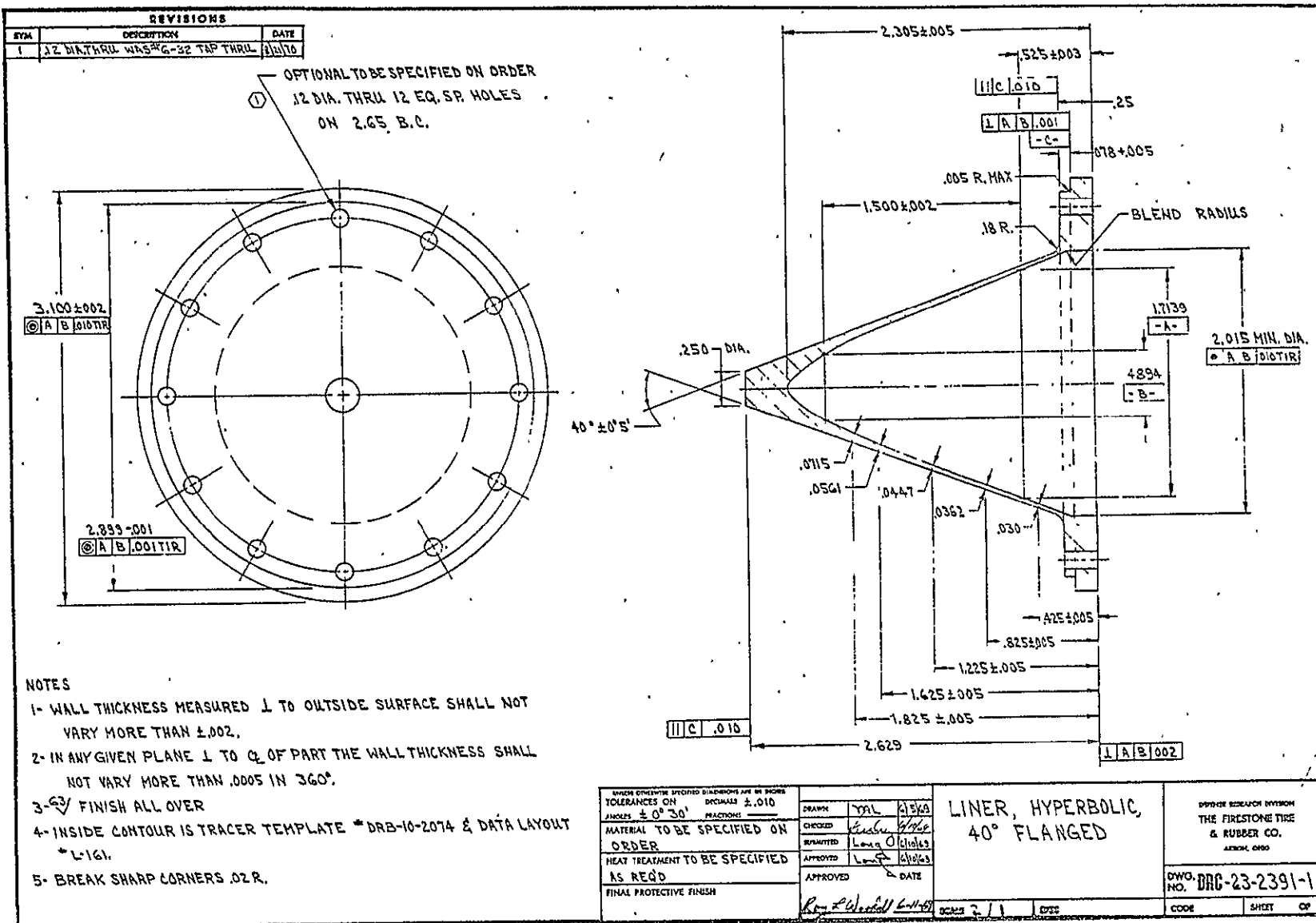


Fig. 4. 40°, 0.030-in. wall thickness hyperbolic liner.

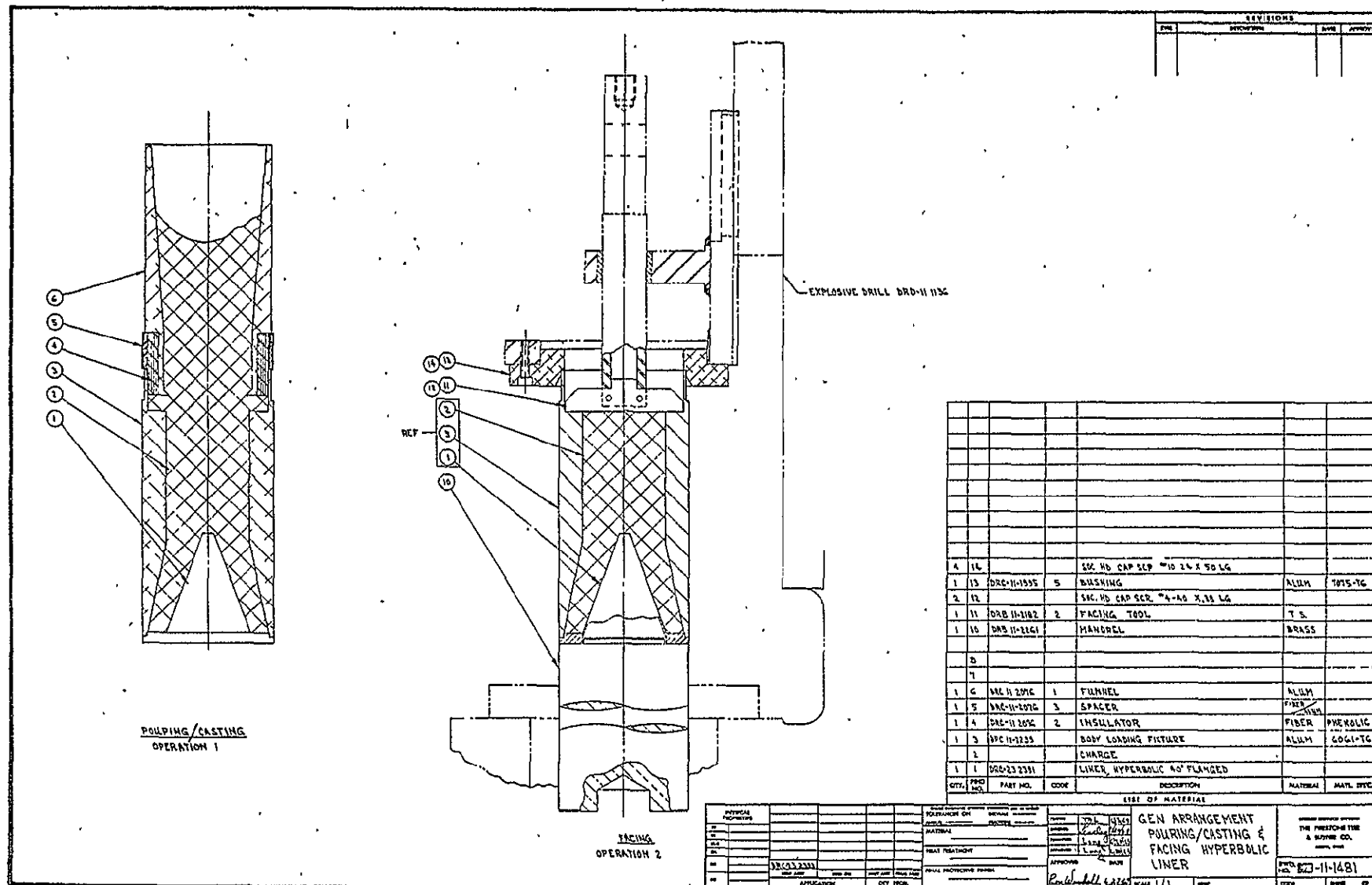


Fig. 5. Explosive loading procedures for hyperbolic charges.

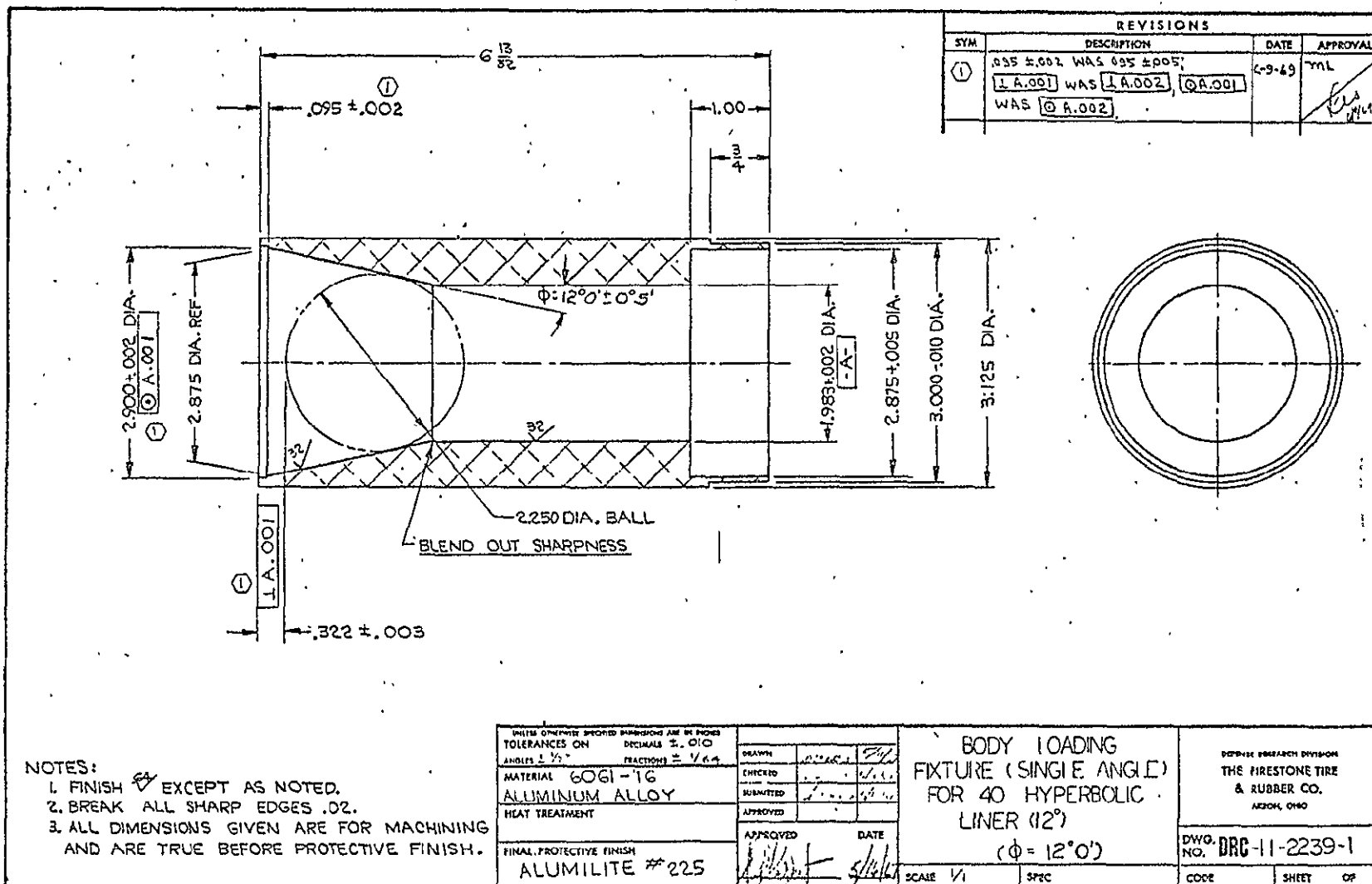


Fig. 6. Loading fixture for 40° hyperbolic charges.

Fig. 7. Explosive loading procedure for 1-in. dia. aperture slug and debris trap charges.

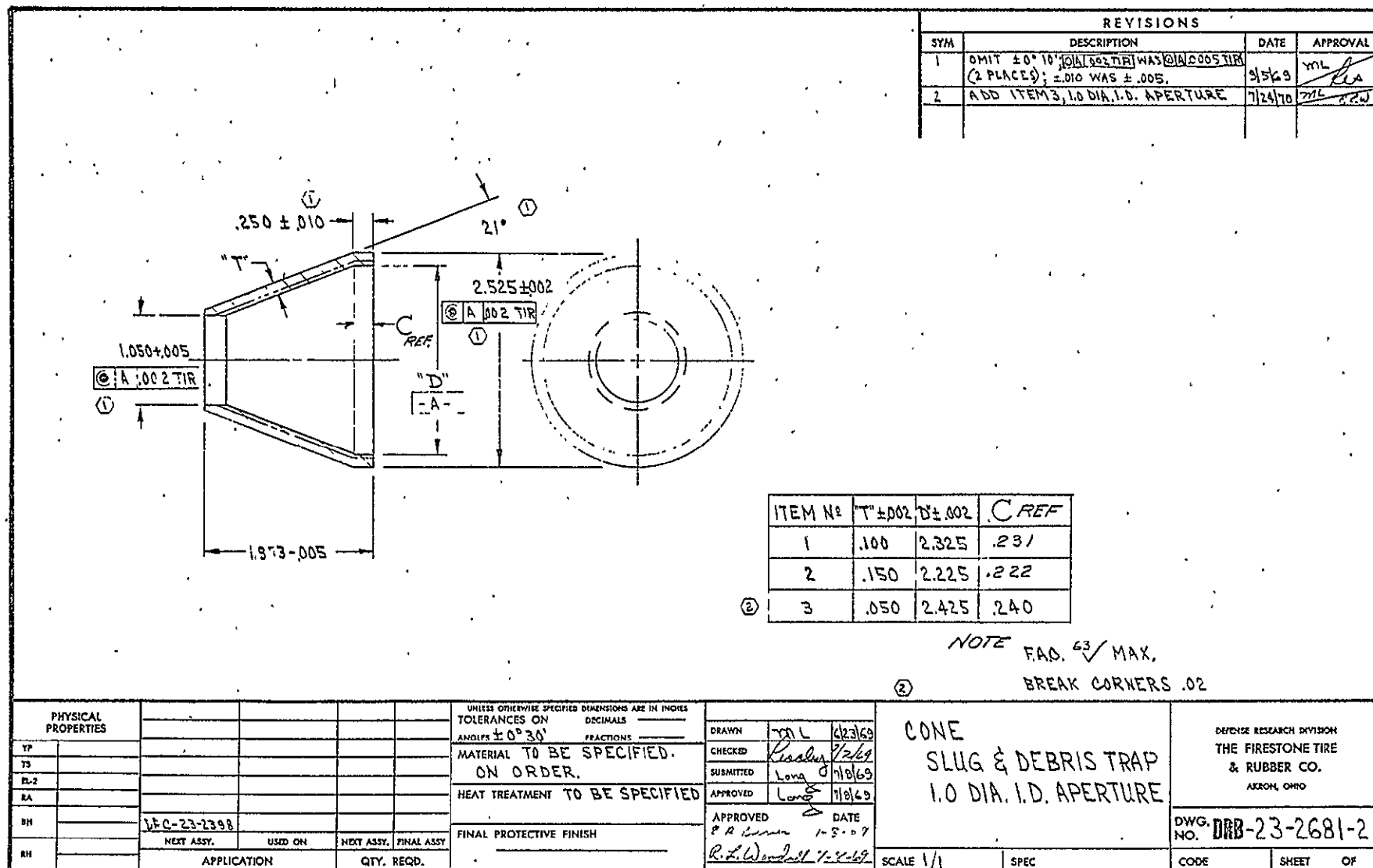


Fig. 8. Liner - 1-in. dia. aperture slug and debris trap.

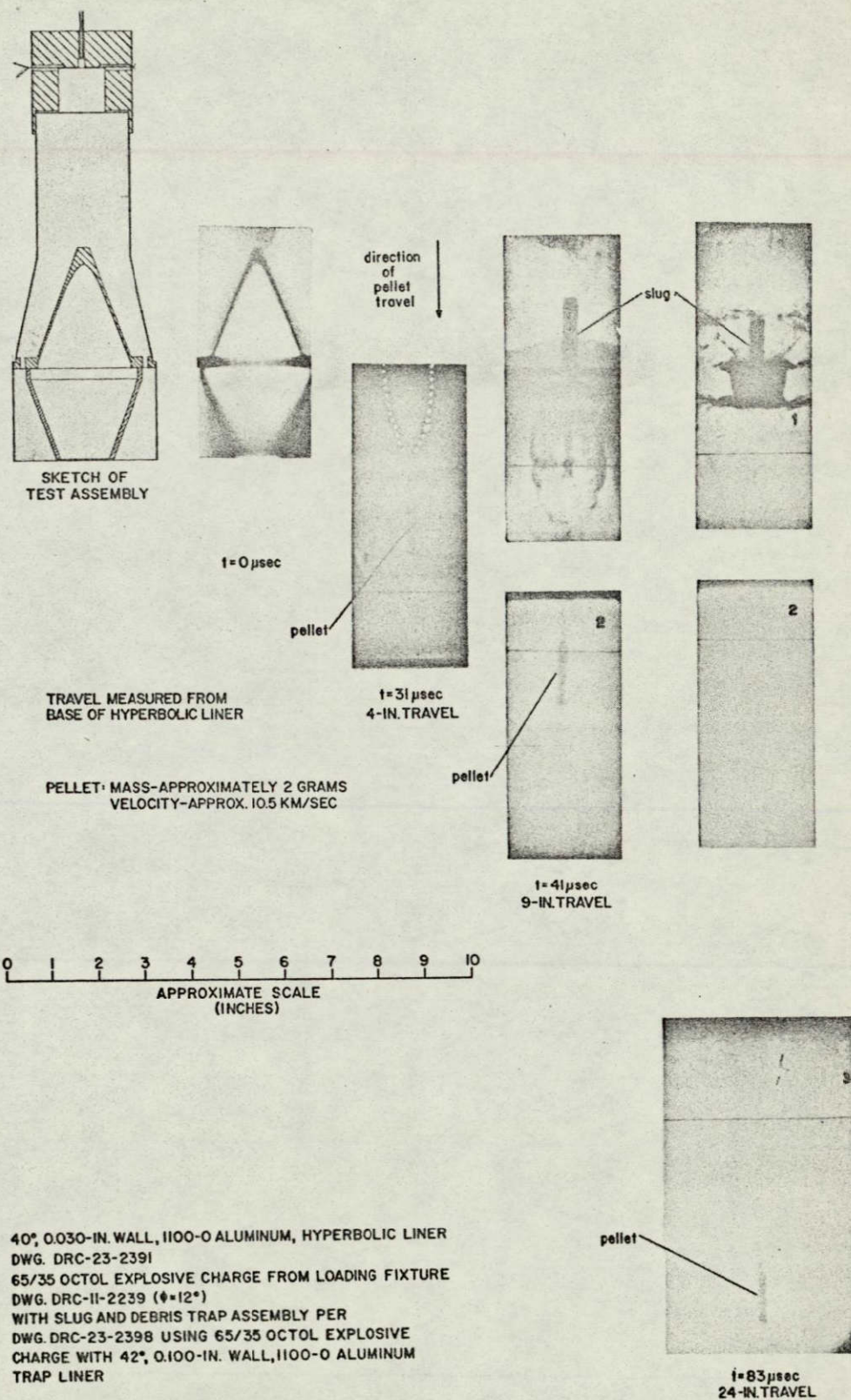


Fig. 9. Radiographs of 1-in. dia. aperture slug and debris trap functioning.



Fig. 10. Liner - 0.5-in. dia. aperture slug and debris trap.

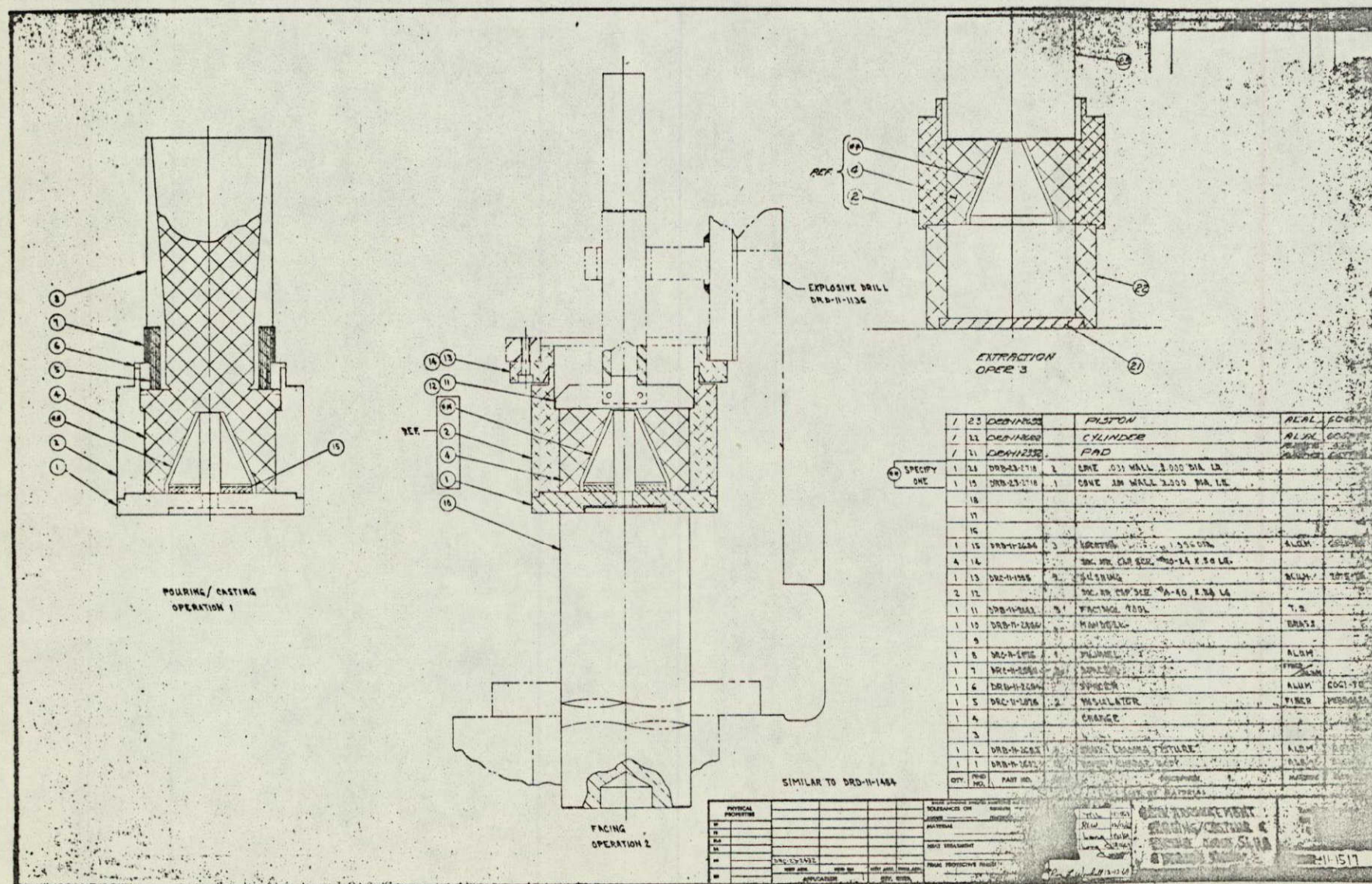


Fig. 11. Explosive loading procedure for 1/2-in. dia. aperture slug and debris trap charges.

1100-O ALUMINUM, 35° HYPERBOLIC LINER, DRC-23-2460, WITH 65/35 OCTOL EXPLOSIVE CHARGE FROM LOADING FIXTURE DRC-II-2427, WITH TWO 0.5-IN. APERTURE DIA. S. & D. TRAPS (0.100-IN. WALL THICKNESS ALUMINUM LINED TRAP FOLLOWED BY AN UNLINED TRAP)

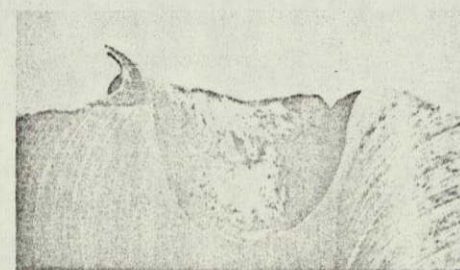
2nd SLUG & DEBRIS TRAP

direction
of
pellet
travel

SHOCKED PELLET
2.7-IN. FROM 2nd TRAP
6.7-IN. FROM HYP. LINER

0 1 2
APPROXIMATE SCALE
(INCHES)

FTR DRD ROUND NO.
1057-3



TARGET
CROSSECTION VIEW
NAS9-9343
ROUND NO. 1057-3
1100-F ALUMINUM TARGET
MAJOR CRATER FORMED BY
1.0 GRAM 1100-O ALUMINUM
MAIN PELLET AT 10.96 KM/SEC
APPROX SCALE (cm.)
0 1 2 3 4 5 6 7 8 9 10

UPPER-HALF
OF ABOVE
VIEW

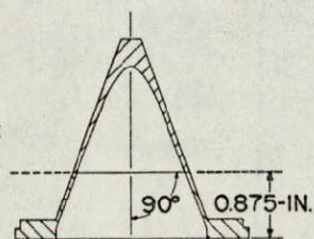
CRATER
VOLUME
(AS MEASURED
WITH WATER)
42.6 cm³

Fig. 12. Photographs of crater formed by 11 km/sec jet-pellet.

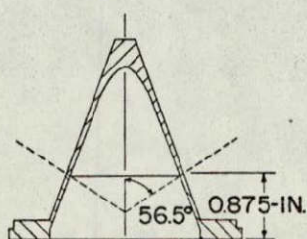
40° 0.030-IN. WALL, 1100-O ALUMINUM,
HYPERBOLIC LINER, DRC-23-2391 M.P.
65/35 OCTOL EXPLOSIVE CHARGE FROM
LOADING FIXTURE DRC-II-2239 ($\phi=12^\circ$)

0 1 2 3 4 5 6 7 8 9 10
APPROXIMATE SCALE
(INCHES)

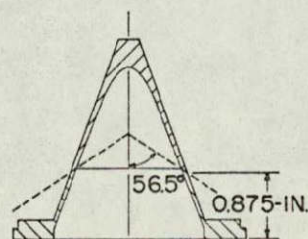
NOTE: DASHED LINES INDICATE
LOCATION AND ORIENTATION
OF CEMENTED JOINTS



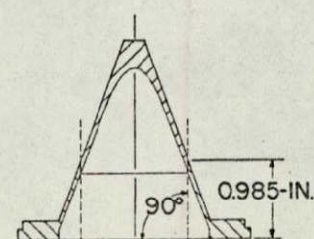
DESIGN 1



DESIGN 2



DESIGN 3



DESIGN 4

direction
of
jet-pellet
travel ↓



JET-PELLET
AFTER 29-IN.
TRAVEL

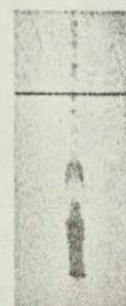
FTR DRD ROUND NO:

1034-1



JET-PELLET
AFTER 25-IN.
TRAVEL

1034-4



JET-PELLET
AFTER 23-IN.
TRAVEL

1034-3



JET-PELLET
AFTER 25-IN.
TRAVEL

1034-5

Fig. 13. Radiographs of composite inhibited jet-pellets.



Fig. 14. 30°, 0.030-in. wall thickness hyperbolic liner.

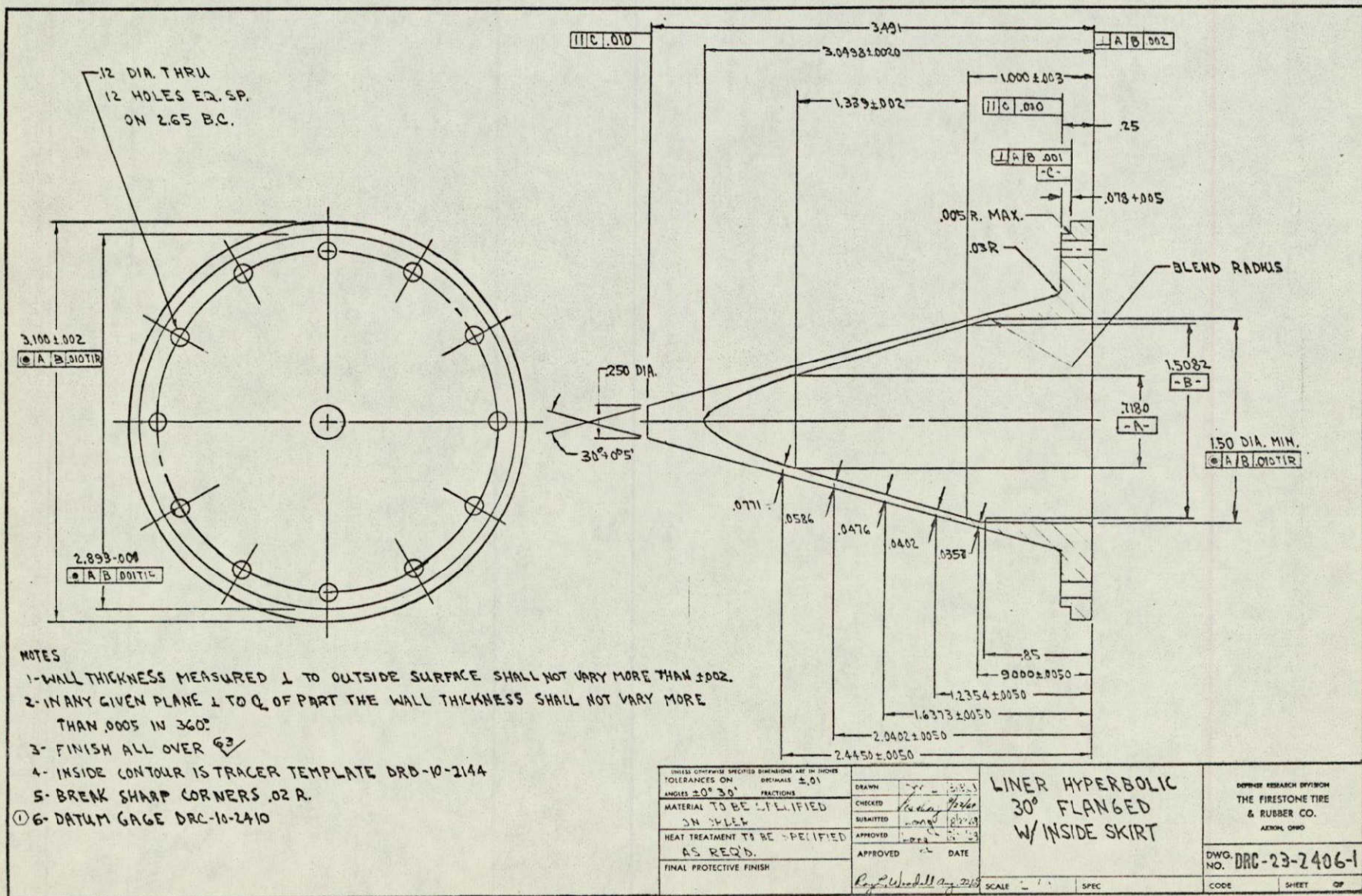


Fig. 15. Inside skirted, inhibited 30°, 0.030-in. wall thickness hyperbolic liner.

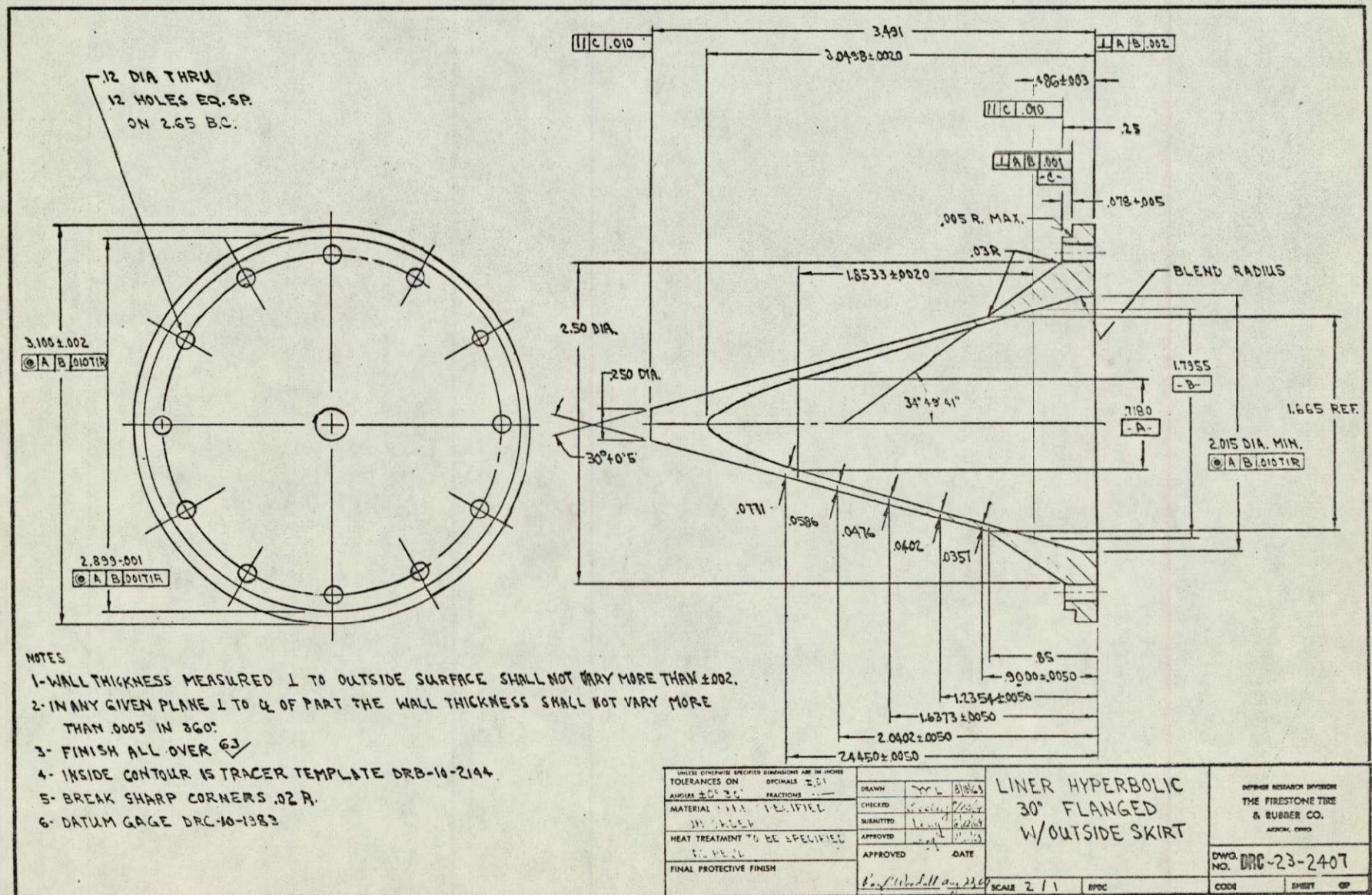


Fig. 16. Outside skirted, inhibited 30°, 0.030-in. wall thickness hyperbolic liner.

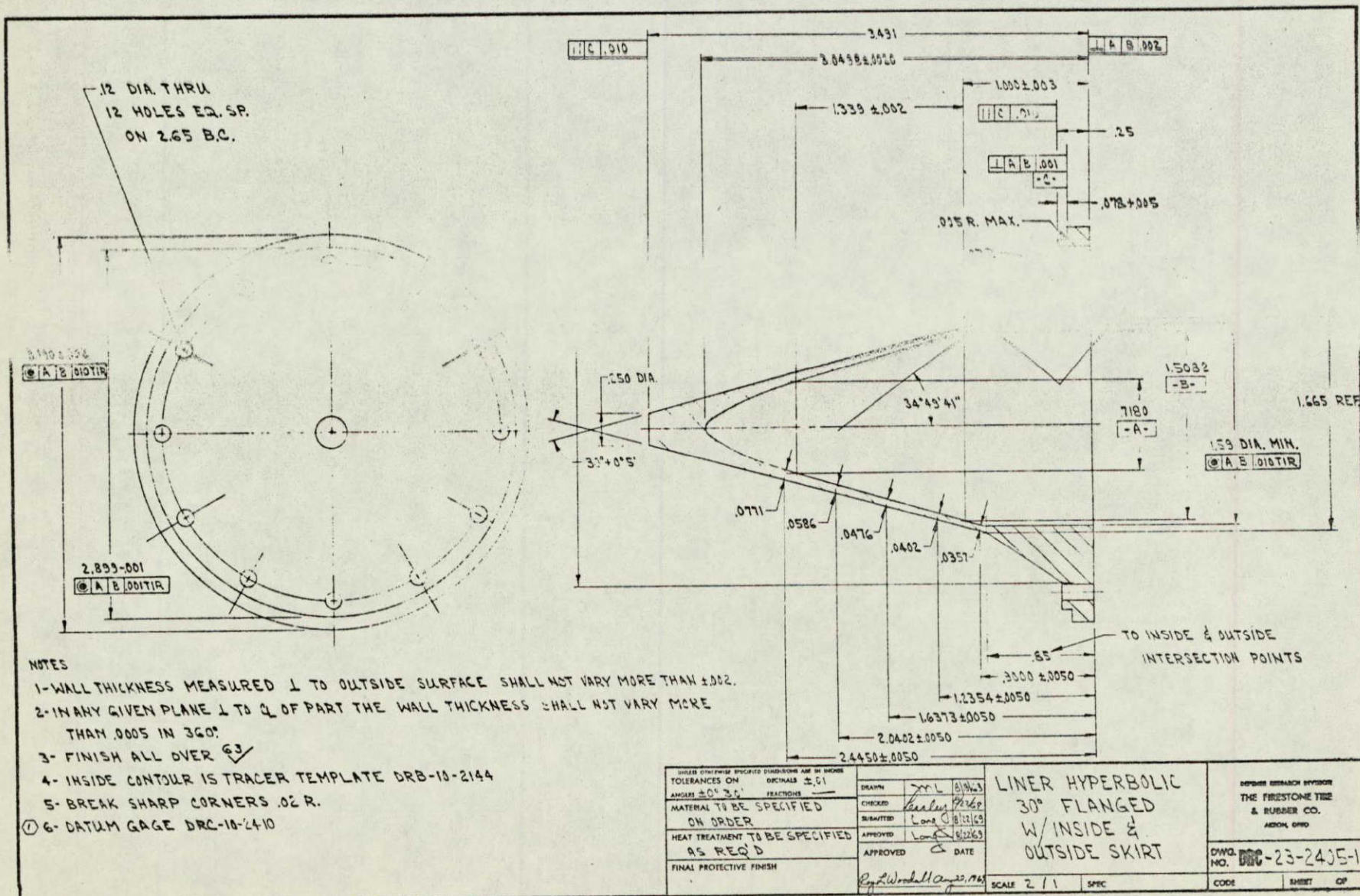


Fig. 17. Inside and outside skirted, inhibited 30°, 0.030-in. wall thickness hyperbolic liner.

30° 0.030-IN. WALL THICKNESS, 1100-O ALUMINUM, HYPERBOLIC LINERS USING 65/35 OCTOL EXPLOSIVE CHARGE FROM LOADING FIXTURE DRC-II-2052

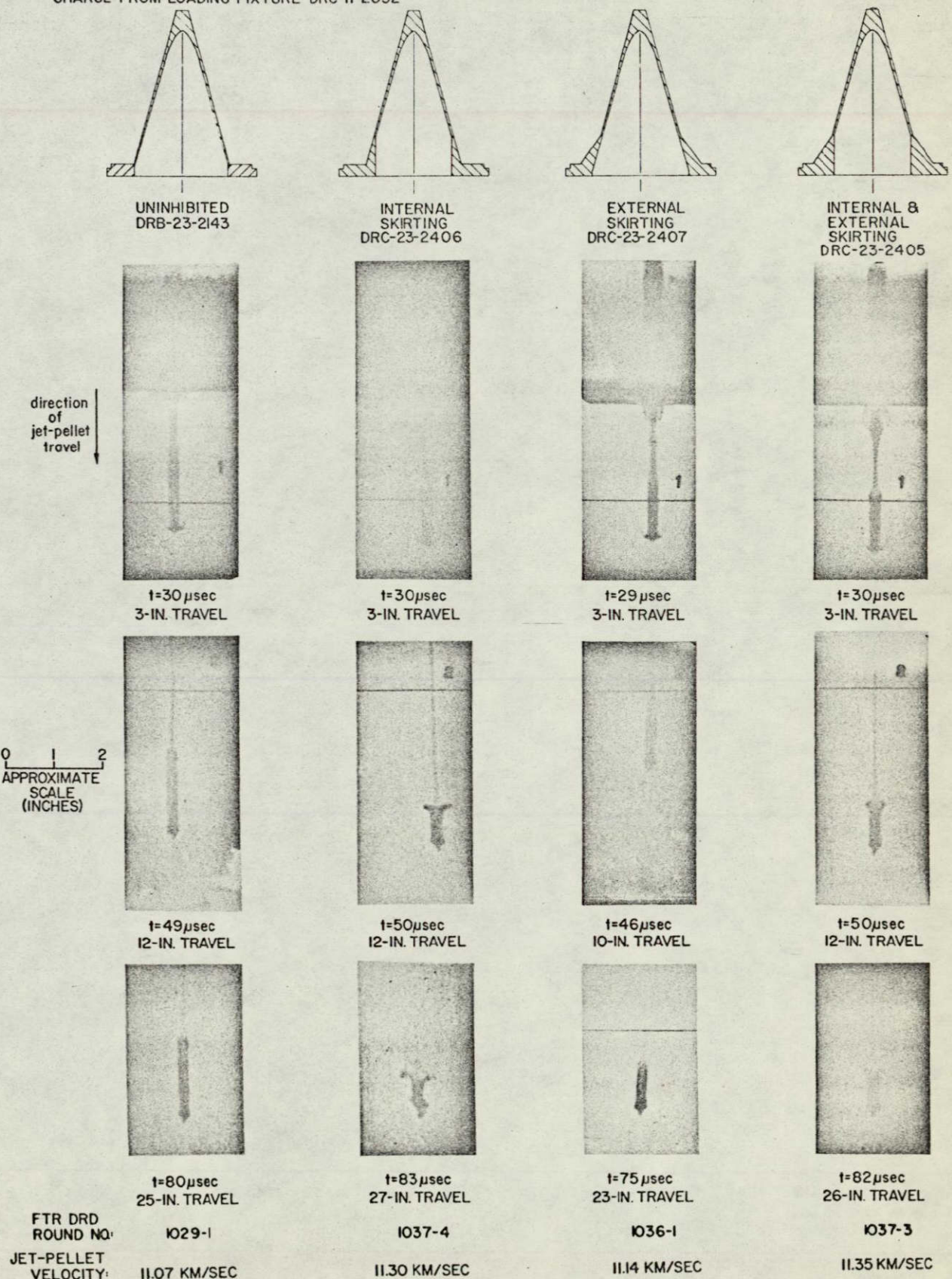


Fig. 18. Radiographs of skirted, inhibited jet-pellets.

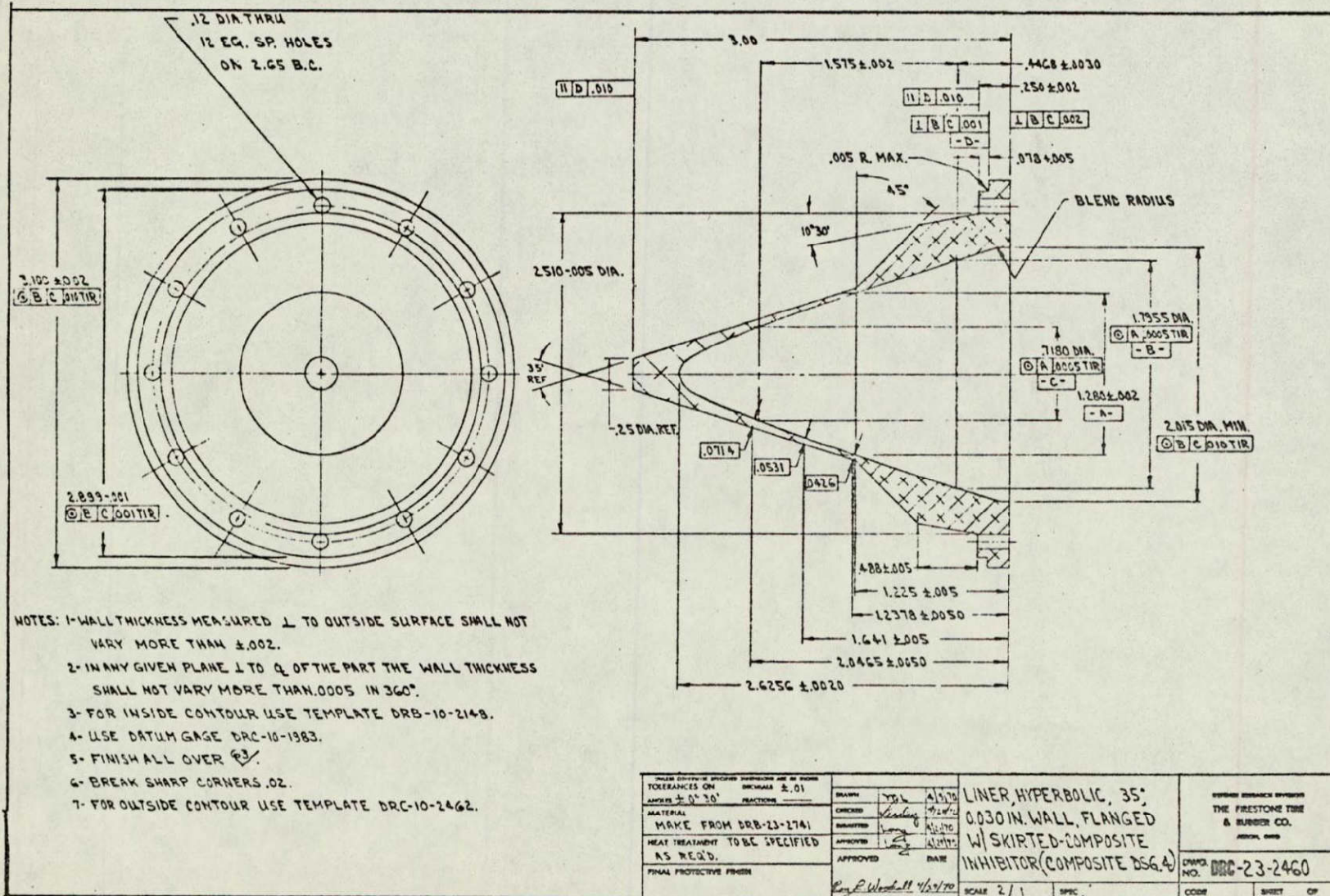


Fig. 19. Skirted, composite, inhibited 35°, 0.030-in. wall thickness hyperbolic liner.

35° 0.030-IN WALL THICKNESS, 1100-O ALUMINUM, HYPERBOLIC LINERS
 USING 65/35 OCTOL EXPLOSIVE CHARGE FROM LOADING FIXTURE
 DRC-II-2427

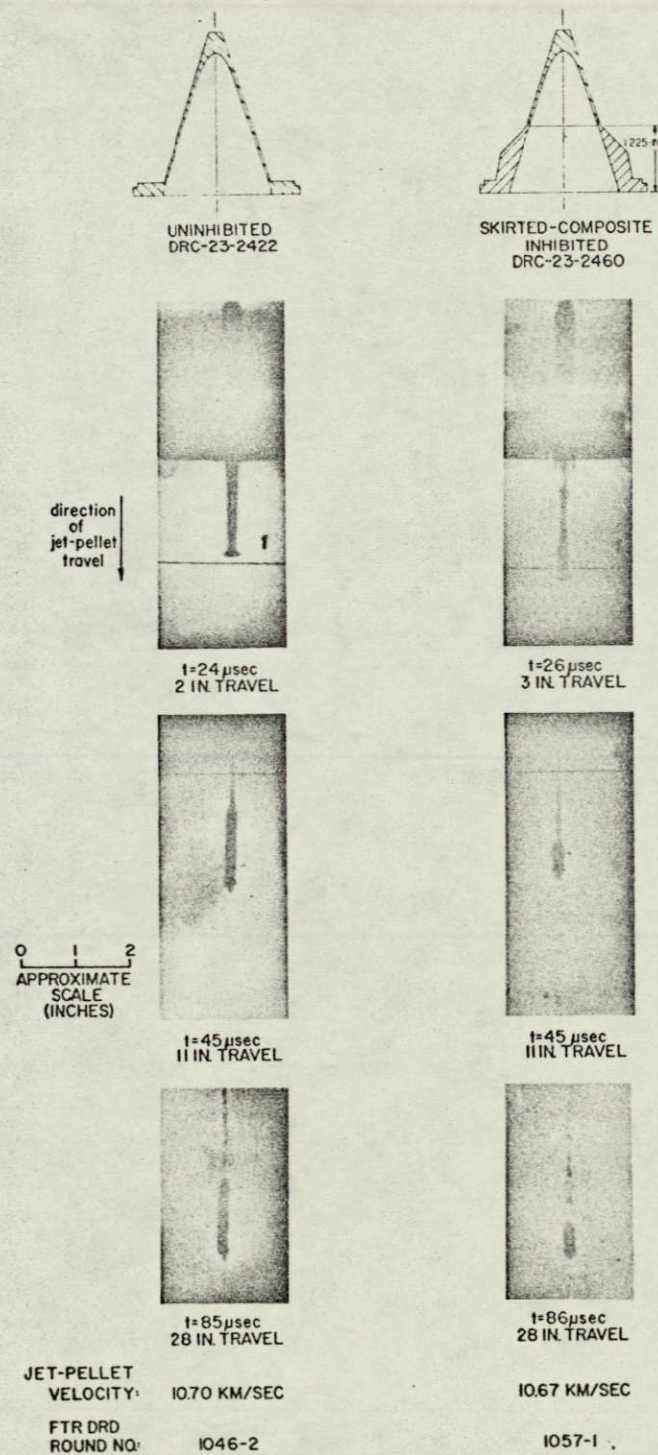


Fig. 20. Radiographs of skirted - composite,
 inhibited jet-pellets.

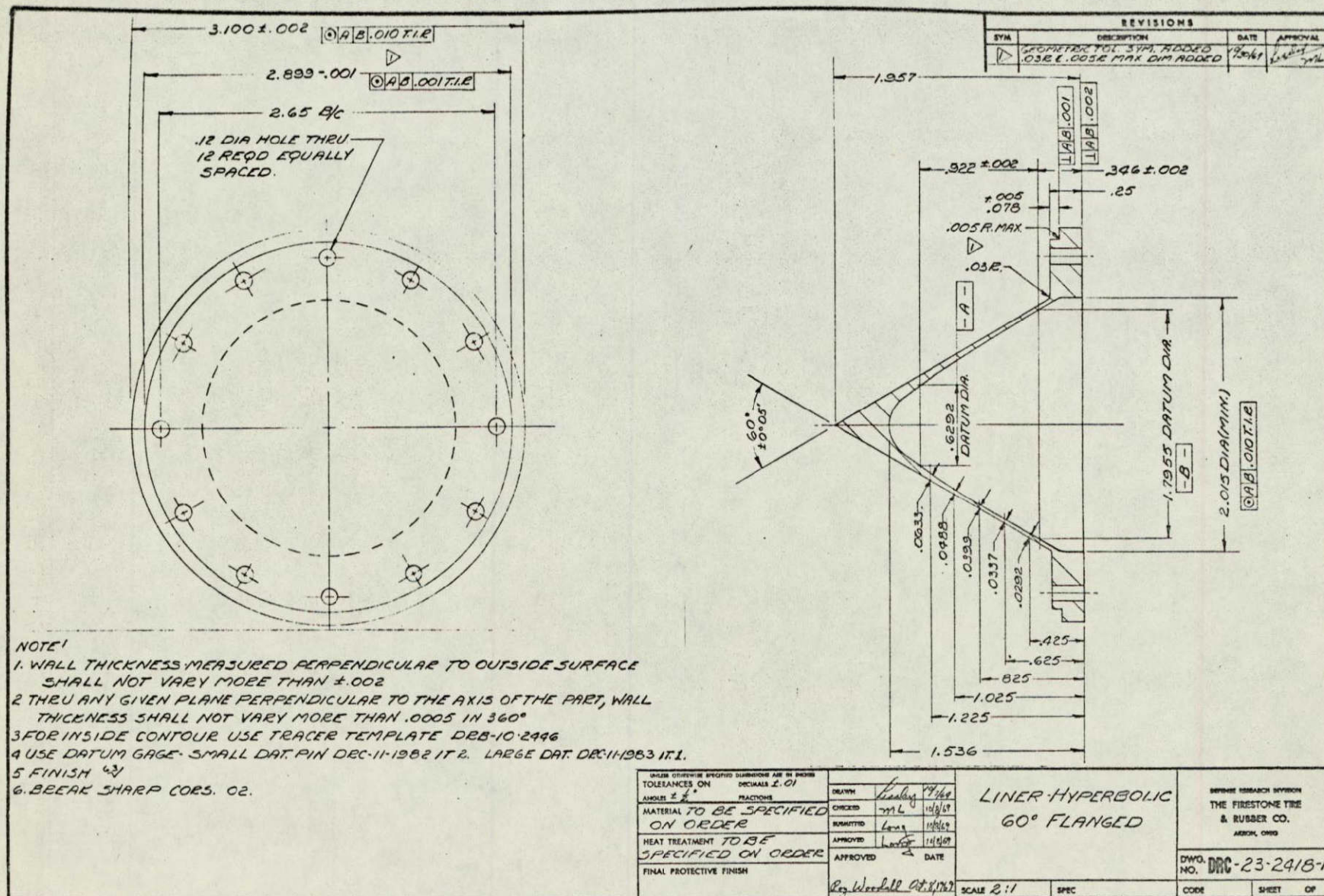


Fig. 21. Flanged 60°, 0.030-in. wall thickness hyperbolic liner.

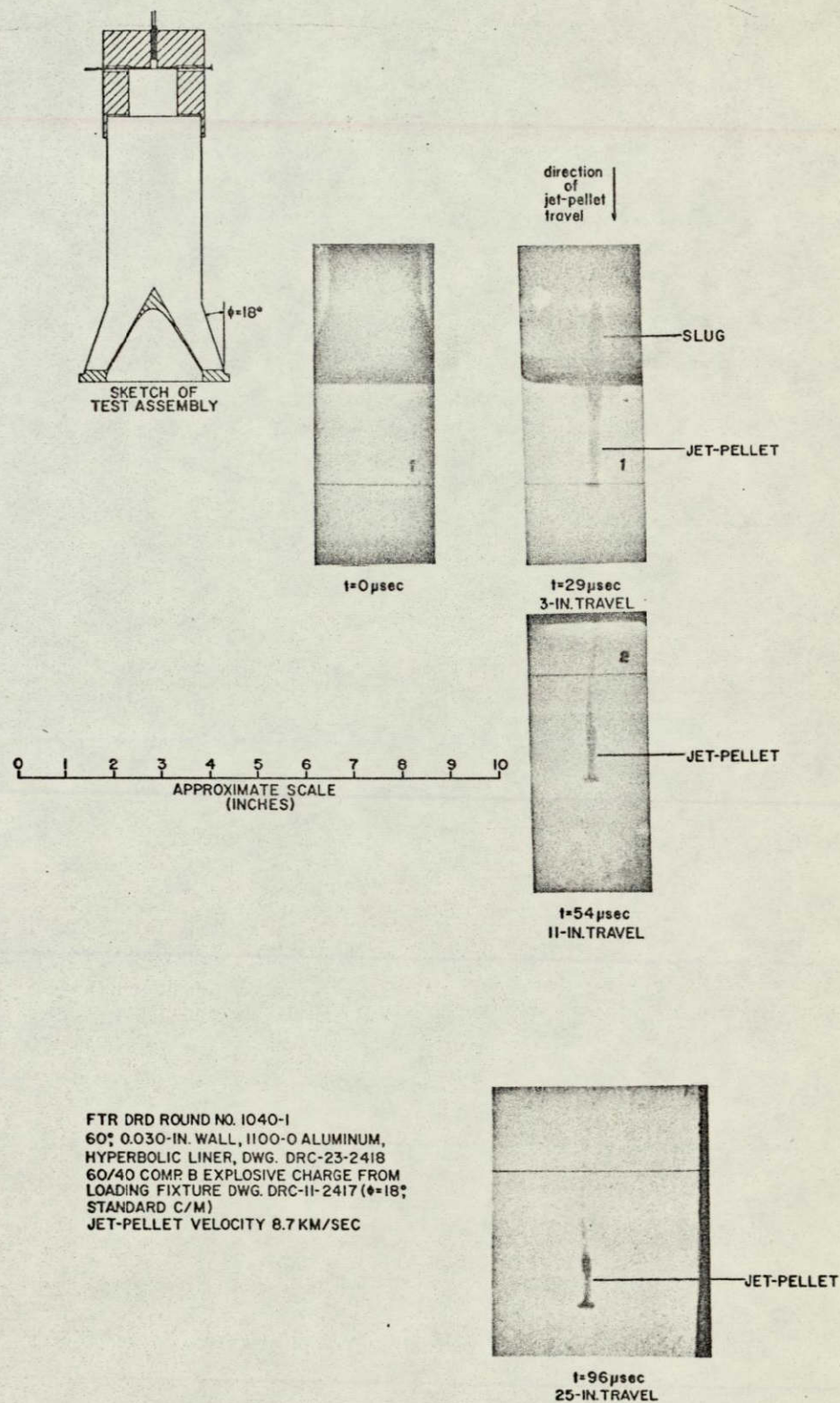


Fig. 22. Radiographs of standard Charge-to Mass Ratio 8 km/sec jet-pellets.

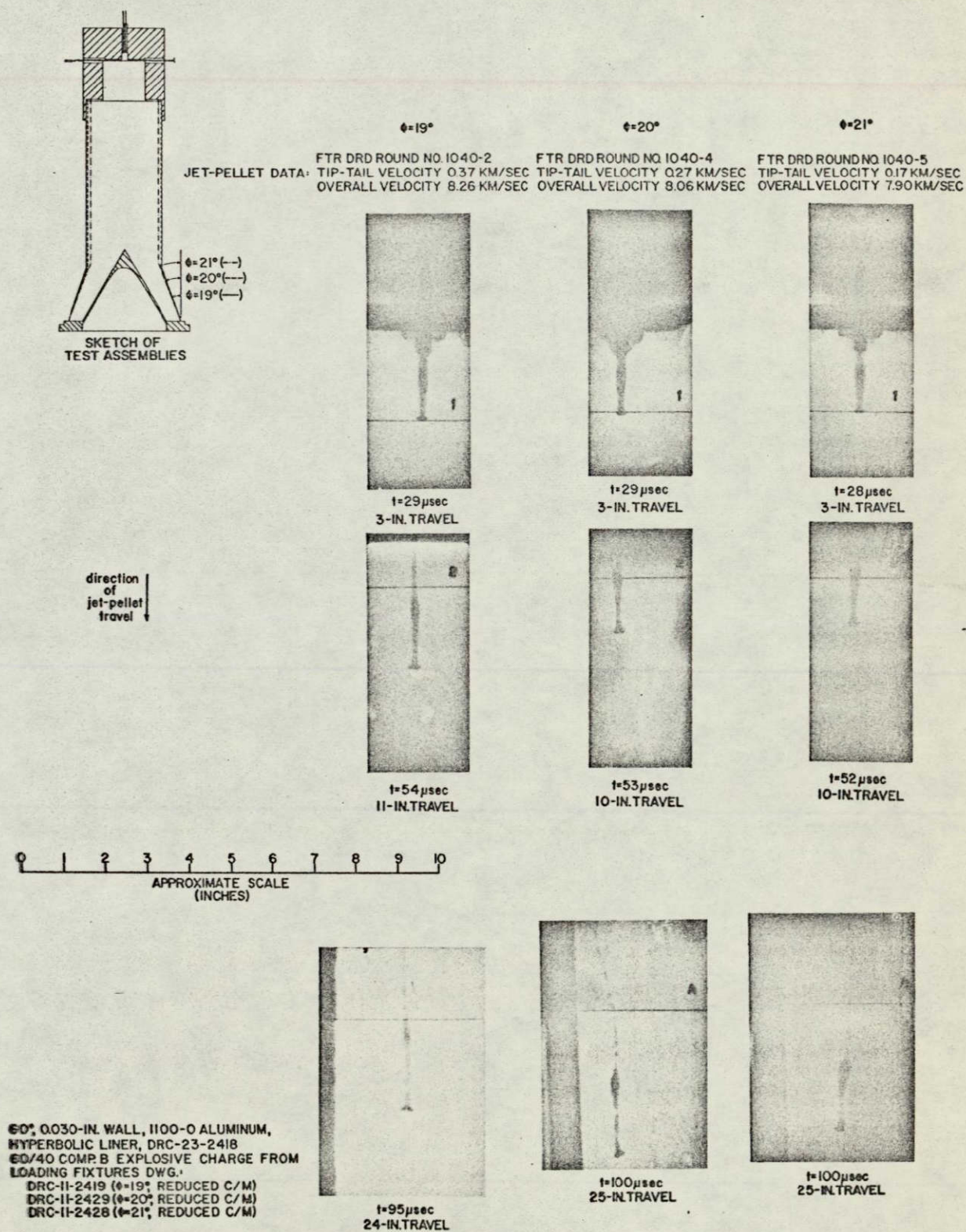


Fig. 23. Radiographs of reduced Charge-to-Mass Ratio 8 km/sec jet-pellets.

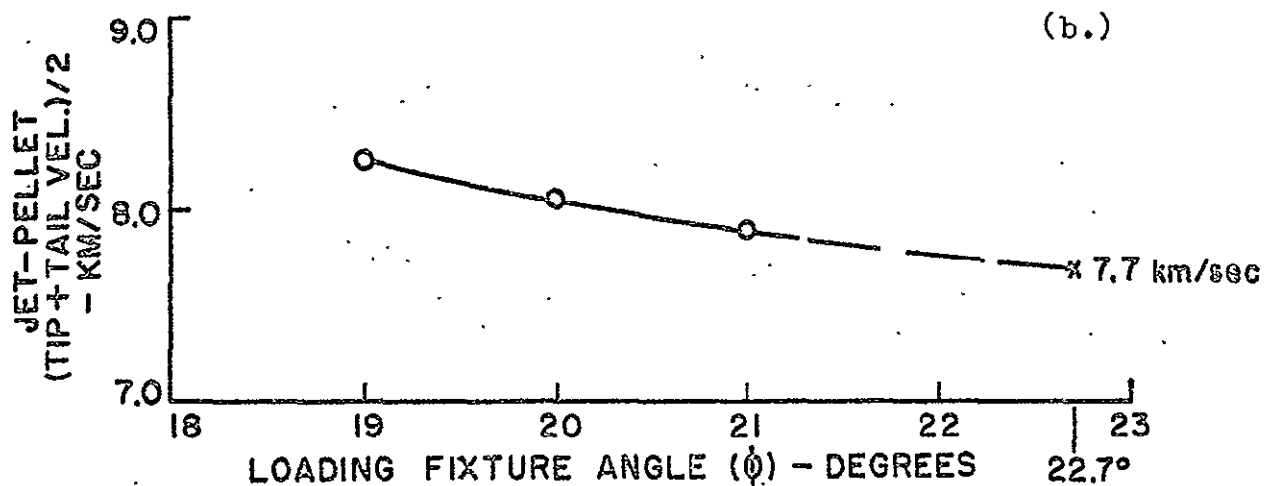
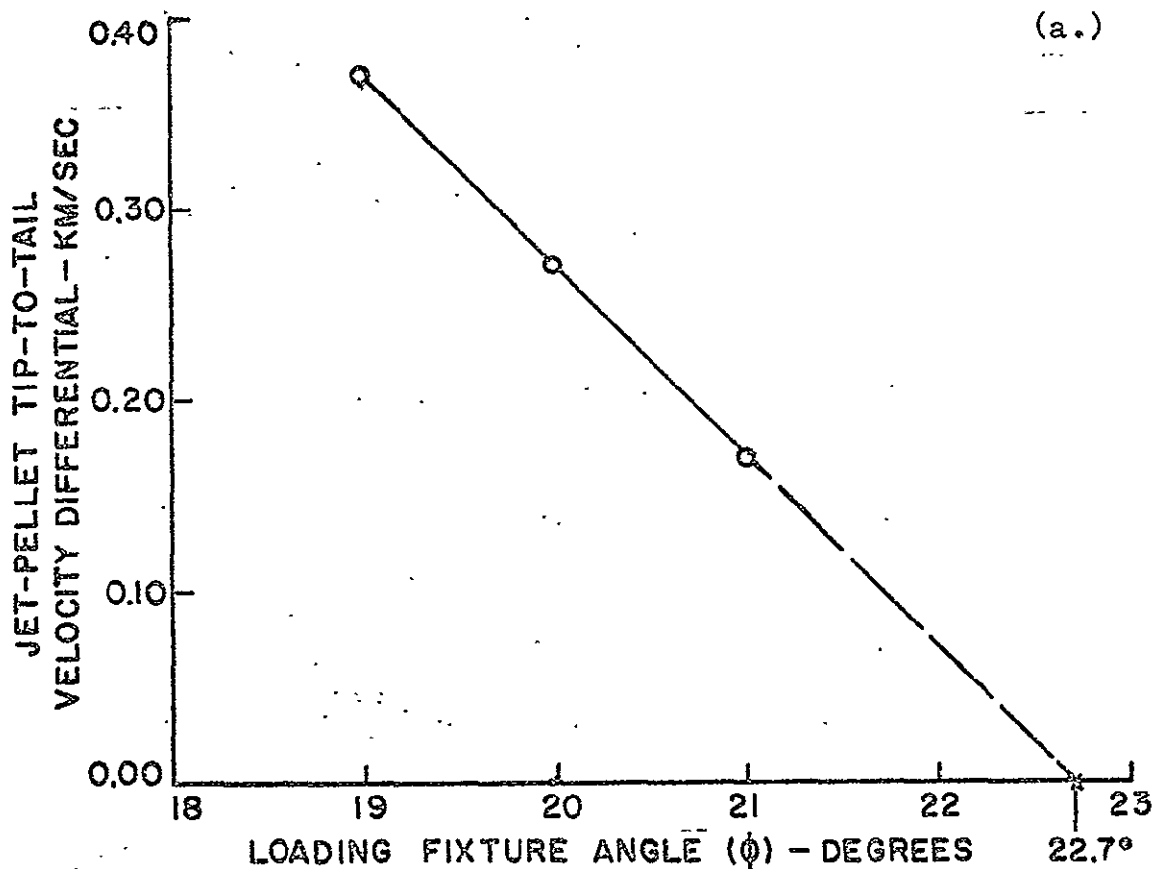


Fig. 24a. Graphic representation of jet-pellet velocity differential vs. reduced C/M loading fixture angle.

b. Graphic representation of jet-pellet velocity vs. reduced C/M loading fixture angle.

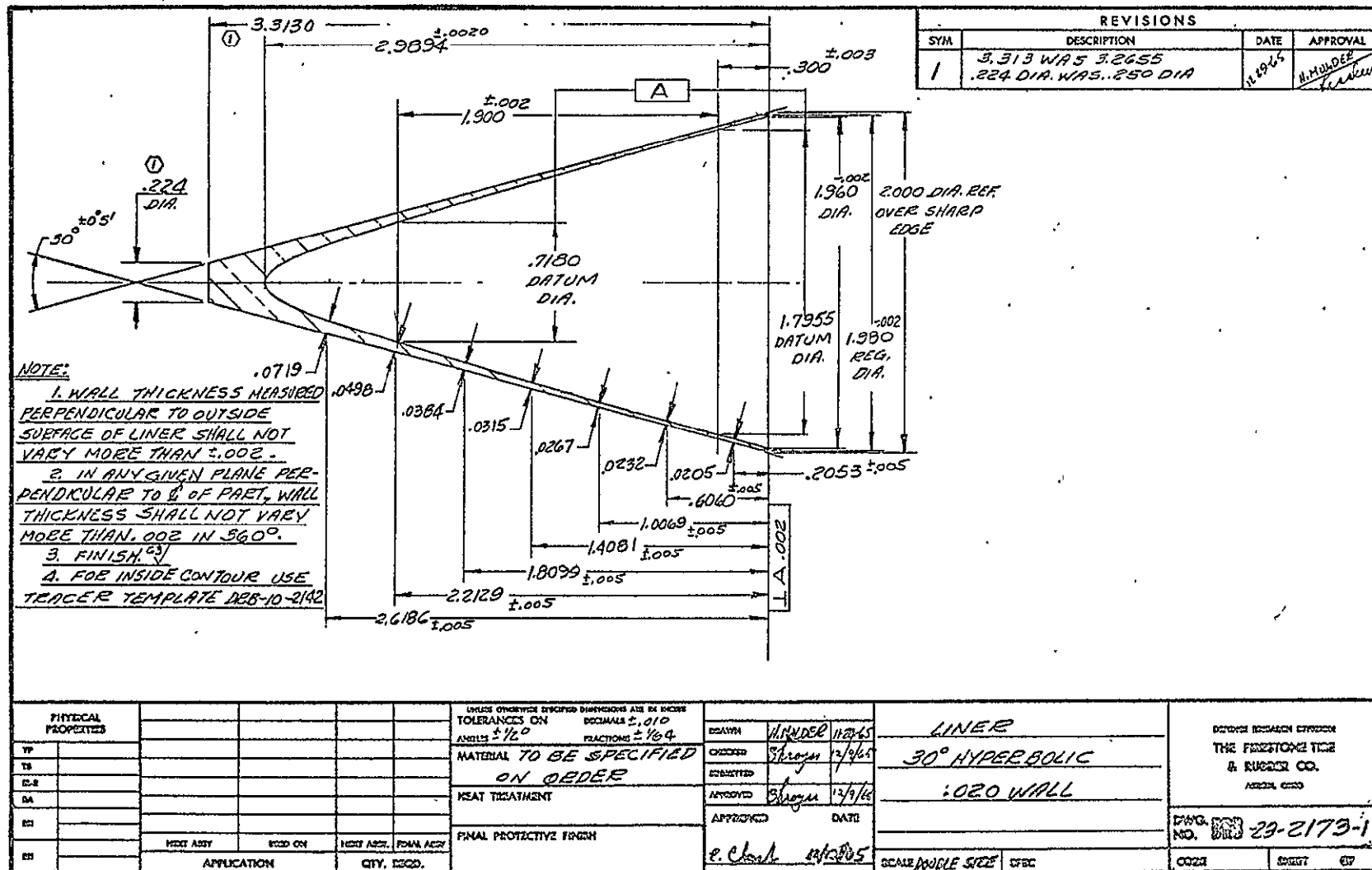


Fig. 25. 30°, 0.020-in. wall thickness hyperbolic liner.

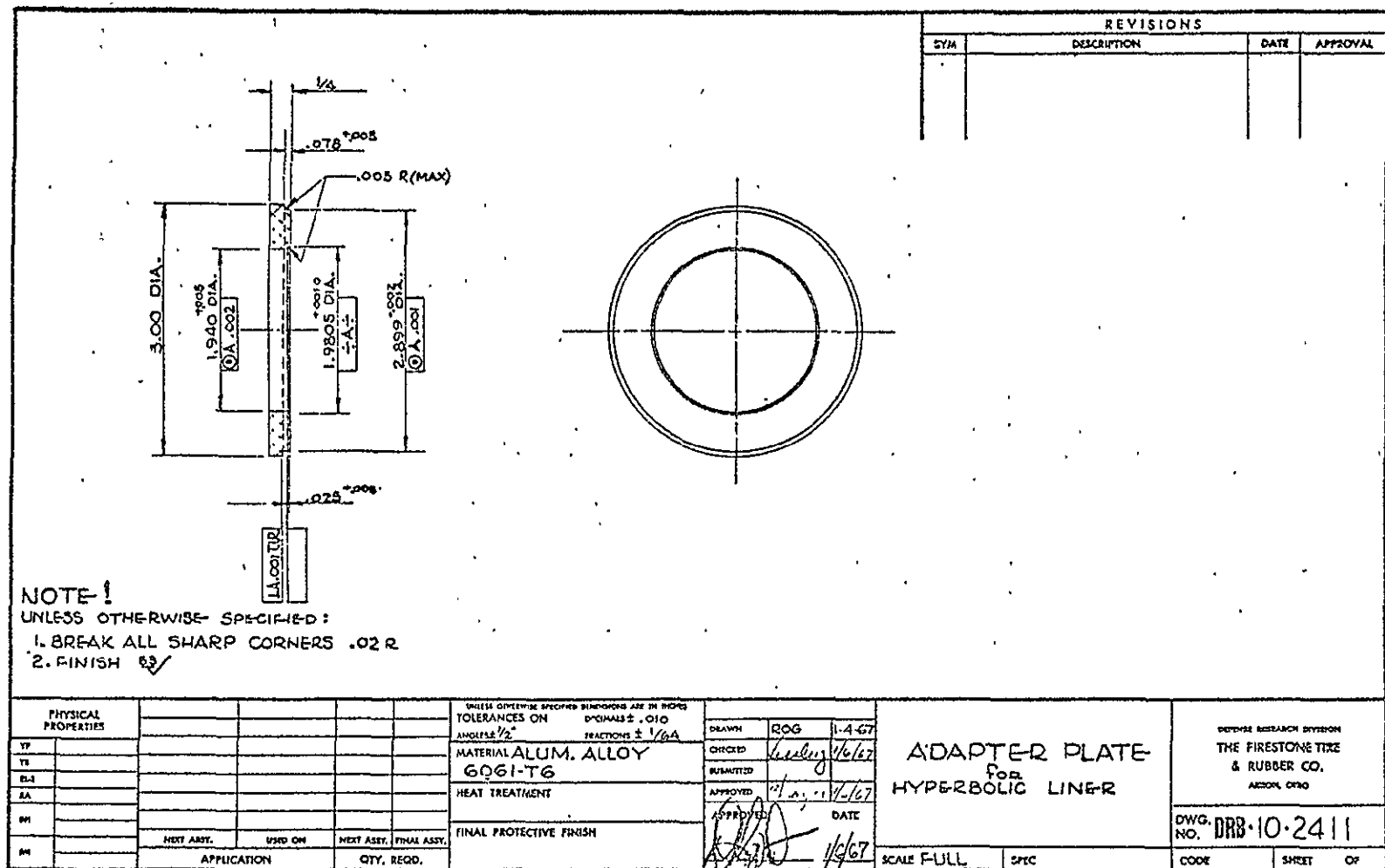


Fig. 26. Adapter plate for hyperbolic liners.

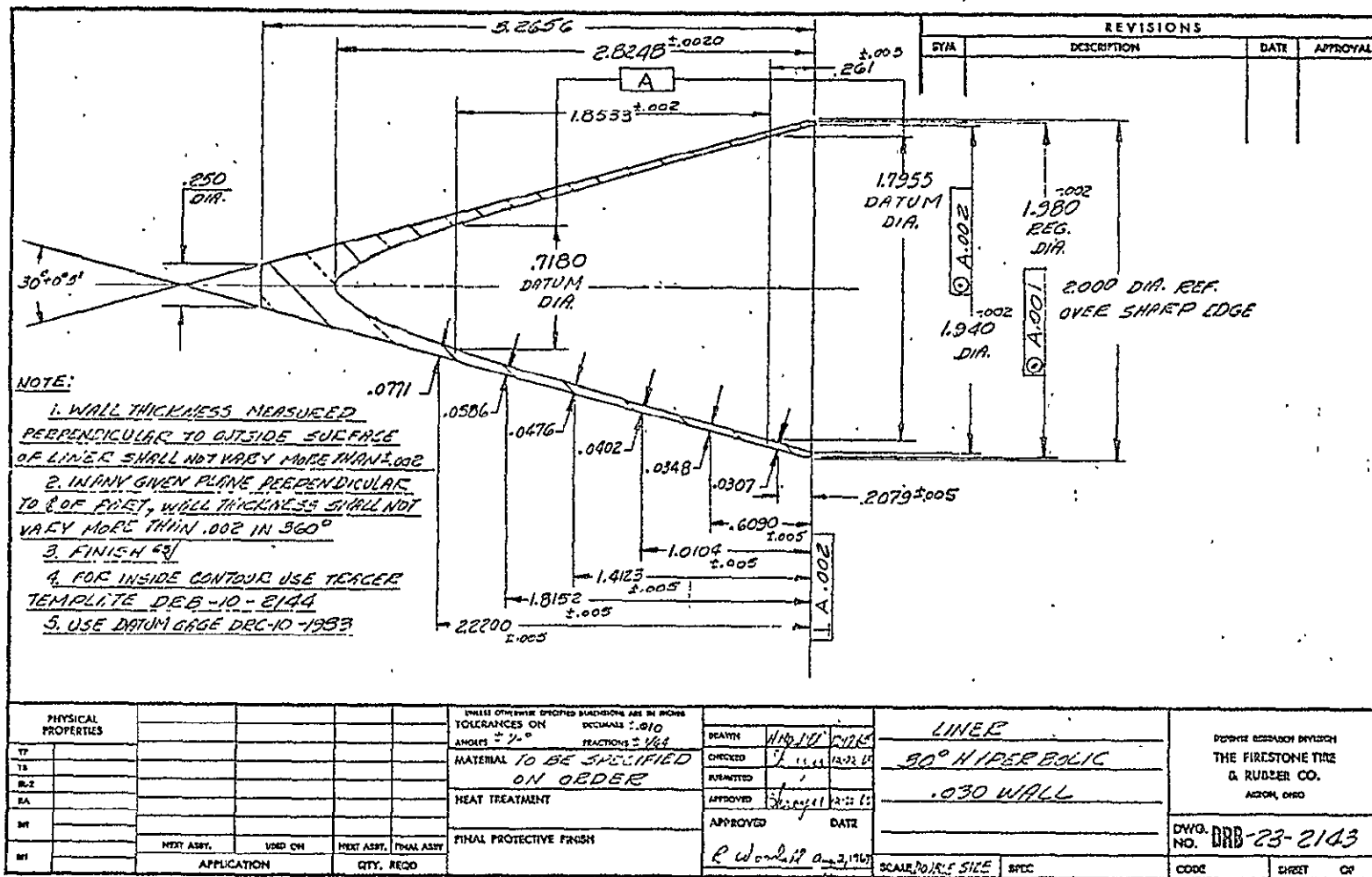


Fig. 27. 30°, 0.030-in. wall thickness hyperbolic liner.



Fig. 28. 30°, 0.040-in. wall thickness hyperbolic liner.

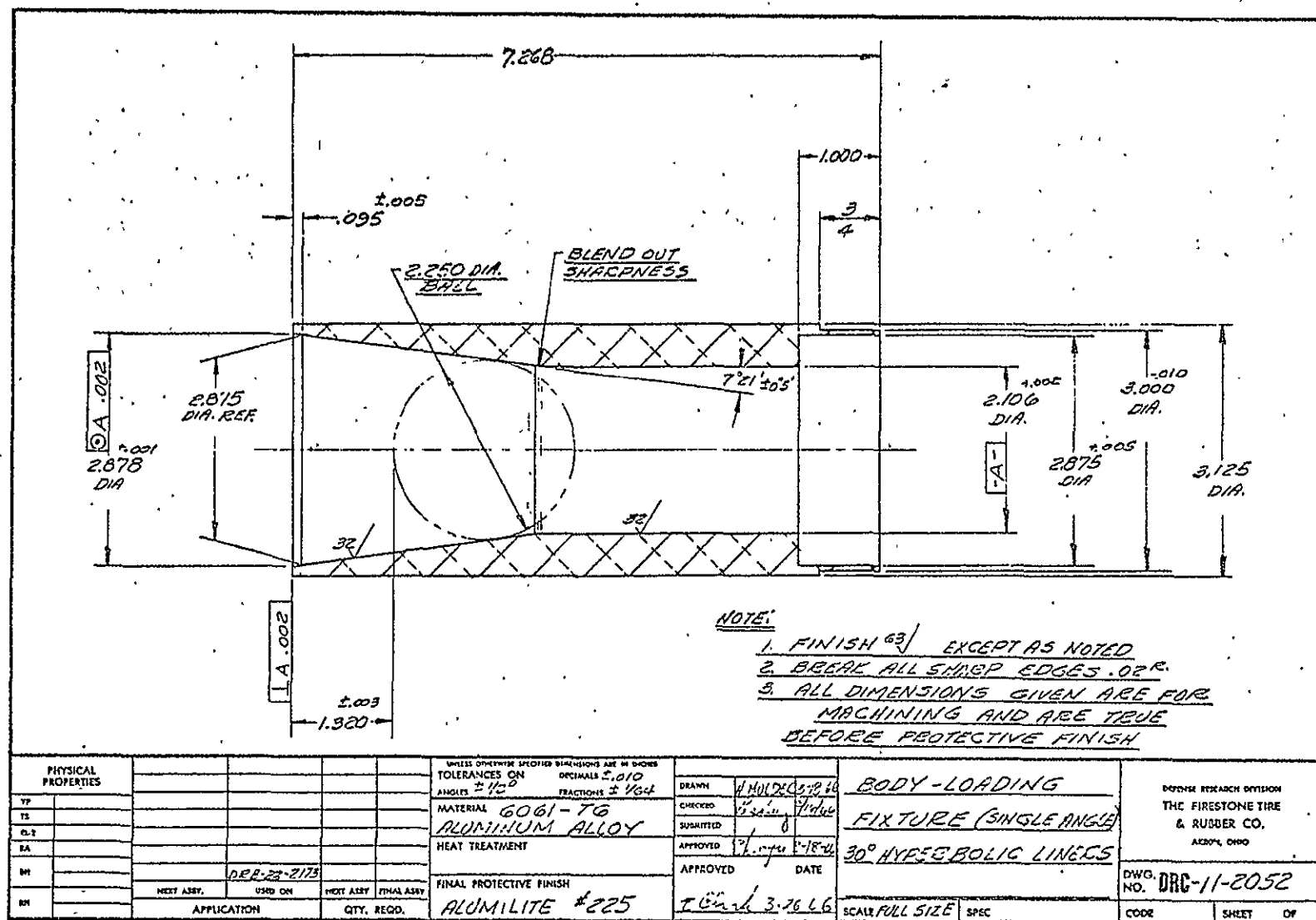


Fig. 29. Loading fixture for 30° hyperbolic liners.

1100-O ALUMINUM,
30° HYPERBOLIC
LINER, DWG.:

WALL THICKNESS:

DRB-23-2173-1
0.020-IN.

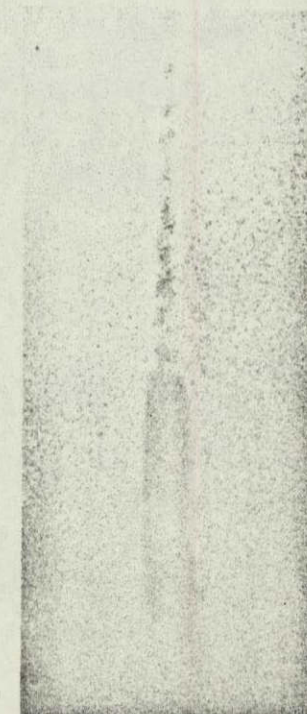
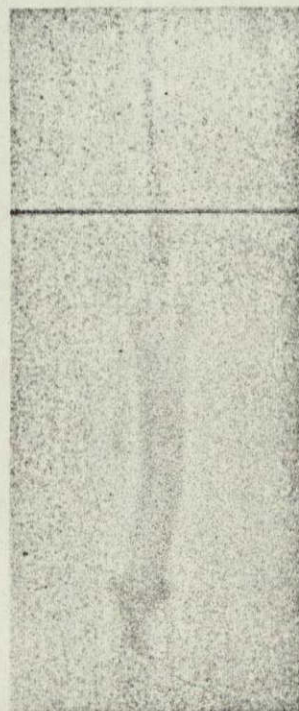
DRB-23-2143
0.030-IN.

DRC-23-2423
0.040-IN.

direction
of
jet-pellet
travel ↓

65/35 OCTOL EXPLO-
SIVE CHARGE FROM
LOADING FIXTURE
DRC-11-2052

0 1 2
APPROXIMATE SCALE
(INCHES)



TRAVEL
DISTANCE :
JET-PELLET
VELOCITY:
FTR DRD
ROUND NO:

24-IN.

11.32 KM/SEC

1029-2

25-IN.

11.07 KM/SEC

1029-1

26-IN.

10.77 KM/SEC

1048-2

NOT REPRODUCIBLE

Fig. 30. Radiographs of jet-pellets from 30° hyperbolic liners
of various wall thicknesses.

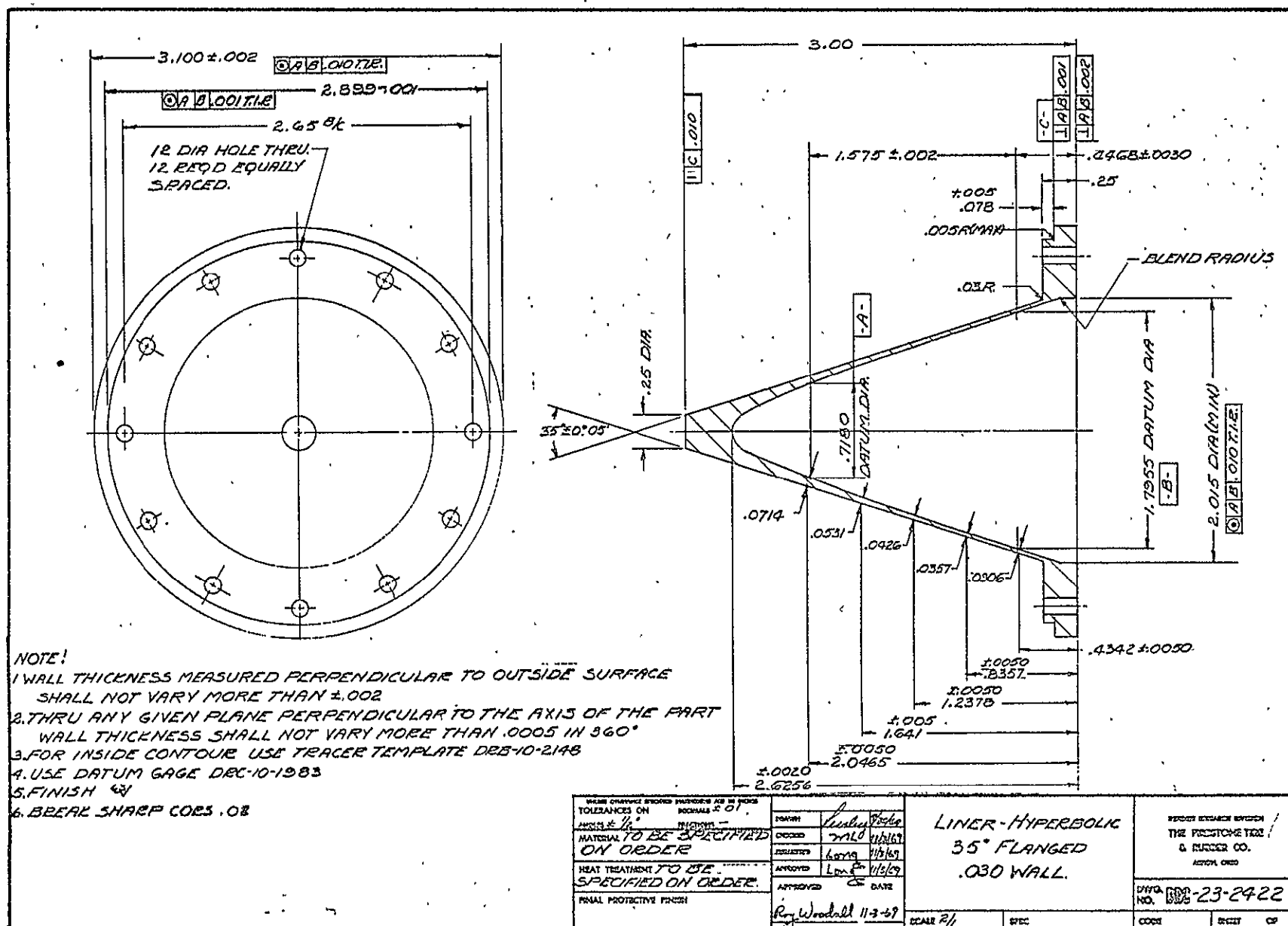
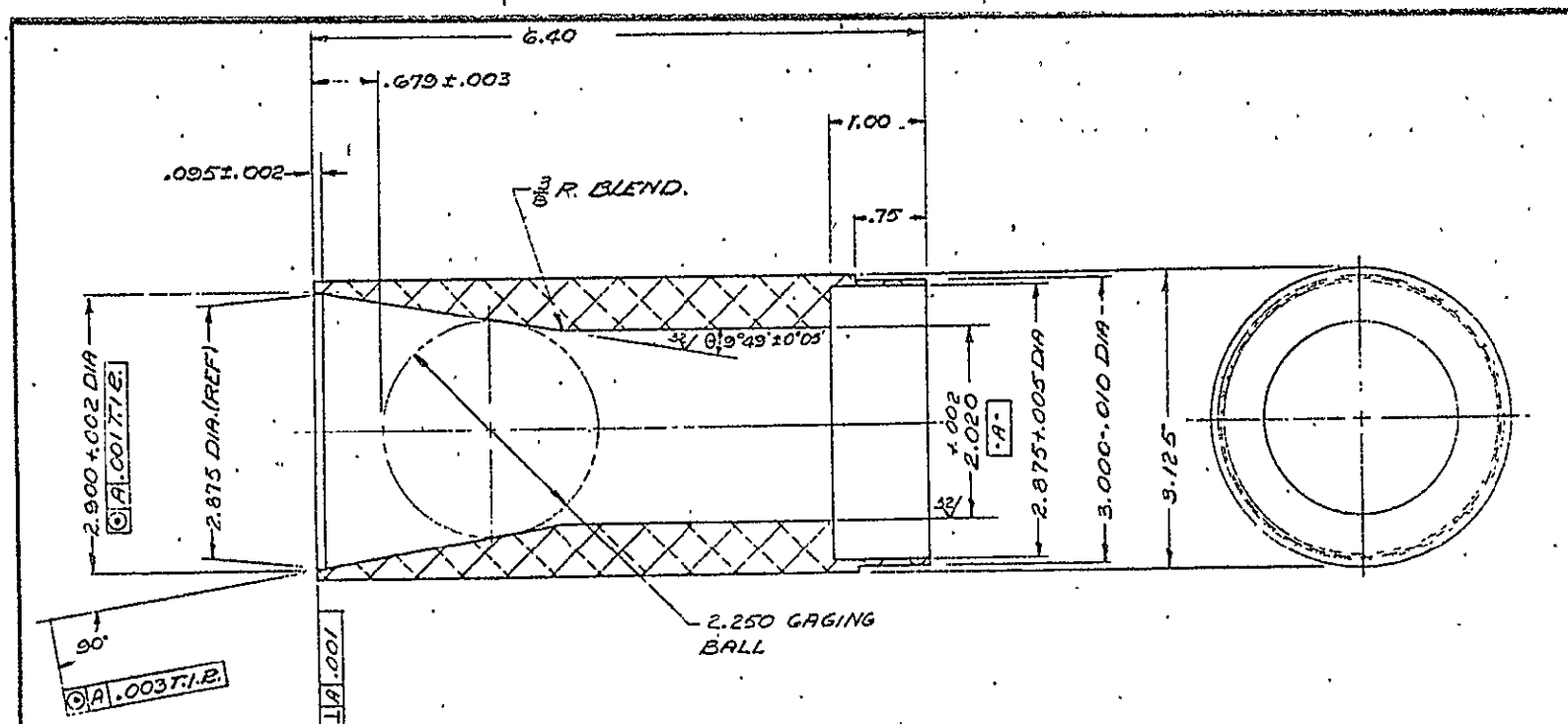


Fig. 31. Flanged 35°, 0.030-in. wall thickness hyperbolic liners.



NOTE

1. FINISH $\frac{3}{4}$ EXCEPT WHERE NOTED OTHERWISE
2. BREAK SHARP CORNS. 02
3. ALL DIMENSION SHOWN ARE FOR MACHINING AND ARE TRUE BEFORE PROTECTIVE FINISH.

PHYSICAL PROPERTIES		TOLERANCES ON DECIMALS $\pm .01$		DRAWN		BODY		DISTANCE RESEARCH DIVISION	
TP						LOADING FIXTURE		THE FIRESTONE TIRE	
TS						(SINGLE ANGLE) FOR		& RUBBER CO.	
IL-3						35° HYPERBOLIC LINER		ACORN, OHIO	
SA						$\theta = 35^\circ 49'$		DWD NO. DRG-11-2427	
MS						SCALE 1:1		SPEC	
DN						CODE		SHEET 07	
APPLICATION		QTY. REQD.		MATERIAL 061-76		HEAT TREATMENT		FINAL PROTECTIVE FINISH	
NEXT Assy		USED ON		AL. AL		APPROVED		DATE	
NEXT Assy		FINAL Assy		ALUMILITE #225		11-11-69		11-11-69	

Fig. 32. Loading fixture for 35° hyperbolic liners.

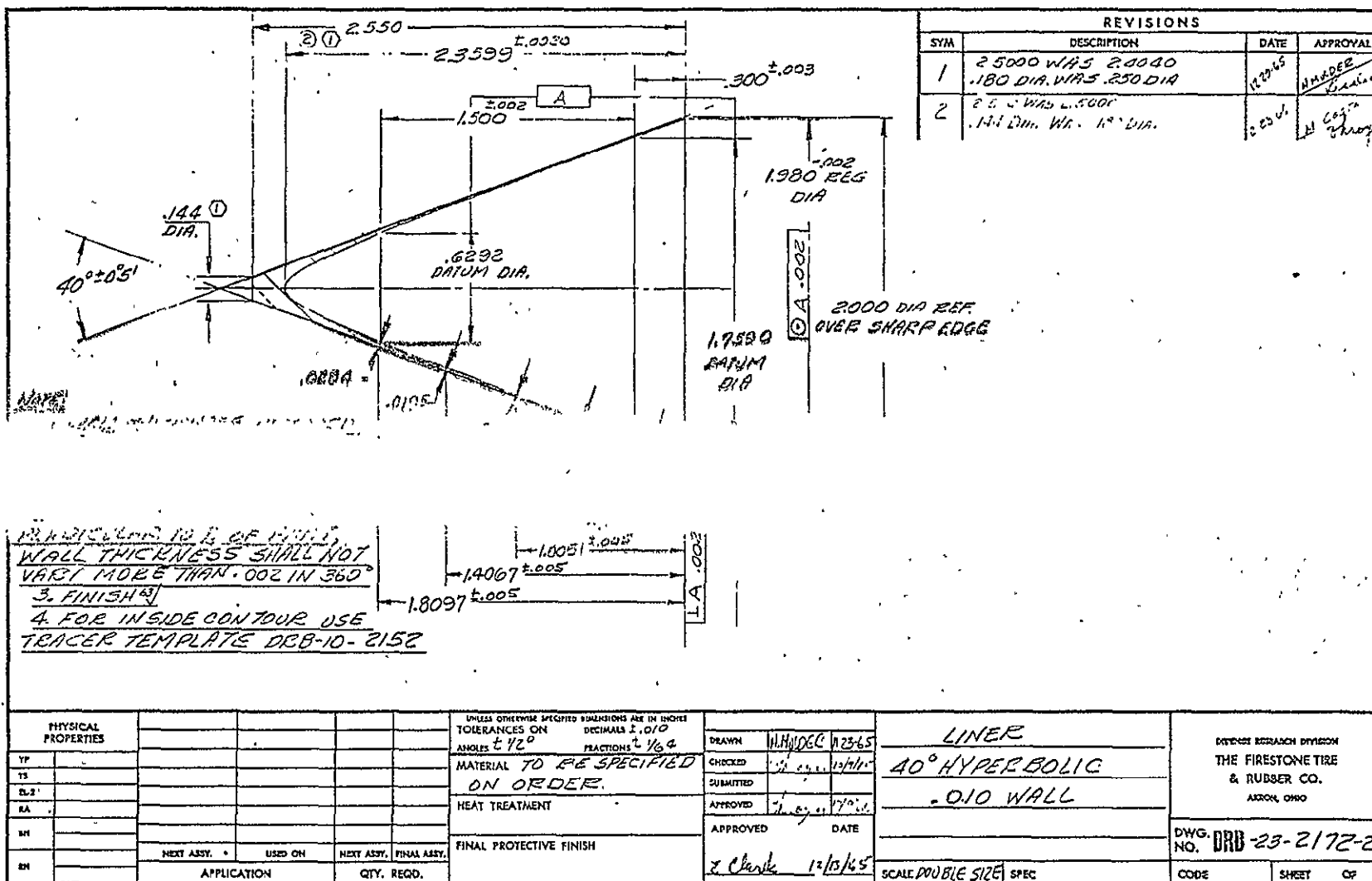


Fig. 33. 40°, 0.010-in. wall thickness hyperbolic liners.

1100-0 ALUMINUM HYPERBOLIC LINERS USING 65/35 OCTOL EXPLOSIVE CHARGE

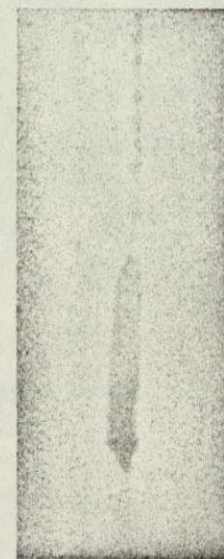
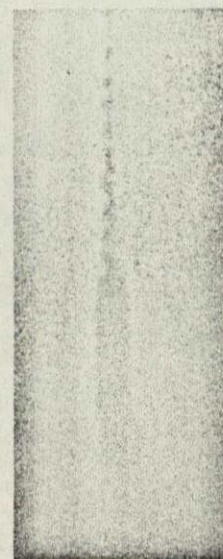
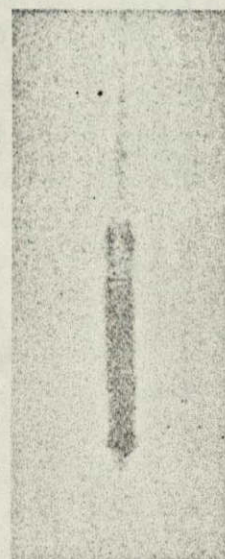
LINER DWG. NO:	DRC-23-2143	DRC-23-2423	DRC-23-2422	DRB-23-2172-2
LOADING FIXTURE DWG. NO:	DRC-II-2052	DRC-II-2052	DRC-II-2427	DRC-II-2239
LINER APEX ANGLE:	30°	30°	35°	40°
LINER WALL THICKNESS:	0.030-IN.	0.040-IN.	0.030-IN.	0.010-IN.

direction
of
jet-pellet
travel



0 1 2
APPROXIMATE SCALE
(INCHES)

NOT REPRODUCIBLE



TRAVEL DISTANCE:	25-IN.	26-IN.	28-IN.	28-IN.
JET-PELLET VELOCITY:	11.07 KM/SEC	10.77 KM/SEC	10.70 KM/SEC	11.28 KM/SEC
FTR DRD ROUND NO:	1029-1	1048-2	1046-2	1043-2

Fig. 34. Radiographs of jet-pellets from hyperbolic liners with various apex angles and wall thicknesses.

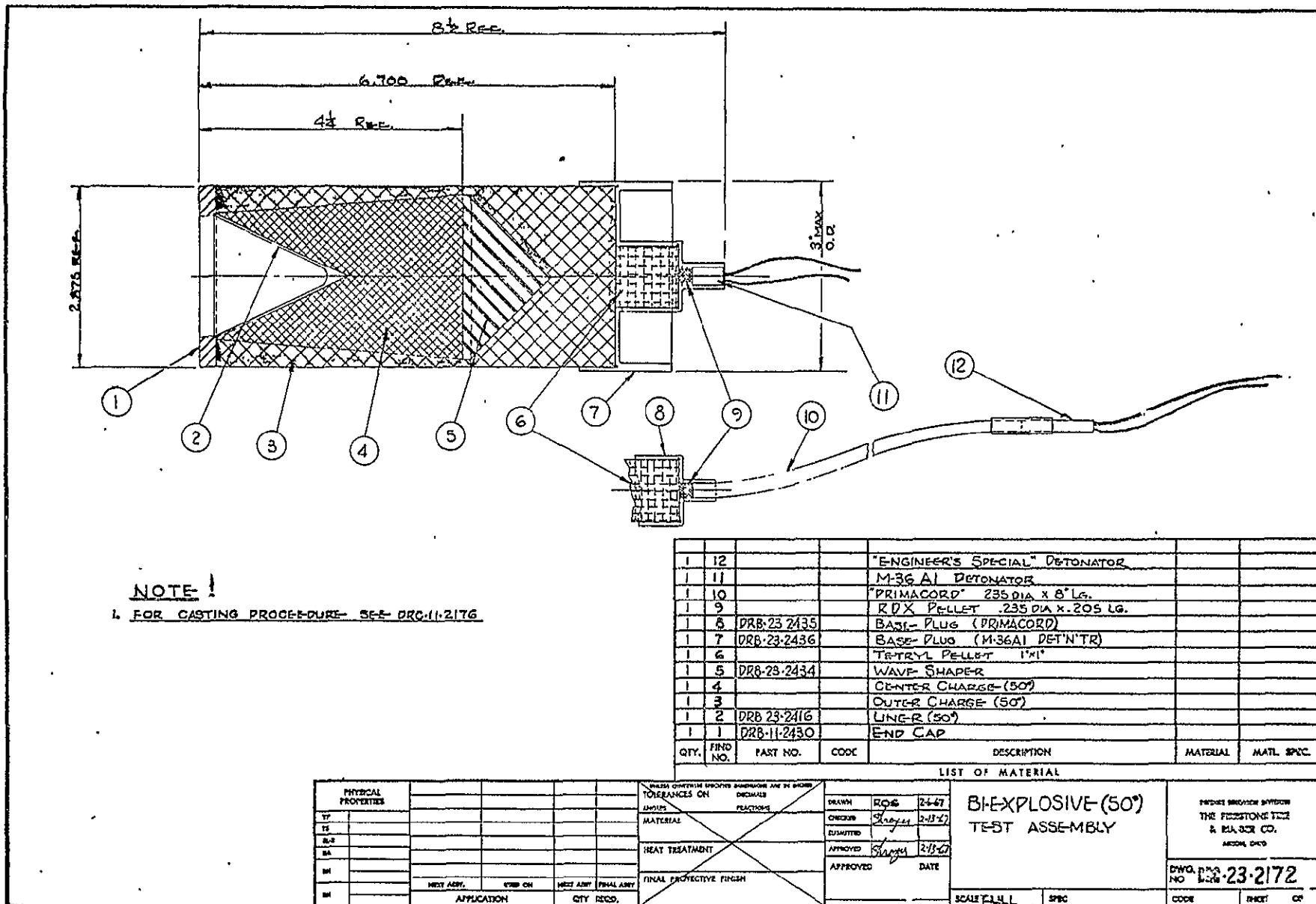


Fig. 35. Bi-explosive test assembly. Developed on NASA Contract NAS 1-6886.

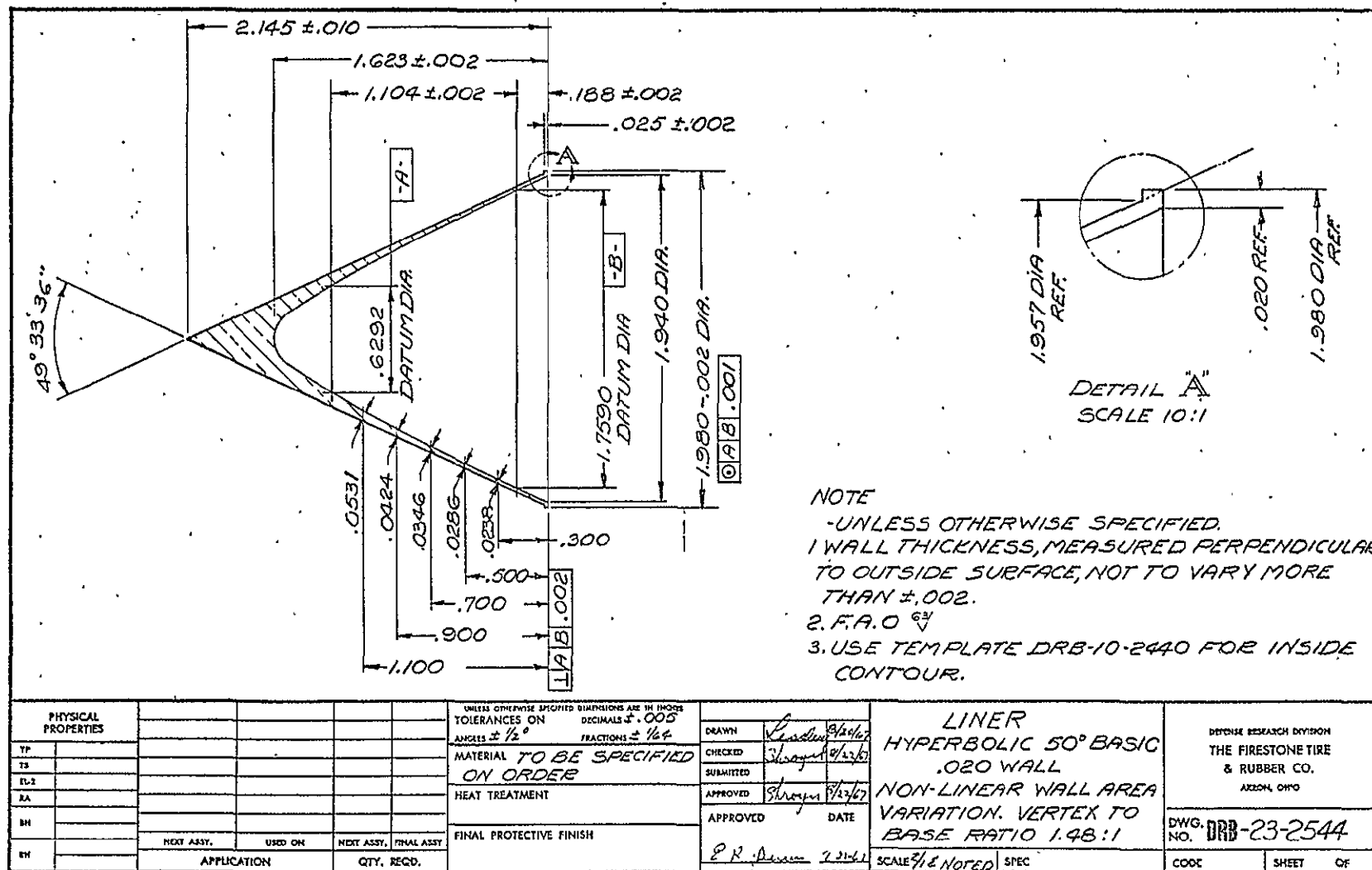


Fig. 36. 50° , 0.020-in. wall thickness (non-linear wall area variation) hyperbolic liner.

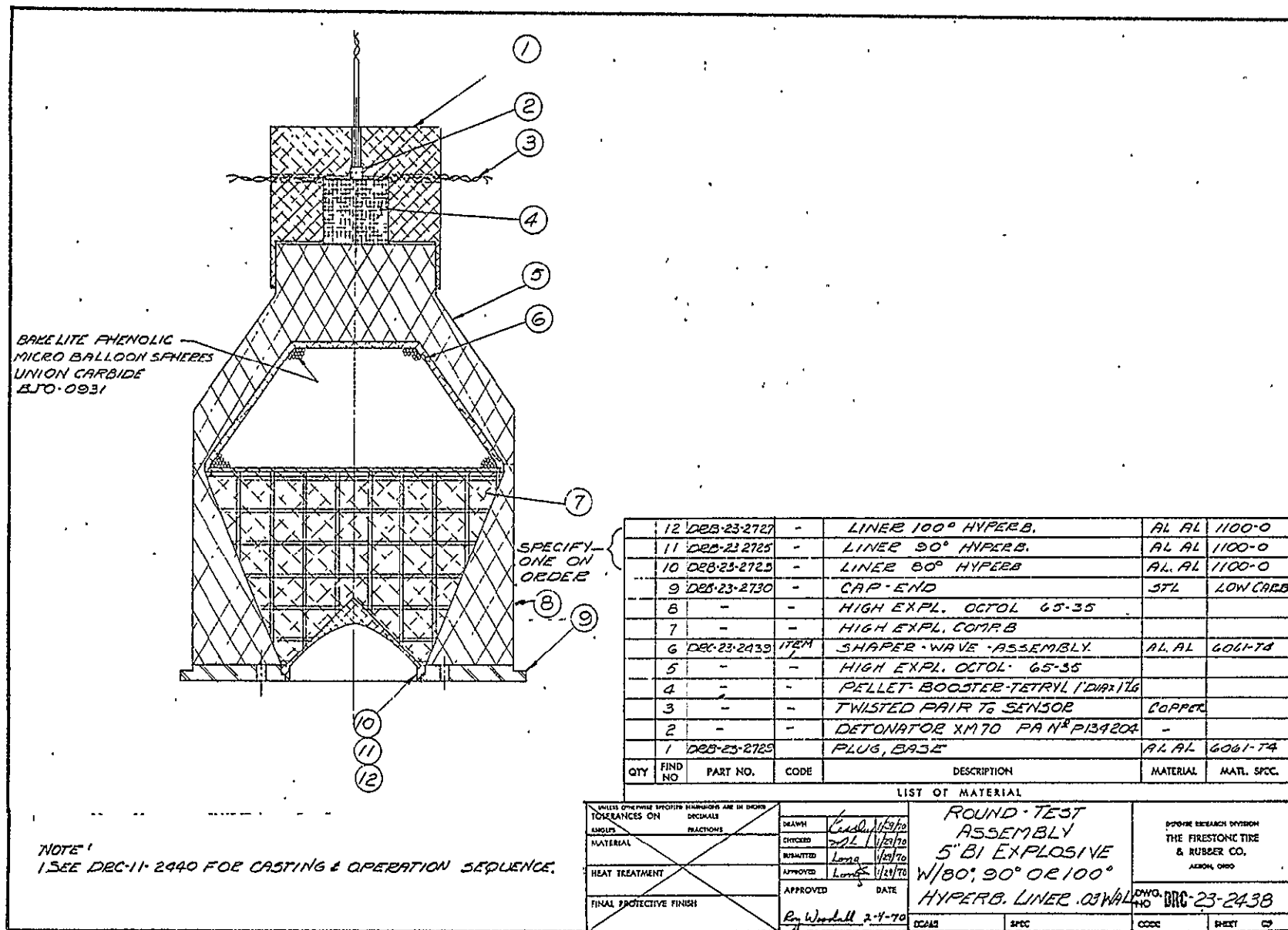
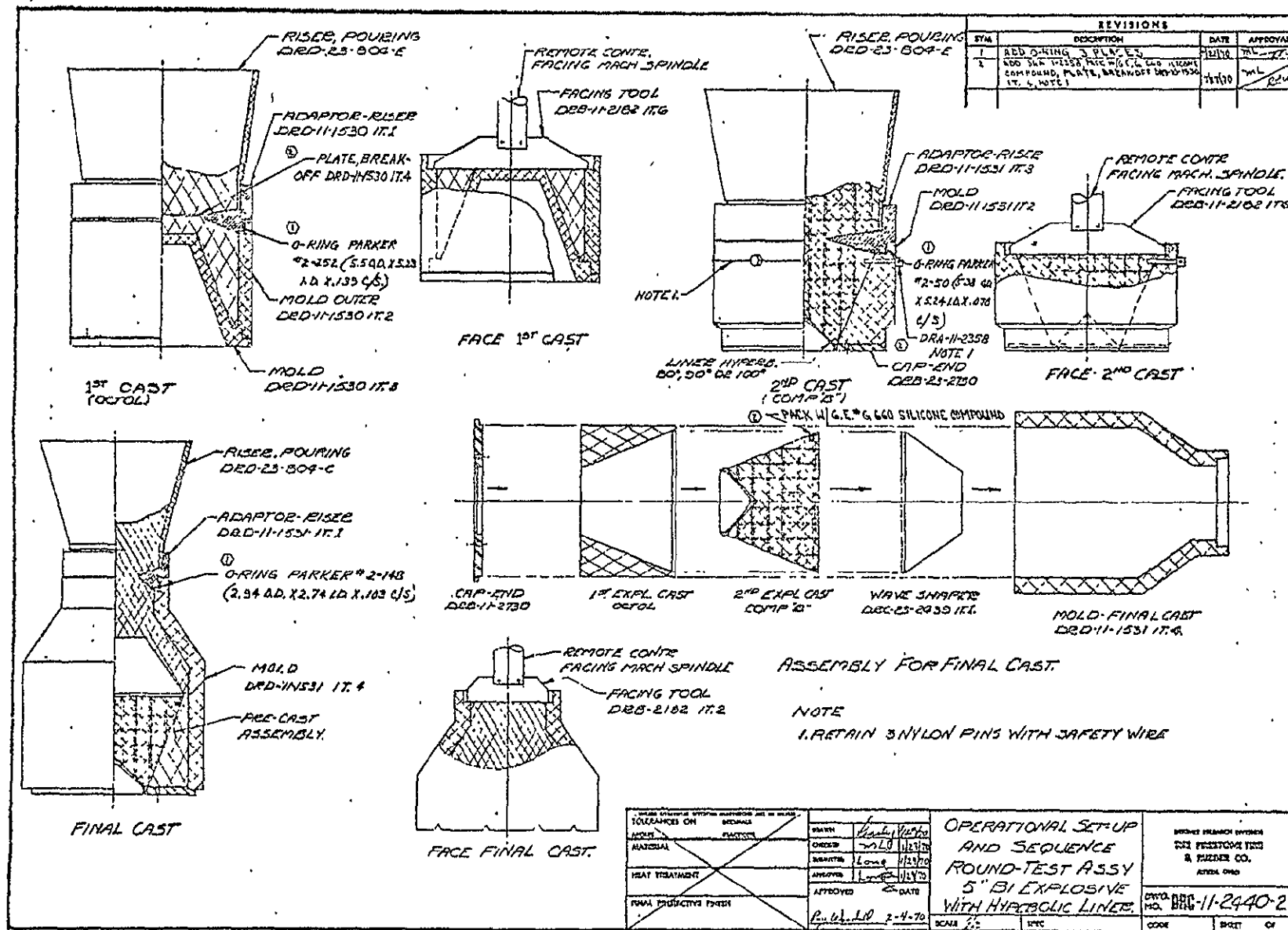


Fig. 37. Bi-explosive charge test assembly, 5-in. dia.



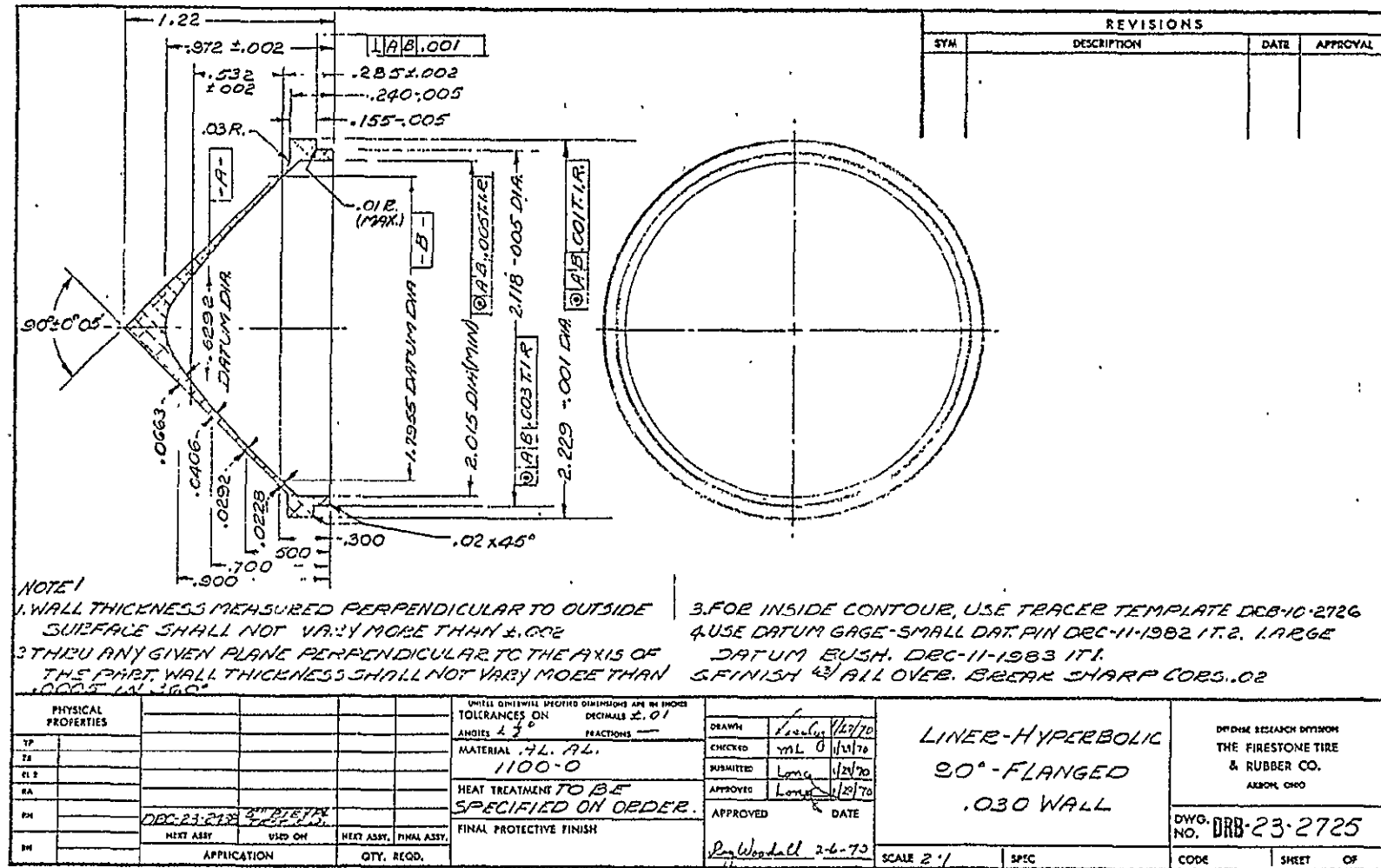
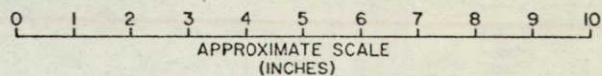
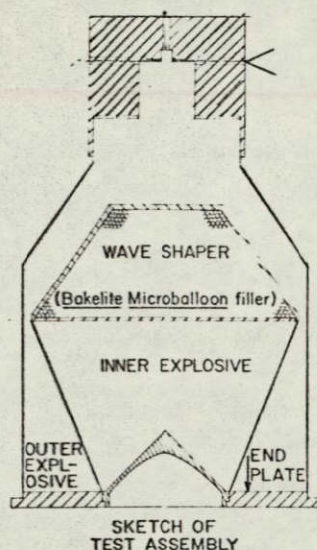


Fig. 39. Flanged, 90°, 0.030-in. wall thickness hyperbolic liner.



INNER
EXPLOSIVE:
OUTER
EXPLOSIVE:

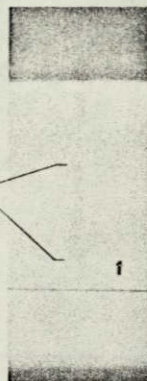
60/40 COMP. B
65/35 OCTOL
ALUMINUM END PLATE

60/40 COMP. B
65/35 OCTOL
STEEL END PLATE

50/50 PENTOLITE
60/40 COMP. B
ALUMINUM END PLATE

direction
of
jet-pellet
travel ↓

JET-PELLET
AFTER 5-IN.
TRAVEL



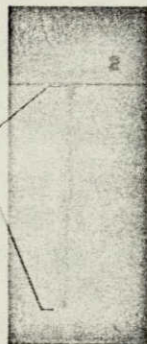
JET-PELLET
AFTER 6-IN.
TRAVEL



JET-PELLET
AFTER 3-IN.
TRAVEL



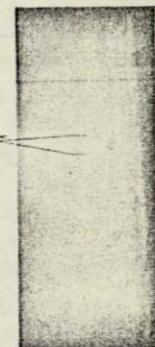
JET-PELLET
AFTER 15-IN.
TRAVEL



JET-PELLET
AFTER 15-IN.
TRAVEL



JET-PELLET
AFTER 13-IN.
TRAVEL



90° 0.030-IN. WALL, 1100-O ALUMINUM,
HYPERBOLIC LINER, DWG. NO. DRB-23-2725
BI-EXPLOSIVE LOADED PER DWG. NO.
DRC-11-2440

JET-PELLET VELOCITY:

FTR DRD ROUND NO. 1056-3
15.3 KM/SEC

FTR DRD ROUND NO. 1056-1
15.1 KM/SEC

FTR DRD ROUND NO. 1056-2
11.6 KM/SEC

Fig. 40. Radiographs of jet-pellets from 5-in. bi-explosive shaped charges.

8

30°, 0.030-IN. WALL, ALUMINUM, HYPERBOLIC LINER, DRC-23-2404
65/35 OCTOL EXPLOSIVE CHARGE FROM LOADING FIXTURE DRC-II-2052.

ALUMINUM TYPE:

1100-F
(as-received)

1100-O
(annealed)

direction
of
jet-pellet
travel



0 1 2
APPROXIMATE SCALE
(INCHES)



FTR DRD ROUND NO:
JET-PELLET VELOCITY:
TRAVEL DISTANCE:

1037-2
11.35 KM/SEC
26-IN.

1029-1
11.07 KM/SEC
25-IN.

Fig. 41. Radiographs of jet-pellets from annealed (1100-O) and unannealed (1100-F) aluminum hyperbolic liners.

40°, 0.030-IN. WALL, ALUMINUM, HYPERBOLIC LINER, DRC-23-2391
65/35 OCTOL EXPLOSIVE CHARGE FROM LOADING FIXTURE DRC-II-2239 ($\phi=12^\circ$)

ALUMINUM TYPE :

6061-T6
(as-received)

6061-O
(annealed)

direction
of
jet-pellet
travel



0 1 2
APPROXIMATE SCALE
(INCHES)



NOT REPRODUCIBLE

TRAVEL DISTANCE: 28-IN.
FTR DRD ROUND NO: 1041-1
JET-PELLET VELOCITY: 10.48 KM/SEC

28-IN.
1041-2
10.53 KM/SEC

Fig. 42. Radiographs of jet-pellets from annealed (6061-O)
and unannealed (6061-T6) aluminum hyperbolic liners.